UNIVERSITA` DEGLI STUDI DI PARMA

FACOLTA DI MEDICINA E CHIRURGIA
DIPARTIMENTO DI NEUROSCIENZE, SEZIONE DI FISIOLOGIA

DOTTORATO DI RICERCA IN NEUROSCIENZE

XXVI° CICLO

The neural correlates of vitality forms

Coordinatore:
Chiar.mo Prof. Vittorio Gallese

Tutor:
Chiar.mo Prof. Giacomo Rizzolatti

Dottorando: Giuseppe Di Cesare

Anno Accademico 2014-2015

Introduction

In everyday life people continuously move, breathe, act, change their facial expression. Movement represents the main demonstration of life and has an important role in conveying the sense of vitality. The continue production of movement supports our sense of vitality, i.e. the sensation to be alive. Important information about others' behavior is carried out by the dynamics of the observed action (the action style). Action dynamics describes the "vitality form", the "how" an action is performed, representing an important aspect that an observer may capture viewing an action performed by others. Differently from action goal (what) and intention (why), vitality form (how) reflects the internal psychological state of the agent, providing also an appraisal, in the case of interpersonal actions, of the affective/communicative quality underlying the relation between the agent and the action recipient (Stern, 2010). Behind each vitality form there is always an internal state that modulates action execution. The change of the internal state anticipates action execution. When the internal state changes people perform the same action using a different vitality form. Without this change, all actions would be performed in the same way and people would move like robots. Being vitality forms observed and performed, they play a double role in social interactions. More specifically, the execution of vitality form allows one to communicate others his internal state, while the observation of vitality form allows the observer to understand others internal state. Vitality forms are composed of different kinematic properties linked together: velocity, trajectory, energy and power. Globally these kinematic properties give a particular experience that reflects the affective/communicative state of the agent.

Vitality forms convey an affective content, not an emotional state. For example, if an action is performed energetically or gently, one can understand if the agent's mood is rude or kind, whether the agent performs the action with willingness or hesitancy. Vitality forms lay in between 'cold' actions, that are actions devoid of an emotional content, where the crucial information is related to the action goal or meaning, and 'hot' actions that are actions expressing emotions, where the crucial information

is related to the emotional dimension of an action (i.e. fear, anger). Vitality forms rest on a *third dimension* of the action processing that describes both the affective and cognitive components of the action. The capacity to express and to understand the vitality forms are already present in infants. These abilities denote a primordial way to relate to and understand others and represent a fundamental constitutive element of interpersonal relations (Stern, 1985; Trevarthen, 1998; Trevarthen and Aitken, 2001; Stern, 2010).

The aim of the present thesis is to investigate the brain areas involved in the vitality form processing. Preliminary to the main experiments concerning this issue, the first study was carried out to clarify which are the specific brain areas involved in the action kinematic processing. In the second study, was delineated the neural correlates involved in vitality forms processing during the observation of vitality form. The results showed a specific activation of the dorso-central insula. This activation, specific for vitality form processing, was also confirmed in the third study. In particular, using multivoxel pattern analysis, the results showed that the most discriminative voxels for the comparison between vitality form and velocity were located, consistently across subjects, in the dorso-central sector of the insula (positive signs, exhibiting a preference for vitality) and a widespread set of voxels around this sector (negative signs, preference for velocity). These results suggest that dorso-central insula is the site where the kinematic aspects of the observed actions are transformed into vitality forms, enabling individuals to understand others' internal state through action observation.

In everyday life, people not only observe vitality forms but also produce them. It is possible to hypothesize that the same neural mechanism underlies both observation and execution of vitality forms. This issue was investigated in the fourth study, which showed that the dorso-central sector of insula is also involved in vitality form imagination and execution.

Taken together, all these findings indicate that vitality form recognition, planning and execution share the same activation pattern, allowing the observer to understand the others' internal state, and the performer to communicate his/her affective internal state to others.

*First Study: The neural correlates of velocity processing during the observation of a biological effector in the parietal and premotor cortex.

1.1 Materials and Methods

1.1.1 Participants

Fourteen English students (7 females and 7 males, mean age 23.5 years) participated in the first experiment (Exp. 1) that was carried out at the Magnetic Resonance and Image Analysis Research Centre (MARIARC) at the University of Liverpool, UK. Sixteen Italian students (9 females and 7 males, mean age 23.6 years) participated in the second experiment (Exp. 2) that was carried out at the Neuroimaging Centre of the University of Parma, Italy. Subjects were right handed and had normal or corrected-to-normal vision and did not report psychiatric or neurological impairments. They gave fully informed written consent of their willingness to participate. The investigations were approved by the Local Ethics Committees (Liverpool for Exp. 1 and Parma for Exp. 2).

1.1.2 Stimuli

An example of the stimuli used in Exp. 1 is shown in Figure 1 Specifically, pairs of video-clips were presented to the subjects showing either an arm (Figure 1 AB) or a cylinder (Figure **1** CD), moving at different velocities, from a start position to reach a target placed at a distance of 35 cm. The video clips ended with the arm or the cylinder touching the target. The reaching movements of the arm and of the cylinder were presented at 3 different velocities: low (arm-V1: 0.38 m/s; cylinder-V1: 0.45 m/s), medium (arm-V2: 0.67 m/s; cylinder-V2: 0.78 m/s), and high (armV3: 1.5 m/s; cylinder-V3: 1.72 m/s). As a control, a still image of the same arm or of the same cylinder was used, which depicted them in either the start or the end position.

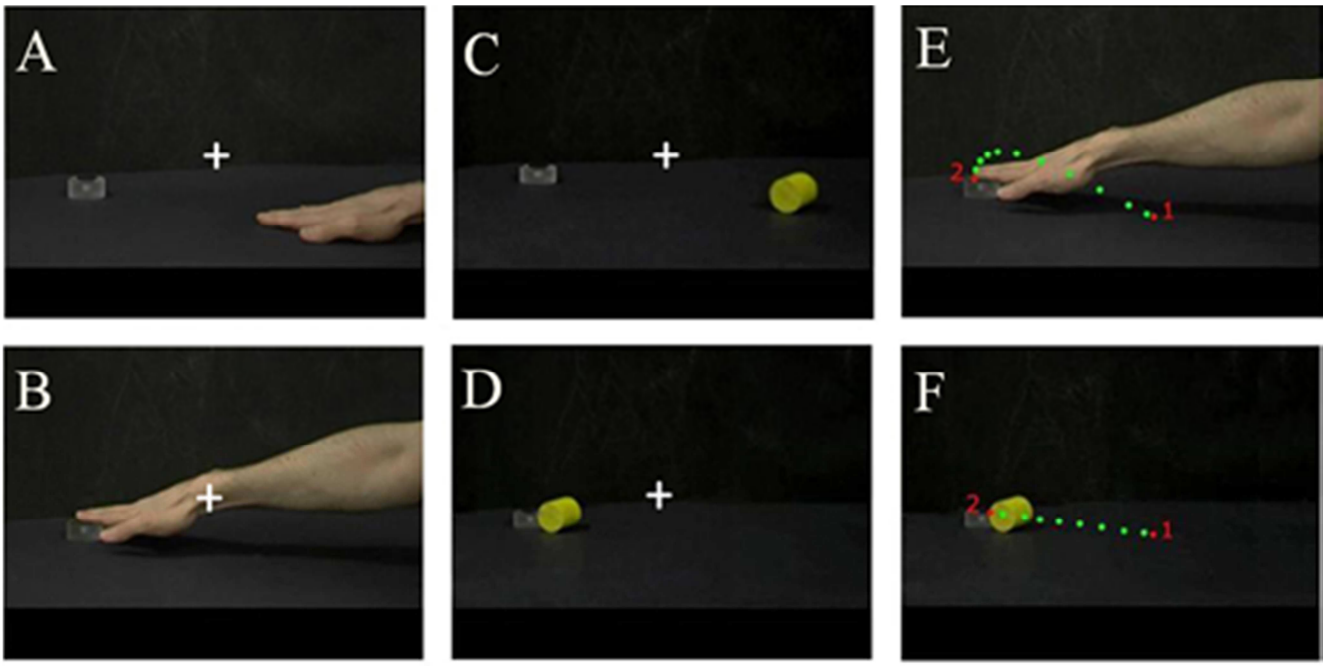

Figure 1: An example of the video-clips as viewed by the participants of Exp. 1. The images show a frame of the arm in the start position (A) and in the end position (B) and of the cylinder in the start position (C) and in the end position (D). The start and the end positions of the arm and of the cylinder were the same. We marked with a green dot for the arm and the cylinder each position occupied every 40ms in the space. The arm reached the end point with a translational motion following a curvilinear trajectory (E); the cylinder reached the target with a complex motion (rotary + translational) using a straight trajectory (F). [Modified from Di Cesare et al. (2013), with kind permission from Elsevier.]

An example of the stimuli used in Exp. 2 is shown in Figure 2. Specifically, the subjects were presented with video-clips showing either a biological effector (arm, Figure 2 AB), a non-biological object (arrow, Figure 2 CD) or a colored biological effector (colored arm – Figure 2 EF). In contrast to Exp. 1, all stimuli moved according to biological motion and reaching started from a fixed point(**Figure 2** C) and ended on a red cross placed at a distance of 46 cm (Figure 2 BD). The video clips ended with the arm, the arrow or the colored arm touching the target. The reaching movements of the arm (Arm) and of the arrow (A) were presented at 3 different velocities: low (Arm-V1: 0.35 m/s; A-V1: 0.33 m/s), medium (Arm-V2: 0.89 m/s; A-V2: 0.96 m/s), and high (Arm-V3: 1.83 m/s; A-V3: 1.32 m/s). The 3 colored arms (blue, red, and yellow; Figure 2 EF) always performed the reaching movement at the same velocity (medium – V2). As a control, a still image of the same arm, arrow or colored arm was used, which depicted them in the end position.

In Exp. 2, the comparison between activations evoked by observation of a biological effector and a non-biological object, both moving following a biological motion, required the construction

of an object with a similar shape and moving with similar kinematic profiles as those of the biological effector, i.e. the arm. For this purpose, the arrow was built using a pink-colored stiff paperboard. The tip of the arrow had the same size as the hand (i.e., 15 cm x 11 cm x 4 cm) while the tail of the arrow was the same size as the arm (60 cm x 7 cm x 4 cm) and, therefore, the arrow and the arm occupied the same space in the video-clips. Five hidden wheel-pairs were mounted under the arrow to allow movement. The arrow was pulled from the tip by a transparent nylon thread. Observation of the arrow moving towards the target gave the impression of a reaching movement. Thus, besides controlling for visual and kinematic aspects, the idea of building an arrow was to control for possible high-order effects evoked by the observation of a reaching movement.

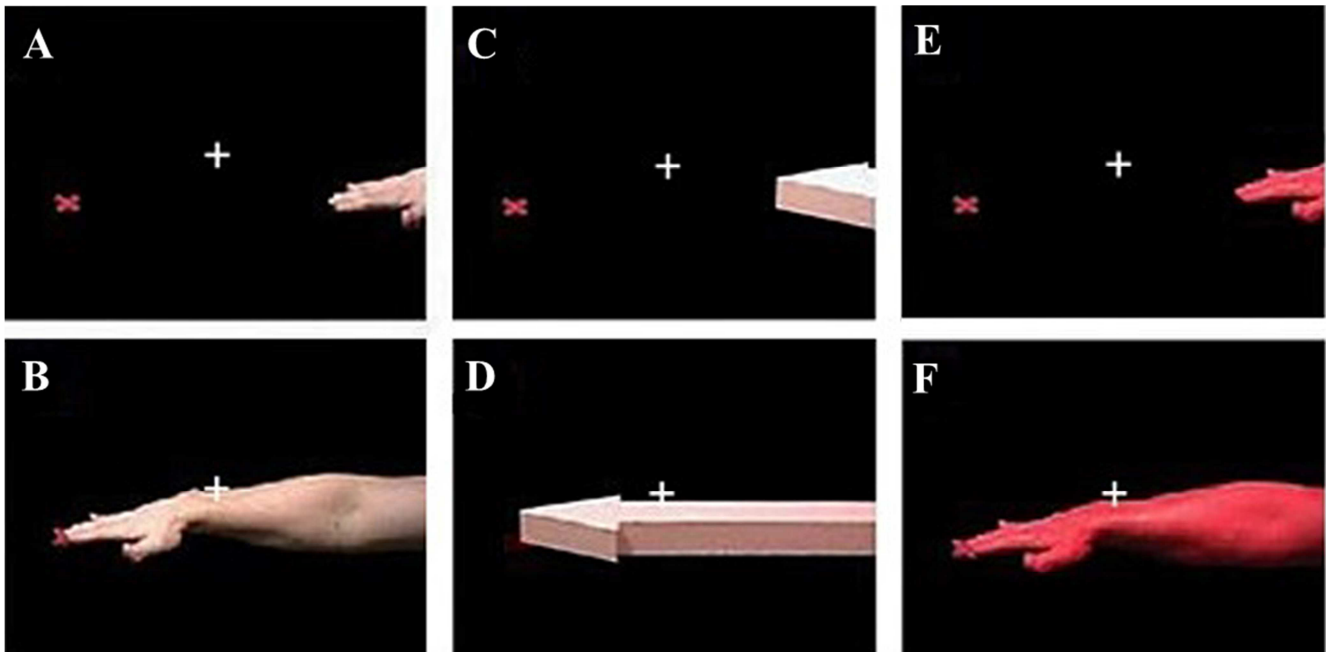

Figure 2: An example of the video-clips as viewed by the participants of Exp. 2. The arm, the arrow and the colored arm are shown at the start position (A, C, E) and at the end position marked by a red cross (B, D, F). In the conditions same, the arm and the arrow reached the end point with the same velocity between video-pairs and, in the conditions different, with different velocities between video-pairs. The colored arm reached the end point always at the same velocity but changing, in the conditions *different*, the arm color between video-pairs. [Modified from Di Cesare et al. (2013), with kind permission from Elsevier.]

The motion profiles of the arm and arrow were studied using the point kinematics method. Using the software Avimeca v2.3, we marked the positions in the videos of the arm and the arrow with a dot on, respectively, the terminal part of the middle finger of the arm and the inferior vertex of the arrow tip in the start position (Figure 3 A, C) and marked each occupied position in space every

40 ms. In this way, was able to verify that the arm and the arrow moved with equivalent trajectory and occupied the same positions in time.

By using Regressi software (version 2.9) velocity curves was obtained for both stimuli (Figure 3 BD). To make sure that velocity varied in the same fashion in the two stimuli (arm and arrow) and within each velocity level (V1, V2, V3), was carried out a 2x3 repeated measures GLM analysis. For homogeneity of comparison between stimuli and across velocity levels, were considered only a number of values ranging ± 6 around the pick of each velocity/type level, totaling 13 values (corresponding to the minimum amount of recorded values associated with V1). Independently of velocity level (V1, V2, V3), the results showed no significant differences in mean velocity between stimuli (P>.05), indicating that the two stimuli had a similar velocity profile.

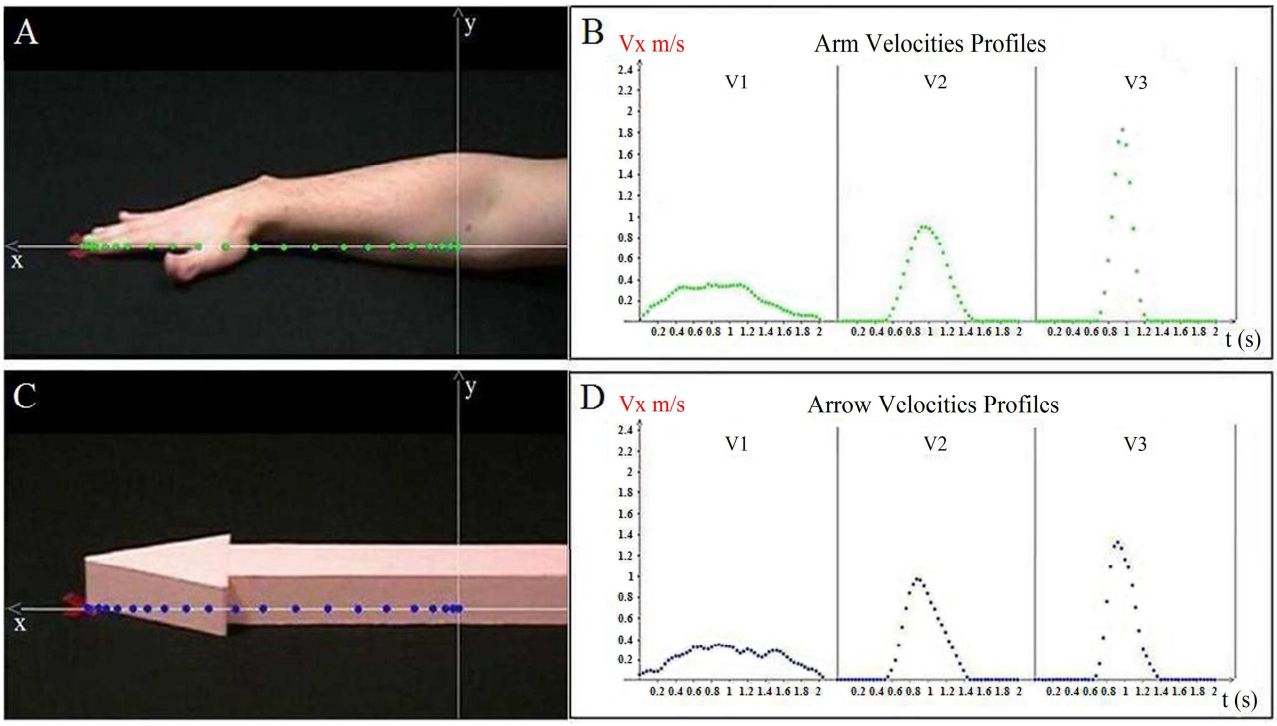

Figure 3: Trajectory profile of the arm (A) and of the arrow (C) reaching the end point with a biological motion. X and Y spatial coordinates are shown on the picture by colored dots that indicate the values of each point occupied in space and time by the arm and arrow moving with a medium velocity (V2). Graphs showing velocity profiles for the arm (B) and for the arrow (D) reaching movements at low velocity (V1 mean peak for the arm: 0.35m/s at 0.75s; V1 mean peak for the arrow: 0.33m/s at 0.88s); medium velocity (V2 mean peak for the arm: 0.89m/s at 0.91s; V2 mean peak for the arrow: 0.96m/s at 0.88s) and high velocity (V3 mean peak for the arm: 1.83m/s. [Di Cesare et al. (2013), with kind permission from Elsevier.]

1.1.3 Paradigm and task

To assess brain responses to observed movement velocity, the RS technique was used in both Exp.1 and Exp. 2. In Exp. 1, pairs of video-clips presented consecutively either the arm or the cylinder moving with the same velocity (condition *same*: 48 trials) or with different velocities (condition *different*: 48 trials). In Exp. 2, pairs of video clips showed the arm, the arrow or the colored arm moving with the same velocity/color between consecutive videos (condition *same*: 30 trials) or with different velocities/color (condition *different*: 30 trials). The trials were constructed so that all possible order combinations of velocity (condition *same*: V1-V1; V2-V2; V3-V3; condition *different*: V1-V2; V1-V3; V2-V3; V3-V1; V3-V2) and of color-C (condition *same*: C1-C1; C2-C2; C3-C3; condition *different*: C1-C2; C1-C3; C2-C3; C3-C1; C3-C2) were presented. Each scanning session (functional run) started with a cross positioned at the center of the screen (500ms), on which subjects were instructed to fixate and this remained on the screen throughout the trials. The first video-clip was presented for 2s followed by a 100ms interval before the second video-clip, which was presented for 2s. The second video was followed by a jittered interval ranging between 2 and 7s. In about 17% of cases in Exp. 1 and 29% of cases in Exp. 2, subjects were asked to provide an explicit response to the stimuli during this interval (catch trials). During the catch trials, cued by the appearance of a question mark after the second video offset, the subjects had to indicate, on a response box, whether the two consecutive videos were the same or different. About 20% of the trials were characterized by two consecutive videos representing a still image of the arm, the cylinder, the arrow or the colored arm (control still image). In Exp. 1, the subjects viewed a total of 342 trials comprising video-pairs distributed among conditions as follows: 96 trials of arm movement (no overt response) plus 18 catch trials (with response); 96 trials of object movement (no overt response) plus 18 catch trials (with response); 32 trials of static arm (no overt response) plus 6 catch trials (with response); 32 trials of static object (no overt response) plus 6 catch trials (with response). In Exp. 2, subjects viewed a total of 315 trials comprising video-pairs distributed among conditions as follows: 60 arm reaching (Arm; 30 same, 30 different), 60 arrow reaching (A; 30 same, 30 different), 60 colored arm reaching

(CArm; 30 same, 30 different), 15 still arm, 15 still arrow, 15 colored arm (still) and 90 catch trials. The experiments lasted approximately 60 min divided in 4 functional runs in Exp. 1 and 5 functional runs in Exp. 2, with each run lasting about 11 min. Stimuli were randomized within each run and balanced across runs so that there was an equal number of trials of each condition type. In Exp. 1, the stimuli were viewed through a frontal mirror mounted on the head coil of the MR system to reflect images displayed on a screen via a projector positioned outside the scanner room. Presentation 11.0 (Neurobehavioral Systems, Albany, CA, http://www.neurobs.com) was used for stimulus presentation and response recording. In Exp. 2, the stimuli were viewed via digital visors (VisuaSTIM) with a resolution of 500,000 pixels per 0.25 square inch and horizontal eye field of 30°. The digital transmission of the signal to the scanner was via optic fiber. E-Prime 2 Professional software (Psychology Software Tools, Inc., Pittsburgh, USA, http://www.pstnet.com) was used for stimulus-presentation and recording of the subjects‟ answers. A training session was given prior to scanning to familiarize subjects with the experimental procedure.

fMRI image acquisition

In Exp. 1, *f*MRI data were acquired on a 3T Trio whole-body scanner with eight-channel head coil (Siemens Medical System, Erlangen, Germany). Echo-planar images (EPIs) were obtained using a gradient-echo sequence with the following parameters: echo time TE = 30ms, repetition time TR =2000ms, flip angle = 90°, field of view FoV = 192 x 192 mm^2, slice thickness = 3 mm, inter-slice gap = 1.2 mm, in-plane resolution = 3 x 3 x 4.2 mm^3, Bandwidth = 2604 Hz/Px, Echo spacing = 0.45 ms. The FoV was tilted by 30° in a clockwise direction to encompass the whole brain with 32 interleaved transverse slices. Each of the 4 functional runs comprised 333 sequential volumes. A T1 weighted structural image was also obtained with the following parameters: TE = 5.57ms, TR = 2040ms, flip angle = 8°, FoV = 224 x 256 mm^2, slice thickness= 1 mm, in-plane resolution = 1x1x1 mm^3, SENSE factor = 2. Total scanning time was approximately 60 min. In Exp. 2, *f*MRI data were acquired with a 3T SIGNA whole-body scanner with eight-channel head coil (General Electrics,

Milwaukee, USA). Echo-planar images (EPIs) were obtained using a gradient-echo sequence with the following parameters: echo time TE = 30ms, repetition time TR = 2100ms, flip angle = 90°, field of view FoV = 192 x 192 mm^2, slice thickness = 3 mm, inter-slice gap = 0.5 mm, in-plane resolution = 2.5 x 2.5 x 2.5 mm^3, Bandwidth = 3906 Hz/Px, Echo spacing = 0.44ms. The FoV was tilted 30° in a clockwise direction to encompass the whole brain with 37 interleaved transverse slices. Each of the 5 functional runs comprised 310 sequential volumes. A T1 weighted structural image was obtained with the following parameters: TE = 3.2 ms, TR = 8200ms, flip angle = 12°, FoV = 256 x 256 mm^2, slice thickness = 1 mm, in-plane resolution = 1 x 1 x 1 mm^3, acceleration factor arc = 2. Total scanning time was approximately 60 min.

1.1.4 Statistical analysis

Data analysis was performed using SPM8 (Statistical Parametric Mapping software; The Wellcome Department of Imaging Neuroscience, London, UK; http://www.fil.ion.ucl.ac.uk) running in MATLAB R2009b (The Mathworks, Inc., Natick, MA). The first four EPI volumes of each functional run were discarded to allow for T1 equilibration effects. For each subject, all volumes were spatially realigned to the first volume of the first functional run and un-warped to correct for between-scan motion. The T1 weighted images were realigned to create a mean image and then segmented into gray, white and cerebrospinal fluid and spatially normalized to the Montreal Neurological Institute (MNI) template. Thereby the EPI volumes were realigned and, after normalization, were re-sampled in 2 x 2 x 2 mm^3 voxels using trilinear interpolation in space. All functional volumes were then spatially smoothed with a 6 mm full-width half-maximum isotropic Gaussian kernel for the group analysis. Data were analyzed using a random-effects model (Friston et al. 1999), implemented in a two-level procedure. In the first level, single-subject *f*MRI responses were modeled using a General Linear Model (GLM), for which a design-matrix included the onsets and durations of each event for each stimulus-type (Exp. 1: Arm, C; Exp. 2: Arm, A, CArm) and condition (same, different) for each functional run. In Exp. 1, eight regressors were modeled (Armsame, Armdiff, Armstill, Csame,

Cdiff, Cstill, CatchTrials and Response). In Exp. 2, eleven regressors were modeled (Armsame, Armdiff, Armstill, Asame, Adiff, Astill, CArmsame, CArmdiff, CArmstill, CatchTrials and Response). In both Exp. 1 and Exp. 2, all regressors, except for Response, included the two consecutive videos of each trial, which were modeled as one single epoch lasting 4.1 s. Responses were modeled as event-related. In the second level analysis (group-analysis), corresponding contrast images of the first level for each subject were entered in two flexible ANOVAs with sphericity-correction for repeated measures (Friston et al., 2002). The first model considered the pattern of activation of the 2 stimulus-types (Arm, C; Exp. 1) and the 3 stimulus-types (Arm, A, CArm; Exp. 2), pooling together the two conditions *same* and *different* minus each respective still image (control still image). This model was used for localization of regions of interest ROIs (ROIs, see next section). The second model was created considering the 2 stimulus-types (Arm, C; Exp. 1) and the 3 stimulus-types (Arm, A, CArm; Exp. 2) for each condition (*same* and *different*) separately minus each respective still image (Armstill, Cstill, Astill and CArmstill). This model was used for signal change extraction at the subject level, as specified in the ROI analysis below. Results were thresholded at $P<0.05$ FWE corrected at the cluster or voxel level as appropriate (cluster size estimated with a voxel-level threshold of P-uncorrected = 0.001). The location of foci of activation is presented in the stereotaxic space of the MNI coordinate system. Activations were also localized with reference to cytoarchitectonical probabilistic maps of the human brain, using the SPM-Anatomy toolbox v1.7 (Eickhoff et al., 2005).

Repetition-suppression and ROI analysis

The RS analysis (Grill-Spector et al., 1999; Hamilton and Grafton, 2009; Kourtzi et al., 2001; Lestou et al., 2008) was used to assess the neural response to observed velocity during observation of the reaching movements. Within the RS analysis, activations obtained when the subjects were presented with pairs of videos showing the same stimulus (condition *same*) were compared with those associated with observation of pairs of videos differing in one specific dimension (condition

different). In Exp. 1, differences for both the arm and the cylinder were analyzed with respect to movement velocity (low – V1; medium – V2; high – V3). In Exp. 2, for the arm and the arrow, differences were analyzed with respect to movement velocity as in Exp. 1; for the colored arm, differences were analyzed with respect to the arm color (red - C1, yellow - C2, blue - C3).

To test the RS effect of movement velocity within the cortical sites active during reaching observation, ROIs were defined on the basis of the functional maps obtained from the second-level group analysis (see statistical model 1 above). More specifically, ROIs were defined within the functional maps reflecting global activation within the parietal and frontal sites in response to at least one of the regressors of interest, namely: only the arm (-still) in Exp. 1 (since the cylinder produced no activation in this sites); the arm, the arrow, and the colored arm (-still) in Exp. 2, independently of conditions *same* and *different* ($P_{FWE\text{-}corr}$<.05 at the voxel level). In total, two ROIs were defined reflecting the cluster of activation in left dorsal premotor (PMd) and left superior parietal lobule (SPL), respectively.

The mean cluster values were calculated for each ROI and stimulus-type (Exp. 1: Arm, C; Exp. 2: Arm, A, CArm) separately for the two conditions (*same* and *different*) *vs.* control still images - see statistical model 2 above. Signal change for each subject was extracted using REX (http://web.mit.edu/swg/rex). One subject of Exp. 2 was excluded from the analysis as an extreme case.

1.2 Results

1.2.1 Experiment 1

Overall effect of reaching observation

The brain activations obtained by comparing arm reaching (independently of the conditions *same* or *different*) *vs.* the control still images of the same arm are shown in Figure 4 A. Activations were found

in occipital lobe, including V6, bilateral human putative MT/V5 complex, left intraparietal sulcus, straddling the inferior and superior banks, left ventral and dorsal premotor cortex and deep structures, including right insula (see Appendix Table 1A-S1 for coordinates and statistical values). The contrast between observation of the rolling cylinder and observation of the control still images of the same cylinder, independently of conditions (*same* or *different)*, produced activations in bilateral human putative MT/V5 complex (Figure 4 B, Appendix Table 1B-S1).

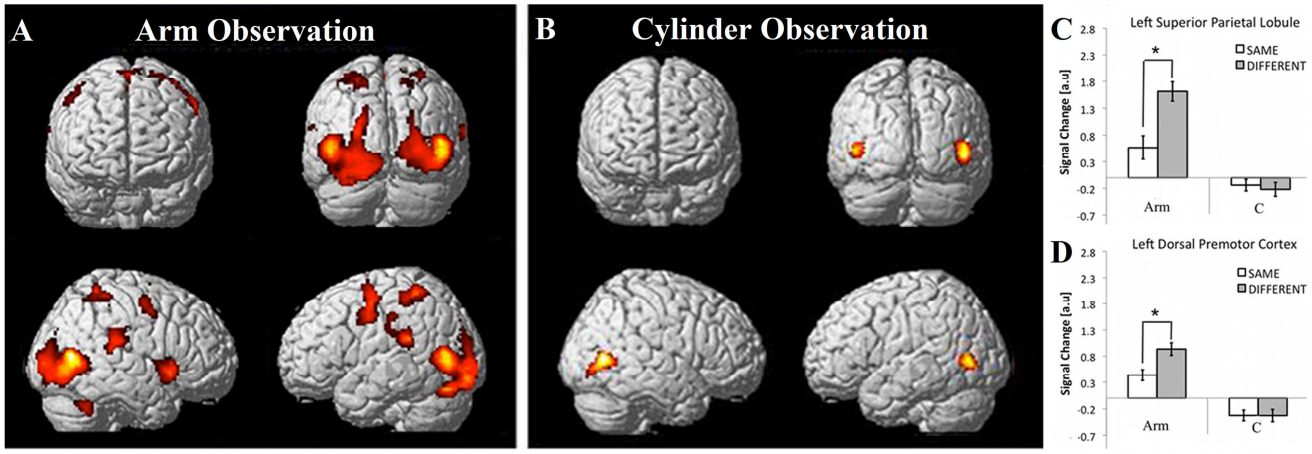

Figure 4: Cerebral activities in Exp. 1 during the observation of the arm reaching movement (A) and of the rolling cylinder (B), pooling together the conditions *same* and *different, vs.* control still images (still images of each respective stimulus-type). The statistical parametric maps (group average) are mapped onto a standard MNI ($P_{FWE-corr} < .05$). The graphs display the mean signal change in arbitrary units (a.u.) in the conditions *same* (white bars) and *different* (gray bars) for each stimulus-type (Arm – Arm, cylinder – C) within (C) the dorsal premotor cortex (PMd; maxima: -22 -8 60) and (D) superior parietal lobule (PLd; maxima -28 -46 56). The error bars represent the standard error of the mean. Asterisk (*) indicates significant differences between the conditions *different* - *same* (p<.025). [Modified from Di Cesare et al. (2013), with kind permission from Elsevier.]

Repetition-suppression effect

Within the RS analysis, were compared activations observed when subjects were presented with pairs of videos showing the arm or the cylinder moving at the same velocity (condition *same*) or at different velocities (condition *different*). The RS analysis was performed for 2 ROIs: one in left dorsal premotor cortex (PMd) and one in left superior parietal lobule (SPL), i.e. in the parietal and frontal regions activated during observation of the arm reaching movement. The difference between the conditions *different* and *same* (RS effect) for the arm and the cylinder were tested in a 2 x 2 repeated measures GLM analysis, with 2 levels of stimulus-type (Arm, C) and 2 levels of stimulus- condition (*same*, *different*) independently for each PMd and SPL ROIs. With respect to the activations observed

for the PMd ROI, results revealed a main effect of stimulus-type (Arm>C; $F_{1,12}$=12.8, p=.004, partial-η^2=.52, δ=.91) and a significant interaction stimulus-type x condition ($F_{1,12}$=14.6, p=.002, partial-η^2=.55, δ=.94). Similarly, results for the SPL ROI revealed a main effect of stimulus type (Arm>C; $F_{1,12}$=9.33, p=.01, partial-η^2=.44, δ=.8) and a significant interaction stimulus-type x condition ($F_{1,12}$=5.3, p=.04, partial-η^2=.31, δ=.56). As shown in Figure 4 CD, independent post-hoc analyses for PMd and SPL revealed a significant difference between conditions *same* and *different* (Diff>Same) for the arm only (PMd: $F_{1,12}$=4.7, p<.05, partial-η^2=.28, δ=.52; SPL: $F_{1,12}$= 5.4, p<.05, partial-η^2=.31, δ=.57).

1.2.2 Experiment 2

In Exp. 2, subjects observed two types of moving stimuli: a biological one, i.e. an arm, and a non-biological one, i.e. an arrow. Both stimuli moved with three different velocities (see Methods section for details). A third stimulus, i.e. a reaching arm whose color – instead of velocity – changed in the conditions *different*, was also introduced to rule out possible attention-related effects on the observed activations (see Bartels et al., 2008).

Overall effect of reaching observation

Arm vs. control still image

The brain activations obtained by comparing observation of the arm reaching movement, pooling together the conditions *same* and *different*, *vs.* the control still images of the same arm are shown in Figure 5 A. Activations were observed in left superior occipital lobe, including area V6, bilateral human putative MT/V5 complex, left superior parietal lobule (SPL) extending into the intraparietal sulcus and left dorsal premotor cortex (PMd), right prefrontal cortex and bilateral insula (see Appendix Table 2A-S1, Arm, for coordinates and statistical values).

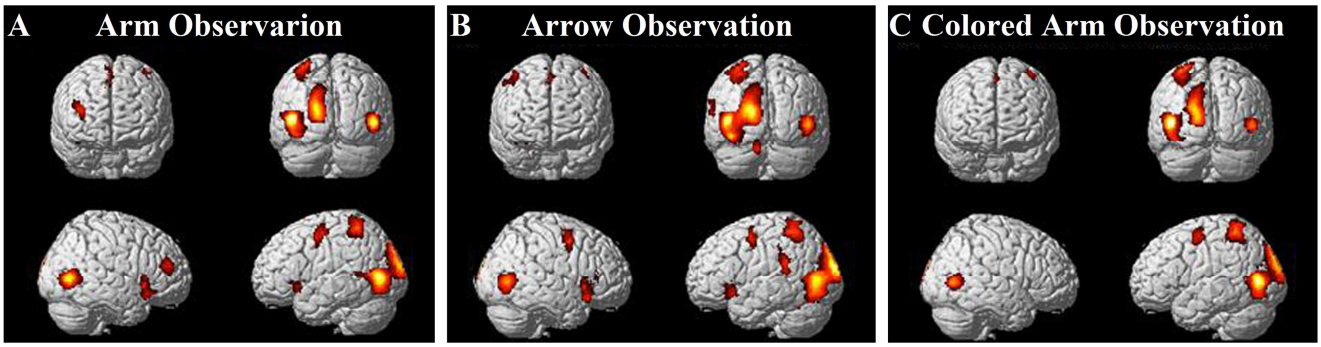

Figure 5: Cerebral activities in Exp. 2 during observation of the arm (A), the arrow (B) and the colored arm (C) reaching movements, pooling together the conditions *same* and *different*, *vs.* control still image (still images of each respective stimulus-type). The statistical parametric maps (group average) are mapped onto a standard MNI ($P_{FWE-corr} \leq .05$). [Di Cesare et al. (2013), with kind permission from Elsevier.]

Arrow vs. control still image

Observation of the non-biological object (arrow - A) performing a reaching movement towards a point with *biological motion*, independently of conditions *same* or *different*, produced signal increase, with respect to the control still images of the same arrow, in areas encoding reaching movement. As shown in **Figure 5** B, the main areas activated involve left superior occipital lobe, including area V6, bilateral human putative MT/V5 complex, an area straddling the superior temporal gyrus and inferior parietal lobule (area TPJ), left superior parietal lobule (SPL) extending into intraparietal sulcus, bilateral dorsal premotor cortex (PMd) and bilateral insula (see Appendix Table 2A-S1, Arrow, for coordinates and statistical values). The interaction between observation of the arm and the arrow reaching movements, relative to their respective static conditions, showed no activation for the arm *vs.* the arrow as well as for the opposite contrast.

Colored Arm vs. control still image

As shown in Figure 5 C, observation of reaching movement of the colored arm (independently of the conditions *same* or *different* color) revealed enhanced activations, with respect to the control still images of the same colored arm, in left superior occipital lobe including area V6, bilateral human putative MT/V5 complex, left superior parietal lobule and left dorsal premotor cortex (see Appendix Table 2A-S1, CArm, for coordinates and statistical values).

Repetition-suppression effect

For the RS analysis, was first carried out a global activation analysis across the three stimulus-types (arm, arrow, colored arm), independently of the conditions *same* and *different*, *vs.* each respective control still images ($P_{FWE\text{-}COR\text{-}VXL}<.05$). As shown in Figure 6 A, global activations were observed in left superior occipital lobe including area V6, human putative MT/V5 complex, superior parietal lobule (mostly on the left side) and bilateral dorsal premotor cortex (see Appendix Table 2B-S1 for coordinates and statistical values). Given lack of activation of right parietal and frontal sites for the arm and colored arm and of right parietal cortex for the arrow reaching movements (with respect to each respective control still images – see analyses above), two ROIs were defined (see Methods) centering on the activations observed in left premotor and parietal cortices. The RS effect for velocity and color were then tested in these ROIs. Within the RS analysis, were compared activations observed when participants were presented with pairs of videos showing the same stimulus (condition *same*) and pairs of videos differing in one specific dimension (condition *different*).

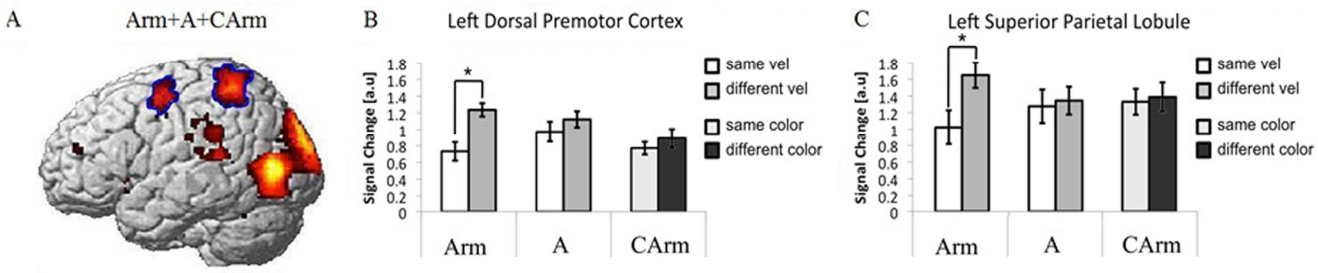

Figure 6: Anatomical locations (A) projected on a standard MNI brain template of the region of interest (ROIs) built within the left dorsal premotor (PMd; maxima: -34 -2 54) and left superior parietal lobule (SPL; -32 -50 68) on the basis of the functional maps obtained from the global analysis among the three stimulus-types (Arm, A, CArm) in Exp. 2. The graphs display signal change produced by the conditions *same* and *different* for each stimulus-type (Arm, arrow – A, colored arm – CArm) within each ROI (B, PMd; C, SPL). The error bars represent the standard error of the mean. Asterisk (*) indicates significant differences *different* - *same* Bonferroni corrected (p≤.017). [Modified from Di Cesare et al. (2013), with kind permission from Elsevier.]

For the arm and the arrow, differences were analyzed with respect to movement velocity (low – V1; medium – V2; high – V3); for the colored arm differences were analyzed with respect to the arm color (red, yellow, blue). Comparisons between conditions *different* and *same* (RS effect) among the 3 stimulus-types (Arm, A, CArm) were tested in 3 x 2 repeated measures GLM analysis, with 3

levels of stimulus- type and 2 levels of stimulus-condition (*same, different*) independently for each ROI. Interaction effects were tested post-hoc and adjusting the p-values according to the Bonferroni correction for multiple comparisons (p=.05/3 = .017). Descriptive analyses and the statistical values relative to the direct comparison between conditions *same* and *different* for each stimulus-type are summarized in Appendix Table 3-S1. As shown in **Figure 6** BC, results for both PMd and SPL showed a main effect of stimulus- condition (D>S; PMd: $F_{1,14}$=15.73, p<0.05, partial-η^2=.53, δ=.96; SPL: $F_{1,14}$=7.96, p<.05, partial-η^2=.36, δ=.75) as well as a significant interaction for stimulus-type x stimulus-condition (PMd: $F_{2,28}$=4.34, p<.05, partial-η^2=.24, δ=.49; SPL: $F_{2,28}$=3.63, p<.05, partial-η^2=.21, δ=.62). For both PMd and SPL, post hoc analysis revealed a significant difference between conditions *same* and *different* for arm reaching observation only (PMd: $F_{1,14}$=30.5, p<.0001, partial-η^2=.69, δ=.99; SPL: $F_{1,14}$=10.9, p=.005, partial-η^2=.44, δ=.87). No differences were observed foreither the arrow or the colored arm (p>.05; see Appendix Table 2-S1 for descriptive statistics).

1.3 Discussion

The aim of the present study was to delineate the cortical regions that are specifically involved in processing the observed of reaching movements and to investigate their sensitivity to biological motion. Additionally, using the RS technique (RS; Grill-Spector et al., 1999; Hamilton and Grafton, 2009; Kourtzi et al., 2005; Lestou et al., 2008) was investigated the responsiveness of these regions to the observation of reaching movements performed with different velocities. Two experiments were carried out. In Exp. 1, video-clips showed either an arm (biological effector) or a cylinder (non-biological object) reaching toward the same target with biological and non-biological motion, respectively. In Exp. 2, the video-clips showed an arm (biological effector) or an arrow (non-biological object) reaching toward a target following the same biological motion. The results of Exp. 1 showed activations specific to the arm reaching movement *vs.* still images of the same arm in visual occipito-temporal areas, including MT/V5 and V6, in intraparietal sulcus straddling the inferior and

superior banks and ventral and dorsal premotor cortex. All activations were bilateral, although stronger in the left hemisphere. The analysis contrasting the rolling movement of the cylinder *vs.* still images of the same cylinder showed enhanced activations in bilateral MT/V5 complex. Lack of activation of the parietal and frontal sites in response to observation of the rolling cylinder confirms previous studies (e.g., Casile et al. 2009; Dayan et al. 2007) showing that these areas do not respond to non-biological movements. The results of Exp. 2, where were compared separately activations observed for the arm and the arrow reaching movements *vs.* their respective still images, revealed, for both stimulus-types, activations of visual and temporal areas, including MT/V5 and V6, left superior parietal lobule and left dorsal premotor cortex. Activation of the parietal and frontal areas during observation of reaching movements is consistent with previous findings showing their involvement in both reaching execution and observation (Filimon et al., 2007). Both studies indicate that activations associated with reaching are located more dorsally than those described for grasping. A large number of investigations, in fact, show that grasping is encoded in the human AIP and the adjacent inferior parietal lobule, as well as in the frontal lobe, mostly in the ventral premotor cortex extending into the posterior part of the inferior frontal gryrus (Buccino et al., 2001; Culham, 2004; Grafton et al., 1996b; Grezes et al, 2003; Rizzolatti et al., 1996).

Comparison of the parietal and premotor activations in response to the arm reaching movement between Exp. 1 and Exp. 2, revealed that the activations in Exp. 1 extended further ventrally than those observed in Exp. 2. A possible explanation for this difference might be the different targets used in the two experiments. Although the videos in Exp. 1 always presented a reaching arm purely touching the object, because the reaching-target was a graspable 3-D object this could have triggered in the observers a motor program for grasping (Gibson, 1986; Grafton et al., 1996b; Grézes et al., 2003; Rizzolatti et al., 1996). In contrast, in Exp. 2 the target-object was a 2-D cross that did not afford any grasping action. This marker primed a grasp-independent reaching movement eliciting activation selectively in the dorsal parietal and superior frontal sites. A significant new finding of the present study is the overlap between the motor activations elicited by the observation of

the arm reaching movements and those elicited by the observation of the reaching arrow. These regions were not activated during the observation of the non-biological movement (rolling cylinder), suggesting that the dorsal parietal and superior frontal sites respond to *biological motion* only, independently of the shape of the moving stimulus (biological or non- biological). In order to investigate sensitivity of the parietal and frontal sites to movement *velocity* using the *f*MRI RS technique, two ROIs were defined for use in both Exp. 1 and Exp. 2, one in left dorsal premotor cortex (PMd) and one in left superior parietal lobule (SPL), that were strongly activated during observation of the biological movements. The RS effect within these regions was tested by contrasting the conditions in which video-pairs presented consecutive stimuli moving with different velocities (condition *different*) with those in which velocity remained unchanged between videos (condition *same*). The RS results revealed, in both premotor and parietal ROIs, a suppression effect only for the arm reaching velocity and not for the arrow, showing that activation of the dorsal parietal and frontal sites is modulated by *velocity* only during observation of movements performed by a biological *effector* (i.e., the arm). In sum, we found that the dorsal parietal and frontal sites specifically encode biological motion (Exp.1) and generalize across different shapes (Exp. 2), whereas these sites only encode velocity when a biological effector is involved (Exp. 2). Some authors have appropriately recommended that caution should be exercised in the interpretation of RS effects on brain activations (see Tolias et al., 2005; Bartels et al., 2008). Nonetheless, the results of the present study show that *f*MRI is capable to highlight functionally relevant processes in response to specific stimulus properties (Bartels et al., 2008). In particular, the RS results of this study revealed activity enhancement in dorsal premotor and superior parietal cortex in response to velocity only for the biological effector, namely the arm, and not for the arrow that underwent the same RS procedure as the arm. Additionally, concerns with respect to the RS technique have been put forward suggesting that attention-related factors may affect brain activation when viewing two consecutive stimuli that differ from one another (Bartels et al., 2008). To control for attention-related confounds, were introduced, alongside the arm and the arrow stimuli, videos showing a reaching colored arm

changing color, instead of velocity, in the condition *different*. Lack of RS effect in the parietal and frontal sites for the colored arm allows us to further rule out the possibility that attention-related factors affected the RS results observed for the arm movement velocity. Although it is not possible to specify the precise neural mechanisms involved in the activation pattern observed in this study, some hypotheses can be advanced on the basis of previous *f*MRI studies as well as from neuroanatomical experiments with non-human primates. In monkeys, the accepted view is that visual information of the dorsal visual stream terminates in IPL and SPL. The classical view on the organization of the dorsal stream was that its nodal area is MT/V5. This area receives direct input from the striate visual area V1 and from other extrastriate visual areas. *f*MRI experiments in humans confirmed the role of MT/V5 as a fundamental node in movement processing (e.g., Sunaert et al., 1999; Zeki et al., 1991). It has been subsequently discovered that visual information travelling the dorsal stream has another nodal area, i.e. area PO (Colby et al., 1988), that has been subdivided into two different areas: the occipital area V6 and the parietal area V6A. In the monkey, V6 is located within the posterior occipital sulcus (POS) and borders with V6A that occupies the dorsal sector of the same bank. While V6 is a purely visual area, receiving input from the striate and extrastriate visual areas, V6A belongs to the parietal lobe and is endowed with more complex properties. In humans, recent *f*MRI studies have shown that the putative V6 complex is located in the occipito-parietal junction (OPJ) (Pitzalis et al., 2009) and it is likely that this complex contains visual and somatic neurons involved in the control of reach-to-grasp movements. One possible explanation for SPL response to movement velocity of the biological effector rests on recent *f*MRI findings with humans showing MT preferred activation for biological movements (hand action) than non-biological movements (Jastorff et al., 2010). Since MT/V5 is connected to area V6, it is possible to hypothesize that visual information about movement of the biological shape reaches SPL through this pathway (see also Galletti et al. 1996, 1999, 2001). Neuroanatomical data in the monkey further suggest that the dorsal sector of V6A (V6Ad; Luppino et al., 2005; Gamberini et al., 2011) receives information also from the inferior parietal lobule (IPL) and, more specifically, from area PG, which, in turn, receives input from

the STS region (Rozzi et al. 2005, 2008) in response to complex biological movements (Grossman and Blake, 2001; Perrett et al., 1999; Thompson et al., 2005). It is therefore possible that the activation of SPL to movement velocity of the biological shape could be also due to its connections with V6 complex and related areas (STS, PG). As far as the activation of dorsal premotor cortex is concerned, the neural substrate for its activation should include again the V6 complex that sends input directly to dorsal premotor cortex, as well as to other connected areas. In the monkey, connections have been suggested between V6and F2 (Gamberini et al., 2009), and with MIP as well as between SPL (PEc) and F2 (Matelli and Luppino, 2001).

In conclusion, in line with the more general mirror mechanism hypothesis, the results obtained in the present study suggest that joint activation of SPL and PMd could represent the neural substrate underpinning the processing of reaching movement performed by others.

*Second Study: The neural correlates of "vitality form" recognition: an fMRI study.

2.1 Materials and Methods

2.1.1 Participants

Nineteen healthy right-handed volunteers (10 females [mean age = 24.1, s.d. = 2, range = 21-28] and 9 males [mean age = 24.4, s.d. = 2.18, range = 22-29]) participated in this study. All participants had normal or corrected-to-normal visual acuity. None reported a history of psychiatric or neurological disorders, or current use of any psychoactive medications. They gave their written informed consent to the experimental procedure, which was approved by the Local Ethics Committee (Parma).

2.1.2 Stimuli

Video-clips were presented to the participants showing two actors (a male and a female) performing a series of different actions, once by the male actor and once by the female. Half of the videos represented actions where the interaction between the two actors was not mediated by an object (for example, executing a stop gesture, Figure 7 A); half of the videos represented actions where the interaction between the two actors occurred using an object (for example, moving a bottle towards the other actor, Figure 7 B). Each actor executed 8 different actions (with object: move a bottle towards the other actor, give a packet of crackers, pass a ball, hand a mug – see Appendix Figure 1-S2; without object: caress, clap hands, stroke the other actor's backhand, stop gesture – see Appendix Figure 2-S2). In all videos, the actors started from a rest position and returned, after action execution, to the same position (Figure 7 A1, B1). All actions were performed with two vitality forms: energetic and gentle. After video-recording, using the software Avimeca v.2.3 (see methods for a detailed description of the calculation) we assessed the kinematic and dynamic profiles associated with each vitality form in terms of action velocity, duration, trajectory and, for the actions with object only, the

*This is a pre-copyedited, author-produced PDF of an article accepted for publication in SCAN following peer review. The version of record is available online at: http://scan.oxfordjournals.org/content/9/7/951.long.

kinetic and potential energy of the object, which give an estimates of the power developed to perform the action. An example of the graphic depiction of each parameter is in Figure 9 A, graphic representation of the parameters for all actions is in Appendix Figures 1-S2, and 2-S2.

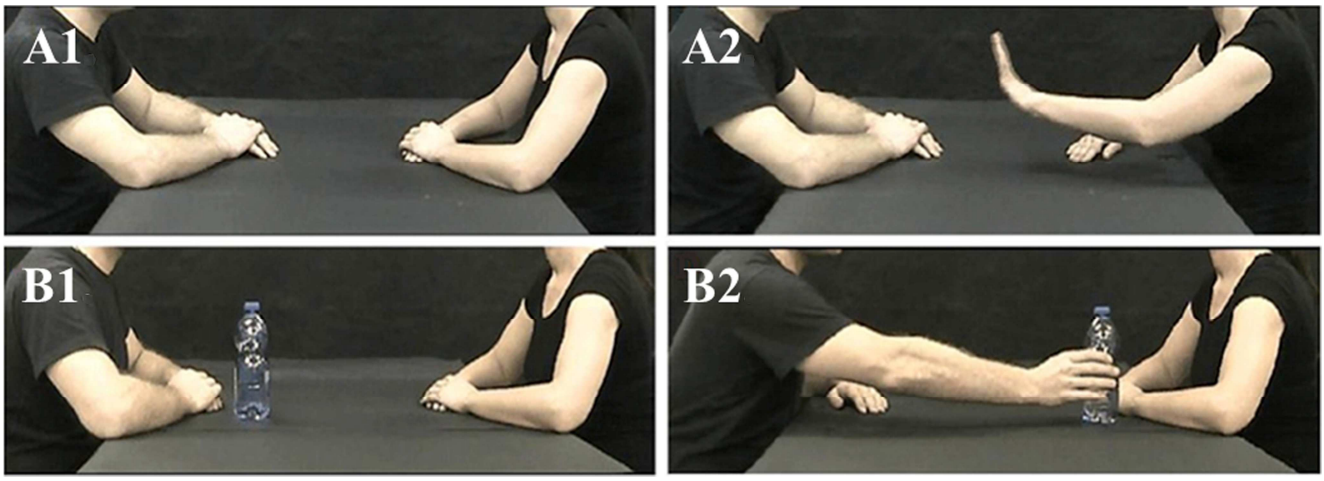

Figure 7: An example of video-clips as viewed by the participants of this study. Frame representing an action without object in the start position (A1); frame representing the actress executing a stop gesture (A2); frame representing an action with object in the start position (B1); frame representing an action with object in the end position (B2, passing a bottle). [Di Cesare et al. (2013), with kind permission from Oxford University Press.]

Using VirtualDubMod software v1.5, the original videos were cropped to remove the head area. This was done to avoid the vision of the face area that represents a highly attractive social cue, which could have deviated the viewer's attention from the performed action on which the participants were required to give judgments. Additionally, to focus participants' attention on the performed actions, the videos were recorded in a dark scenario and the actors wore black shirts to emphasize the forelimb area. Finally, each recorded video was flipped to balance the actors' placement within the scene across each action type. Each video lasted 3s. A total of 64 stimuli were produced (8 actions x 2 vitality forms x 2 actors x 2 actors' placements in the videos).

Kinematics and dynamics profiles of the actions performed by the actors

The movement characteristics of the actors during action performance were studied using the 2D point kinematics method. After video recording, using the software Avimeca v2.3, was marked a specific point of the hand of the actor for all video clips (point 1, 8). For the actions that were performed

without an object such us, for example, stroking the back hand of the other actor, the origin point of the X/Y axes was fixed in the start position of the actor and marked each position in the space every 40ms (Figure 8 A). The tracking terminated when the actor reached the other actor (point 3, Figure 8 A). For the actions performed using an object, the origin of the X/Y axes was fixed in the position of the object at rest (just before lifting the object) and marked each occupied position in space every 40ms (Figure 8 B).

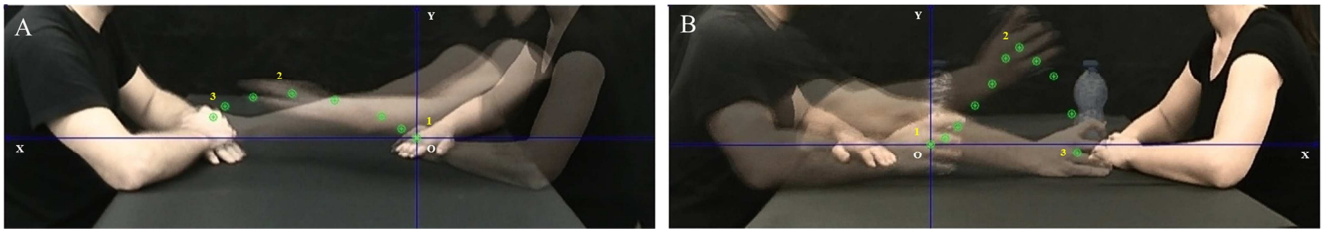

Figure 8: Example of hand tracking during actions performed without an object by the female actress (A) and with an object by the male actor (B). The green dots indicate the X and Y positions occupied by the hand in space every 40ms. For the actions performed without object, the origin of the axes is fixed in the start position on the actor's hand (A). For the actions performed with an object the origin of the axes is fixed in the position of the object at rest (just before lifting the object) (B). The numbers show the start (1), intermediate (2), and final (3) position occupied by the hand in space during the action. [Di Cesare et al. (2013), with kind permission from Oxford University Press.]

The tracking of the action terminated when the object was placed at the end position (point 3, Figure 7B). Using Regressi software (v2.9) the velocity and trajectory curves were calculated for all actions performed with two different vitalities (gentle and energetic). The module of velocity was calculated using both X and Y values for each point during the execution of gentle and energetic actions (Appendix Figures 1A-S2, 3A-S2). This kinematic analysis reveals that the velocity profiles change as a function of vitality form. More specifically, during the execution of an energetic action, such us passing a bottle (Figure 9 A), the actor performs the action with a higher velocity than when performing the same action in a gentle form. This data further show that, when performing the same action with different vitality forms (gentle and energetic), besides the velocity, also the action trajectories differ (Appendix Figures 1B-S2, 3B-S2). Only for actions performed with an object, we estimated the kinetic energy ($E_k = ½\, mv^2$), the potential energy ($E_u = mgh$) and the power ($P = d(E_k + E_u)/dt$) required to perform the action on the object. To this purpose, the mass of each object (bottle

0.250 Kg; cup 0.200 Kg; ball 0.100 Kg; cracker 0.025 Kg) was calculated. The potential and kinetic energy curves related to female bottle movement is shown in Figure 9 D, while movements performed with other objects are shown in Appendix Figures 1-S2 and 2-S2. Potential and kinetic energy was normalized with respect to the mass (Nm/Kg) in order to compare the curves of the different objects. The curves indicate that energetic and gentle actions performed with objects are characterized by a different peak values for both energy profiles (potential and kinetic). Finally, we calculated the power ($P = d(E_k + E_u)/dt$) used by the actor to move the bottle in association with specific velocities and trajectories (Figure 9 D). Also in this case we normalized the power with respect to the mass (J/Kg) to compare the curves of the different objects.

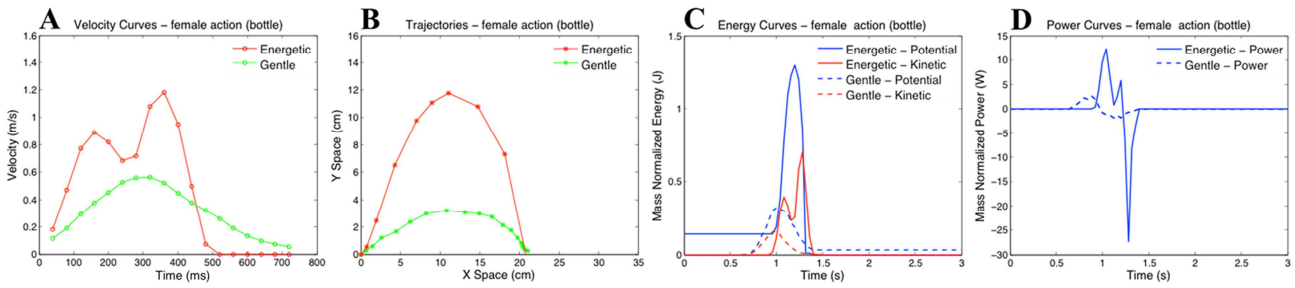

Figure 9: Kinematic and dynamic profiles associated with the one of the action (passing a bottle) performed by the female actress with the two vitality forms (gentle, energetic). (A) Velocity profiles (gentle, green line; energetic, red line); (B) Trajectories; (C) Potential energy (blue line), Kinetic energy (red line); (D) Power required to perform a vitality form (energetic, blue solid line; gentle, blue dashed line). [Di Cesare et al. (2013), with kind permission from Oxford University Press.]

These data indicate that to perform the action in an energetic way the actor used a higher power than when he/she performed the same action in a gentle way. In sum, using kinematics and energy information, we delineated 4 important components of vitality form: velocity, trajectory, energy and power.

2.1.3 Paradigm and Task

The stimuli were presented to the participants in pairs of consecutive videos, where the observed action (*what*) and vitality (*how*) could be the same or change between video-pairs. To counterbalance all what-how possibilities, 4 different combinations of action-vitality were created: 1. same action –

same vitality (SASV); 2. same action – different vitality (SADV); 3. different action – same vitality (DASV); 4. different action – different vitality (DADV). All video combinations were presented in two tasks. The *what* task required the participants to pay attention to the type of action observed in the two consecutive videos and to decide whether the represented action was the same or different regardless of vitality form. The *how* task required the participants to pay attention to the vitality form and to decide whether the represented vitality was the same or different between the two consecutive videos regardless of the type of action performed. Each video combination was presented 32 times within each task. The participants lay in the scanner in a dimly lit environment. The stimuli were viewed via digital visors (VisuaSTIM) with a 500,000 px x 0.25 square inch resolution and horizontal eye field of 30°. The digital transmission of the signal to the scanner was via optic fiber. The software E-Prime 2 Professional (Psychology Software Tools, Inc., Pittsburgh, USA, http://www.pstnet.com) was used both for stimuli presentation and the recording of participants' answers. In each scanning session (functional run), *what* task started with the instruction "Pay attention to WHAT". The instruction was written in a blue color and instructed the participants to focus on the type of action. The *how* task started with the instruction "Pay attention to HOW". The instruction was written in green color and instructed the participants to focus on how the action was performed (the action vitality form). Each trial started with a colored fixation point (blue for *what* task and green for *how* task) positioned at the centre of a black screen for 500ms. The color of the fixation point corresponded to the color of the instructions provided (see above) to help the participants remembering the current task. The fixation point was followed by the presentation of pairs of video-clips. The first video-clip was presented for 3s followed by a 100ms fixed interval and by the second video-clip lasting 3s. The second video was followed by a jittered interval ranging between 2.5-4s (fixation cross), in which, in about 10% of cases, the participants had to provide an explicit response to the stimuli (catch trials). More specifically, the participants had to indicate, on a response box placed inside the scanner, whether the two consecutive videos were the same or different according to the task type. One sixth of the experimental trials was characterized by three consecutive videos representing a still image of the

actors during rest position before action performance (static control). All video-pairs were shown in 4 functional runs. Within each run, the two tasks (*what* and *how)* were presented, each, in 4 independent mini-blocks in a sequential order. Within each mini-block/task, the video-pairs were presented 8 times (4 with object, 4 without object) in a randomized order. The stimuli were randomized within each run and balanced across runs so to make an equal number of trial types. In total, the participants viewed 256 experimental video-pairs. Each functional run lasted about 13min. The whole study lasted approximately 60min. Before the scanning session, the participants underwent a training session with different stimuli than those used during scanning to familiarize with the experimental procedure.

fMRI data acquisition

Anatomical T1-weighted and functional T2*-weighted MR images were acquired with a 3 Tesla General Electrics scanner equipped with an 8-channel receiver head-coil. Functional images were acquired using a T2*-weighted gradient-echo, echo-planar (EPI) pulse sequence (acceleration factor asset 2, 37 interleaved transverse slices covering the whole brain, TR = 2100ms, TE = 30ms., flip-angle = 90 degrees, FOV = 205 x 205 mm^2, inter-slice gap = 0.5 mm, slice thickness = 3 mm, in-plane resolution 2.5 x 2.5 x 2.5 mm^3). Each scanning sequence comprised 366 sequential volumes. Immediately after the functional scanning a high-resolution inversion recovery prepared T1-weighted anatomical scan (acceleration factor arc 2, 156 sagittal slices, matrix 256x256, isotropic resolution 1x1x1 mm^3, TI=450ms, TR =8100ms, TE = 3.2ms, flip angle 12°) was acquired for each participants.

2.1.4 Statistical analysis

Data analysis was performed with SPM8 (Statistical Parametric Mapping software; The Wellcome Department of Imaging Neuroscience, London, UK; http://www.fil.ion.ucl.ac.uk) running on MATLAB R2009b (The Mathworks, Inc., Natick, MA). The first four EPI volumes of each functional run were discarded to allow for T1 equilibration effects. For each subject, all volumes were spatially realigned to the first volume of the first functional run and un-warped to correct for between-scan motion. The T1 weighted image was segmented into gray, white and cerebrospinal fluid and spatially

normalized to the Montreal Neurological Institute (MNI) space. The spatial transformation derived from this segmentation was then applied to the realigned EPIs for normalization and re-sampled in $2\times2\times2$ mm^3 voxels using trilinear interpolation in space. All functional volumes were then spatially smoothed with a 6 mm full-width half-maximum isotropic Gaussian kernel for the group analysis. Data were analysed using a random-effects model (Friston et al., 1999), implemented in a two-level procedure. In the first level, single-subject *f*MRI responses were entered in three independent General Linear Models (GLM) by design-matrixes modelling the onsets and durations of each trial for each functional run according to specific experimental demands. In particular, the first model ("task-related" model) was created to assess and compare the global activation patterns evoked by the tasks *what* and *how* modelling, in two separate regressors, all what-how combinations (independently for *what* and *how tasks).* The second ("vitality form") and third ("action-type") models (of the first level) were created purposely for the ROI analyses testing for possible interactions between stimulus-driven and task-related effects on observed activations during the *how* task. More specifically, in the second model, we regressed the experimental trials as a function of vitality form (gentle *vs*. energetic) entering in two main regressors the what-how pair-combinations having the same vitality, gentle or energetic, for each task. The what-how combinations having different vitalities (SADV, DADV) were modelled separately for the two tasks *what* and *how*. In the third model, we regressed the experimental trials as a function of action-type (with object *vs*. without object). Here, we modelled the actions carried out with and without object in two separate regressors for each task (*how* and *what).* In all three first level models, 3 additional regressors were entered, modelling the static control images, the instructions and the participants' responses. All trials representing the video-pairs were modelled as one single epoch lasting 6.1s. The static controls, instructions and responses were modelled as events having duration 0s.

In the second level analysis (group-analysis), corresponding contrast images from the "task-related" model of the first level were entered for each participant into two independent flexible ANOVAs with sphericity-correction for repeated measures (Friston et al., 2002). In the first model, we

compared the pattern of activations within and between tasks (*what* and *how*) *versus* implicit baseline (fixation cross). In the second model, we compared the pattern of activations for each task (*what* and *how*) *versus* explicit baseline (static controls) (P_{FWE} <0.05 corrected at the cluster or voxel level, cluster size estimated with a voxel-level threshold of *P*-uncorrected = 0.001). To test possible stimulus-driven effects on specific activations observed in the *how* task, regions of interest (ROIs) were created on the basis of the functional maps obtained from the group analysis directly comparing *how* and *what* tasks (effect of vitality form). Accordingly, a ROI was defined within right dorso-central insula, centering the sphere (radium 5mm) around the maximum x=34, y=12, z=12 from the contrast "*how vs. what*" using MarsBaR region of interest toolbox for SPM (release 0.42). Mean cluster values associated with each vitality form (gentle and energetic) and action-type (with object and without object) were then calculated for each subject on the basis of contrast images from the "vitality-form" and "action-type" models of the first level (see above). Signal change for each subject was extracted using REX (http://web.mit.edu/swg/rex). For all the analyses, the location of the activation foci was determined in the stereotaxic space of MNI coordinates system. Those cerebral regions for which maps are provided were also localized with reference to cytoarchitectonical probabilistic maps of the human brain, using the SPM-Anatomy toolbox v1.7 (Eickhoff et al, 2005).

Testing for task-complexity: Behavioral analysis

Our contrast of interest, *how vs. what*, although producing activations specifically related to vitality forms, could have also reflected some effects associated with task demand. To test this possibility, we carried out a further analysis, based on the responses given by the participants during the scanning sessions when presented with the catch trials, i.e., those trials in which the participants were required to give an explicit response to two consecutive videos presented in a trial, indicating if they were the same or different in terms of vitality form (*how* task) or action type (*what* task; see Methods above). Sixteen responses were recorded for each task for each participant. The dependent variable was the percent of correct responses (‘‘hits’’). Depending on the type of data, both nonparametric (Hollander

and Wolfe, 1999; Siegel and Castellan, 1988), and parametric statistical procedures were applied. The data were obtained for 16 participants. Three participants were excluded from analyses because of technical problems reported during response recording in at least one functional run.

2.2 Results

Overall effect of "what" and "how" tasks

The observation of all video-clips, pooling together the activations obtained during *what* and *how* tasks, *versus* implicit baseline (fixation cross) showed signal increase in visual occipito-temporal areas, hippocampus, posterior parietal lobe, SMA, inferior frontal gyrus and cerebellum bilaterally. Additional activations were observed in the left hemisphere in the ventral and dorsal premotor cortex and in the insula. Analyses carried-out within each task independently *versus* implicit baseline revealed for both *what* and *how* tasks a similar activation pattern (Figure 10 AB). However, the activations observed for *what* task (Figure 10 A) were more extended compared to those observed for *how* task (Figure 10 B), particularly in the frontal areas (see Appendix Table 1AB-S2 for coordinates and statistical values).

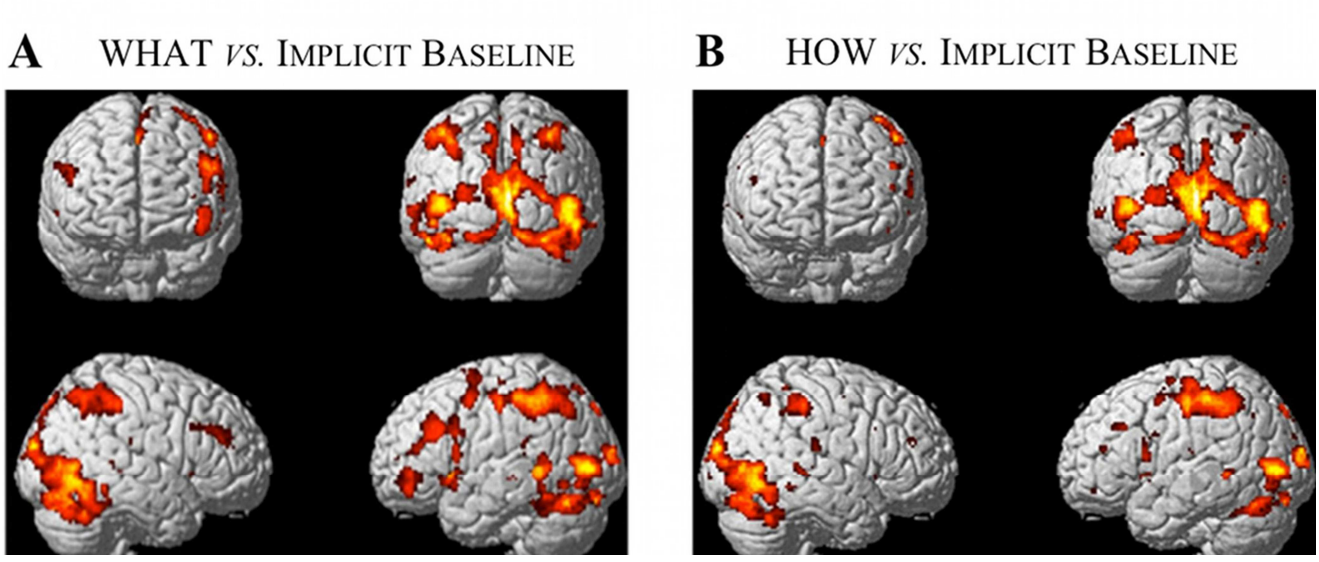

Figure 10: Signal change during A. the task what and B. the task how vs. implicit baseline (fixation cross). The activations (PFWE<.05 at vxl level) are rendered into a standard MNI brain template. [Di Cesare et al. (2013), with kind permission from Oxford University Press.]

A similar activation pattern was obtained when subtracting static controls from observation of the video-clips showing actions. As expected, there was a clear decrease in the activation of occipito-temporal visual areas, with the exception of those specifically tuned for movement as area MT. With respect to the analysis *vs.* implicit baseline, an additional activation was found in the inferior parietal lobe extending to superior temporal gyrus. This activation was due to a reduced BOLD signal (with respect to implicit baseline) when observing the static controls. Analyses carried-out within each task independently *versus* static controls revealed a large overlap between activations during *what* and *how* tasks. As in the analysis *vs.* implicit baseline, the activations were more widespread during *what* task than during *how* task.

Contrast between what and how tasks

As shown in Figure 11 A, the direct contrast between *what vs. how* tasks produced stronger activations for *what* task in posterior parietal lobe and premotor cortex extending rostrally to include the caudal part of inferior frontal gyrus, bilaterally. Additional activations were observed in the left hemisphere in the posterior part of inferior temporal gyrus and in the anterior part of inferior frontal gyrus (see also in Appendix Table 2A-S2 for coordinates and statistical values). The opposite contrast (*how vs. what*), revealed a specific activation for *how* task in the right dorso-central insula (Figure 11 BC; see in Appendix Table 2B-S2 for coordinates and statistical values).

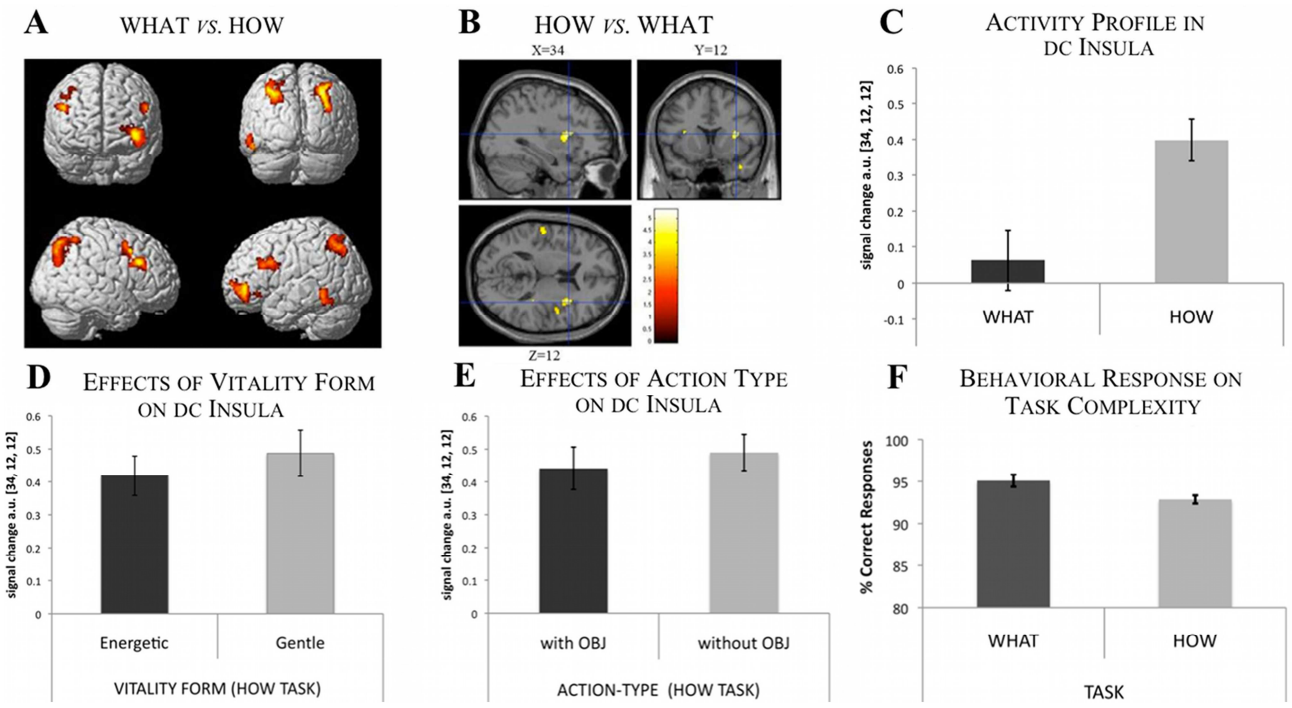

Figure 11:Brain activations resulting from the direct contrast between (A) what vs how task and (B) how vs what task. These activations (PFWE < 0.05 at cluster level) are rendered into a standard MNI brain template. (C) Activation profile within right dorso-central insula (maxima: 34 12 12) in the direct contrast how vs what task. (D) Activation profile in dorso-central insula as a function of vitality form (energetic, gentle) during how task (E) Activation profile in dorso-central insula as a function of action-type (with object, without object) during how task. (F) Percent correct responses (hits) during discrimination of what (is it the same or a different type of action?) and how (is it the same or a different form of vitality?) within each respective task, showing no differences in performance difficulty between tasks (P > 0.05). [Di Cesare et al. (2013), with kind permission from Oxford University Press.]

Testing for task-related and bottom-up stimulus- driven effects: ROI analysis

To assess possible effects exerted by bottom-up stimulus-driven processes on activations observed in the contrast *how vs. what,* we created a ROI centered at dorso-central insula (see Methods). Task-related and stimulus-driven processes were tested in two independent 2x2 GLM analyses, where we assessed separately the effects of vitality form (gentle, energetic) and action-type (with object, without object) on task-related activations (what, how). The results relative to the effects of task (what, how) and vitality form (gentle, energetic) on insular activation revealed a main effect of task (how>what; $F_{1,18}$=5.66, P=.029, partial-η^2=.24, δ=.62) but no effect of vitality form nor interaction effects between vitality form and task, indicating that insular activation was not modulated by a specific form of vitality (P>.05; see D). Similarly, the results relative to the effects of task (what, how) and action-type (with object, without object) on insular activation revealed a main effect of task (how>what; $F_{1,18}$=11.55, P=.003, partial-η^2=.39, δ=.9) but no effect of action-type nor interaction effects between action-type and task (P>.05; see E). Altogether, these results indicate that insular activation is not associated with effects due to bottom-up stimulus-driven processes.

Task-complexity: Behavioral analysis

To rule out the possibility that our contrast of interest, *how vs. what,* reflected activations associated with task demand, we assessed the level of complexity in discriminating the *what* and *how* of an action within each respective task. To this purpose, we carried out a behavioral analysis based on percent correct responses (hits) given by the participants during the scanning sessions (see Methods). The null hypothesis that the percent correct responses for *what* and *how* tasks be equal was tested using the related-samples Wilcoxon Signed Rank test (Z=-1.03; P>.05), indicating no difference in difficulty between the two tasks. Additionally, hits were calculated for each what-how combination to assess possible interaction effects of sequence complexity and task-type. To this purpose, we carried out a repeated measure GLM analysis with two levels of task (*what* and *how*) and 4 levels of what-how combination (see Methods), using the Greenhouse-Geisser correction for sphericity violation (P<.05).

The results revealed only a main effect of what-how combination (how>what; $F_{3,45}$=4.47, P=.02, partial-η^2=.23, δ=.72; see Appendix Table 3-S2 for details), showing that difficulties in judging whether pairs of stimuli were same or different did not depend on task type (see Figure 11 F).

2.3 Discussion

The aim of the present study was to identify the brain areas underlying the recognition of vitality forms during the observation of actions done by others. Participants were presented with pairs of video-clips showing two actors performing actions towards each other. The same action was carried out with two vitality forms, energetic and gentle. The participants viewed the stimuli in two tasks, *what* and *how*, in which they had to decide whether the observed action goal (*what*) and vitality form (*how*) were the same or different between two consecutive videos. Overall, action observation, independently of task (*what, how*), produced activations, besides visual areas, in posterior parietal lobe bilaterally, left inferior and dorsal premotor cortex and inferior and middle frontal gyrus. Additional activations were found in hippocampus and insula. Although there was a large overlap between the activations observed for the two tasks, cortical activations were more extended during the discrimination of the action-*what* (e.g., passing a ball) with respect to the action-*how* (e.g., gently). This cortical activation pattern is similar to that typically described for execution and observation of goal-directed actions (mirror mechanism; see Grafton et al., 1996; Rizzolatti et al., 1996; Decety et al., 1997; Iacoboni et al., 1999; Buccino et al., 2001; Rizzolatti and Craighero, 2004; Keysers and Fadiga, 2008; Iacoboni, 2009; Caspers et al., 2010; Rizzolatti and Sinigaglia, 2010; Grosbras et al., 2012; Molenberghs et al., 2012). In line with these general results, the contrast between *what* and *how* revealed greater activations, for *what* task, in posterior parietal lobe bilaterally, premotor cortex extending rostrally to include the caudal part of inferior frontal gyrus, and in the rostralmost part of inferior frontal gyrus. These data indicate that the analysis of actions aimed at goal recognition requires a more extensive activation of the parieto-frontal circuit subserving this function. It is interesting to note that, as far as the parietal lobe is concerned, its activation was located in a more

posterior location than that typically observed in studies investigating hand actions, such as grasping (Grafton et al., 1996b; Rizzolatti et al., 1996; Binkofski et al., 1999; Buccino et al., 2001; Grèzes et al., 2003). A similar activation was found in Calvo-Merino et al. (2005) during observation of complex actions such as classical ballet or capoeira. It is then likely that activation of the posterior part of the parietal lobe observed in our study represented a bias of the viewer towards a more "global" description of the observed action in the attempt to extract its goal-related meaning. With respect to the contrast *how vs. what*, the results revealed enhanced activation for *how* task in right dorso-central insular cortex. Note that this activation cannot be ascribed to some effects exerted by task demand, as shown by our behavioral analysis indicating no significant differences between *what* and *how* tasks (see Behavioral Results).The insula is an extremely complex and heterogeneous structure including a posterior granular (sensory part), a central large dysgranular and a small rostro-ventral agranular (motor parts) sector (see Mesulam et al., 1982, 1985; Augustine, 1996). A recent neurophysiologial study (Jezzini et al., 2012) showed that, in the monkey, the insula is constituted of two major functional subdivisions: (a) a sensorimotor sector, occupying the dorso-central portion of the insula, which appears to be a functional extension of the parietal lobe, (b) a large anterior and ventral sector consisting of a mosaic of oro-facial motor programs. In the anterior and ventral insula there is a progressive dorso-ventral shift from motor programs without emotional content to motor programs with such a content. A similar pattern of functional organization has been recently described in a meta-analysis by Kurth et al. (2010) for the human insula. In this meta-analysis, consisting of large number of *f*MRI studies, they found four functional distinct regions corresponding to sensory-motor (Showers and Lauer, 1961), olfacto-gustatory (Kringelbach et al., 2004; Poellinger et al., 2001; Royet and Plailly, 2004; Small et al., 1999), socio-emotional (Dolan, 2002; Phillips et al., 2003; Iacoboni and Dapretto, 2006) and cognitive networks of the brain (Mayer et al., 2007; Soros et al., 2007). Socio-emotional aspects activate the ventro-rostral part of the insula while all tested functions, except for the sensory-motor function, overlap on its anterior dorsal portion, often found activated by cognitive demands (Chong et al., 2009), stimulus or task complexity (Menon and Uddin, 2010), and

stimulus emotional salience (Grosbras and Paus, 2005; Pichon et al., 2009, 2011). The view that the most anterior sector of the insula is functionally segregated from its dorso-central sector is consistent with our findings supporting Stern's (1985, 2010) notion that vitality forms do not represent a basic emotional state like anger and fear that, differently from our results, determine a consistent activation of the rostral insula (e.g., Wicker et al., 2003; Gallese et al., 2004; Singer et al., 2004; Grosbras et al., 2005; de Gelder, 2006; Jabbi et al., 2008; Pichon et al., 2009). Instead, our data suggest that vitality forms represent a specific aspect of movement processing, subserved by anatomically and functionally distinct areas from those described for emotion processing. To exclude the possibility that our dorso-central insular activation was affected by some stimulus properties intrinsically describing the type of vitality form (gentle, energetic) or the type of action (with object, without object), we carried out additional analyses. In particular, the dorso-central insular sector showed no statistical difference with respect to the different types of vitality (energetic or gentle). Of course, we cannot exclude the possibility that, within this insular sector, specific neuronal populations are attuned to one or to the other type of vitality. Likewise, the results of these analyses showed that dorso-central insula responded similarly to actions mediated by the presence or absence of an object. Taken together, these data suggest that processing of low-order stimulus-features is not responsible for the activation of the dorso-central insula. What is then the functional role played by dorso-central insula in the processing of vitality affects? Single neuron studies showed that this sector is endowed with sensorimotor properties (Robinson and Burton, 1980a; Schneider et al., 1993). Anatomically, it is connected with the somatosensory cortex (e.g., Mishkin, 1979; Friedman et al., 1986; Augustine, 1996). Furthermore, unlike the anterior part of the insula, which is linked with the frontal lobe and subcortical emotional centers, this posterior sector is connected with medial temporal areas and, in particular, with the hippocampus and the amygdala (e.g., Friedman et al., 1986). A cue clarifying the functional role of dorso-central insula may come from findings showing that this sector receives information from a specific set of unmyelinated cutaneous fibres. These fibres (CT-afferents; see Löken et al., 2009) are activated when the skin is stroked at a pleasant, caress-like speed and their discharge correlates with

the subjective hedonic experience of the caress (Morrison et al., 2011). In Morrison et al. (2011) there was also evidence that dorso-central insula was activated during the observation of other individuals being caressed. CT-like processing being triggered also during others' observation suggests that this insular sector may serve as a platform for the evaluation of specific interaction patterns between individuals. The coding of vitality forms during action observation suggests the involvement of somato-motor processing, as well as of visual processing. Unfortunately, the perusal of our activations does not allow us to give a precise localization of such putative visual input, although one might suggest the existence of a cortical visual pathway to the insular cortex. Such input may originate from higher order visual areas, such as STS, to which dorsal granular/dysgranual insula is shown to be connected (Seltzer and Pandya, 1991; Mesulam and, Mufson, 1982). The proposal of a direct visual path reaching the dorso-central insula is in line with the results by Hadjikhani and Roland (1998), who suggested the involvement of this sector in cross-modal transfer of information. More specifically, dorso-central insula may be a site of interaction between modality specific areas, namely somatosensory and visual. In sum, the present data show that recognition of vitality forms involves the activation of a specific sector (the dorso-central sector) of the insula. Given the anatomical connections of this sector with other cortical areas, it appears that vitality form processing involves a pathway different from those mediating both "cold" and emotional actions. This pathway links, via dorso-central insula (see also Dijkerman and de Haan, 2007), sensorimotor cortical areas with the medial limbic temporal areas, and particularly the hippocampus. Activation of the hippocampus could be functional to storage and retrieval of memories associated with specific forms of vitality. Thus, this sensorimotor-insular-limbic network could provide the specific feeling characterizing vitality forms intrinsic to action processing.

Third Study: Vitality forms and velocity processing involve different sectors of the insula during action observation: a multivoxel pattern analysis.

3.1: Materials and Methods: Behavioral study

3.1.1 Participants

Eighteen healthy right-handed participants (mean age=23.5, s.d.=1,85) took part to the behavioral study. All participants had normal or corrected-to-normal visual acuity. They gave their written informed consent to the experimental procedure, which was approved by the Local Ethics Committee (Parma).

3.1.2 Stimuli and experimental design

The participants were shown video-clips representing two actors, one of which moved an object (a bottle, a can, or a jar) with his right hand towards the other actor. All three actions were performed with 12 different velocities. In all videos, the actor started from the same initial position and reached the same final position. Figure 12 AB shows the action performed with a jar.

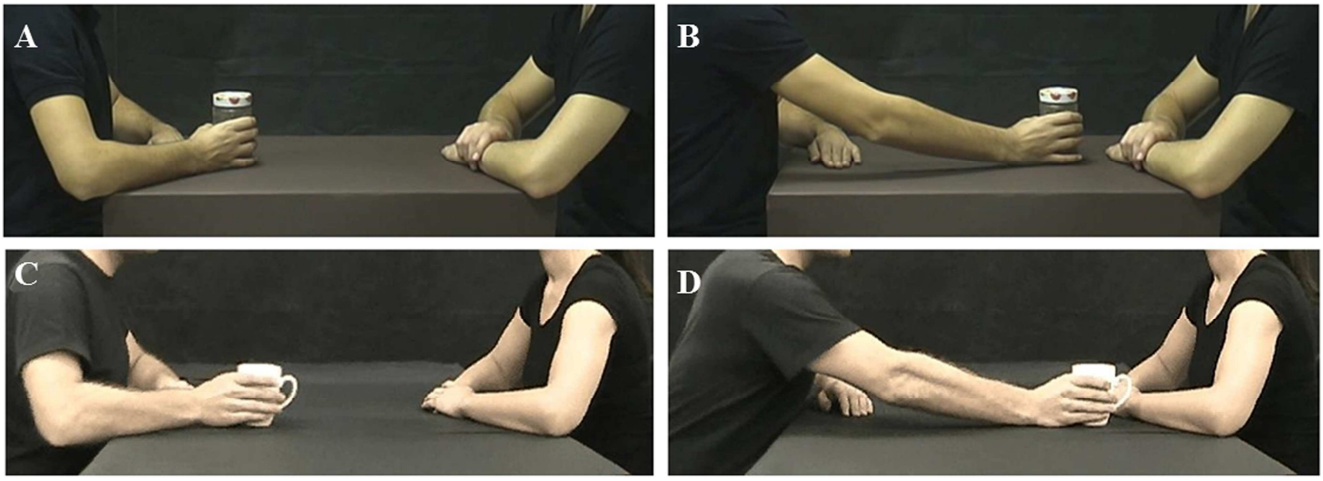

Figure 12: Example of video-clips as viewed by the participants in the Exp. 1 (AB, pass a jar) and Exp. 2 (CD, hand a cup). (AC) frame representing an action with the object in the start position; (BD) frame represents the same action in the end position.

Each video lasted 2s. A total of 36 stimuli were presented (3 objects x 12 velocities). The experimental design was a 2 x 12 factorial with two levels of Task (*vitality, velocity*) and twelve levels of Velocities (execution time from 500ms to 1600ms).

3.1.3 Paradigm and task

The experiment consisted of four experimental sessions. In the first two sessions, participants were instructed to judge the vitality forms of the actions shown in the video-clips (*vitality task*) and judge them as “very rude”, “rude”, “neutral”, “gentle”, or “very gentle” using a five point scale. In the third and fourth sessions, participants were asked to evaluate the velocity of the observed actions (*velocity task*) and to judge them as “very fast”, “fast”, “medium”, “slow”, and “very slow” using again a five point scale,

Using E-Prime software, a total of 36 stimuli were presented for the vitality and velocity tasks (3 actions, i.e. move a bottle, move a jar, move a can, each one presented with 12 different velocity). Each action was presented 10 times per task. Each experimental session consisted of 180 trials presented in a randomized order. Each session lasted about 10 minutes, the whole experiment lasting about 45 minutes. Before the experiment, participants underwent two training sessions (vitality training, velocity training), with stimuli different from those used during the experiment, to familiarize with the experimental procedures and tasks. To avoid a possible bias elicited by velocity on vitality judgment, we preferred to present the vitality judgment tasks first.

The velocity profile of each action was assessed by placing a reflective marker on the object using 3D motion capture system (Vicon OMG, UK). In particular, six infrared cameras (MX2 model) recorded the position occupied by the marker in the 3D space for each action performed by the actor with the object. After recording with Vicon Nexus at 100Hz, all recorded data were used to perform a kinematic analysis, using MATLAB (The Mathworks, Natick, MA) software.

The 36 stimuli (3 objects x 12 velocities) used in the experiment have been compared by means of the Dynamic Time Warp metrics that allows to take into account the little differences in

duration of the trajectories. The metrics has been applied to the modulus of the velocity of each trajectory (and on vx,vy,vz independently) and it produces a 36 by 36 matrix of distances. The distance matrix has been analyzed for understanding if, for every duration level, the distance among the objects inside each level, is less than the ones of other duration levels. The results of this analysis showed that there is no difference between the three objects. For this reason we grouped the three objects and calculated the average profiles of the velocity of the three objects (bottle, can, jar; Figure 13).

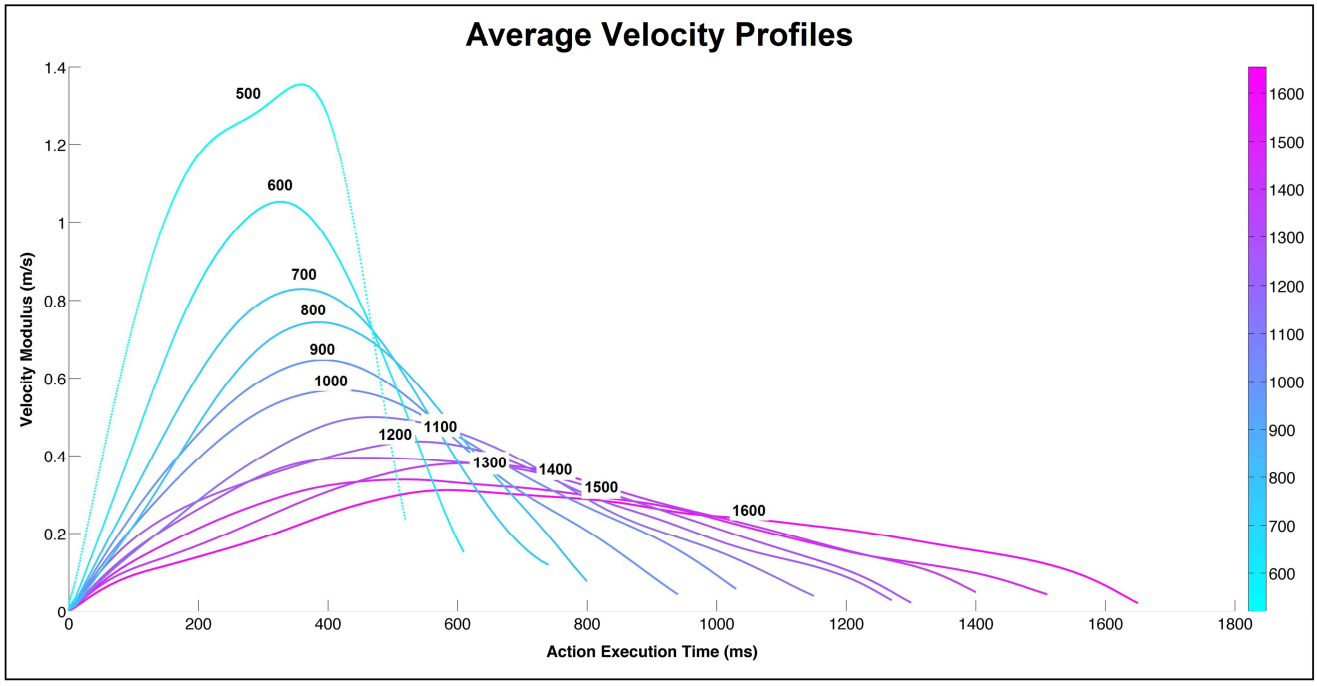

Figure 13: The graph depicts the average velocity profiles of the actions performed by the male actor during twelve different execution times. Each velocity curve represents the mean velocity used by the actor to perform the action (pass an object towards the other actor) using three different objects (bottle, can and jam) at twelve different execution times.

3.2 Materials and Methods: fMRI studies

3.2.1 Participants

Two fMRI experiments were carried out. Eighteen healthy right-handed volunteers [8 females (mean age = 24.1, s.d. = 2, range = 21-28) and 10 males (mean age = 24.4, s.d. = 2.18, range = 22-29)] participated in Experiment 1. The same participants took part also to Experiment 2. From this sample,

two male participants were excluded from Exp. 2 for technical problems related to image acquisition. All participants had normal or corrected-to-normal visual acuity. They gave their written informed consent to the experimental procedure, which was approved by the Local Ethics Committee (Parma).

3.2.2 Experimental Design

The two experiments were carried out in the same experimental session. Exp. 1 (run 1) aimed at mapping the anatomical areas specifically involved in vitality form processing. Exp. 2 (runs 2-5) aimed at understanding if, *within these areas*, the coding of velocity and vitality forms are characterized, at least partially, by different activation patterns.

The experimental design of Exp. 1 was a 2 x 2 factorial with two levels of task (*what, how*) and two levels of vitality forms (*gentle and rude*). The experimental design of Exp. 2 was a 2 x 3 factorial with two levels of task (*vitality, velocity*) and three levels of vitalities/velocities (*gentle/slow, neutral/medium, rude/fast*).

3.2.3 Stimuli

During Exp. 1 (run 1), participants were presented with video-clips showing two actors (1 male and 1 female) performing 4 different actions. The actions were performed either by the male actor or by the female. All actions consisted of transitive actions in which one actor moved an object towards the other actor (an example is shown in Figure 12 CD). Each actor executed 4 different actions (move a bottle, hand a cup, pass a ball, give a packet of crackers). All actions were performed using two different vitality forms: gentle and rude. In all videos, the actors started from an initial position and reached a final position (Figure 12 CD). Each video lasted 2s. A total of 16 stimuli were shown (4 actions x 2 vitality forms x 2 actors). Using VirtualDubMod software v1.5, all the original videos were cropped to remove the head area. This was done to avoid the vision of the face area that represents a highly attractive social cue and which could have averted the viewer's attention from the action that the participants were required to judge. Additionally, to focus participants' attention on the performed

actions, the videos were recorded in a dark scenario and actors wore black shirts to emphasize the forelimbs.

The physical characteristics of the presented actions were assessed using the 2D point kinematics method. After video recording, using the software Avimeca v2.3, we marked a specific point of the hand of the actor for all video clips. For all actions, we fixed the origin of the X/Y axes in the position of the object at rest and marked each occupied position in space every 40ms. The tracking of the action terminated when the object was placed at the end position. Using Regressi software (v2.9), we calculated the velocity and trajectory curves for all actions performed with the two different vitalities (gentle and rude). The module of velocity $\left(|v| = \sqrt{v_x^2 + v_y^2}\right)$ was calculated using both X and Y values for each point during the execution of gentle and rude actions (Figure 14 A).

The kinematics analysis revealed that the velocity profiles changed as a function of *vitality form*. More specifically, the execution of an action performed in a rude way was characterized by a higher velocity than the same action performed in a gentle form (Figure 14 A). Additionally, when the same action was performed with different *vitality forms* (Exp. 1: gentle, rude;), besides velocity, a difference was also found in the action trajectories (Figure 14 B).

Additionally the kinetic energy ($E_k = ½ mv^2$), the potential energy ($E_u = mgh$) and the power ($P = d(E_k + E_u)/dt$) required to perform the action with the object were also measured. To this purpose, the mass of each object (bottle 0.250 Kg, cup 0.200 Kg, ball 0.100 Kg, cracker 0.025 Kg) was calculated. The potential and kinetic energy curves related to movements performed with these objects are shown in 14 C. The potential and kinetic energy was normalized with respect to the mass (Nm/Kg) in order to compare the curves of the different objects that had different weights. The curves indicate that gentle and rude actions are characterized by different peak values for both energy profiles (potential and kinetic).

Finally, the power ($P = d(E_k + E_u)/dt$) used by the actor to move the objects in association with specific velocities and trajectories was measured (Figure 14 D). The power with respect to the mass

(J/Kg) was then normalized to compare the curves of the different objects that had different weights. Our data indicate that, in order to perform the action in a rude way, the actor used a higher power than when he/she performed the same action in a gentle way.

During Exp. 2 (runs 2-5), participants were shown video-clips representing two male actors, one of which (the one sitting on the left side of the screen) performed an action towards the other actor using his right hand. To keep the observer's attention, the action was executed using three different objects (move a bottle, a can, a jar). All actions were performed using 3 different velocities (execution times: 600ms, 1000ms, 1400ms; mean velocity: 1.06 m/s, 0.57 m/s, 0.38 m/s) These times were selected on the basis of the behavioral data (see Results of the behavioral experiment). They corresponded to fast/rude, medium/neutral and slow/gentle velocity/vitality. In all videos, the actor started from the same initial position and reached the same final position (Figure 12 AB). Each video lasted 2s. A total of 9 stimuli were shown (3 *objects* x 3 *execution times*).

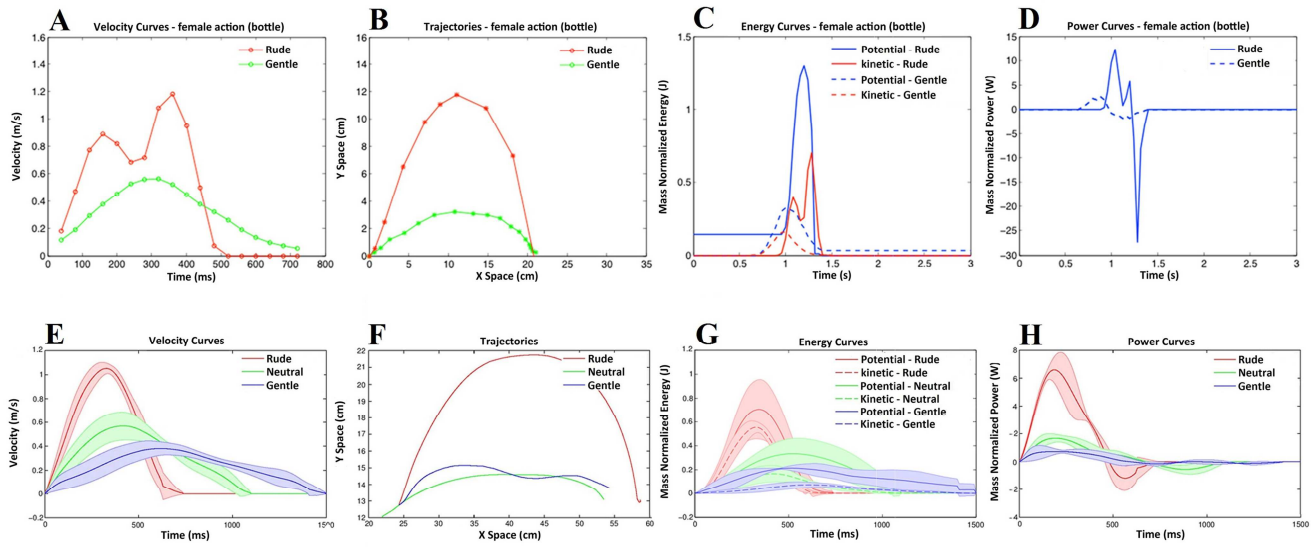

Figure 14: Kinematic and dynamic profiles of the actions performed by the female actress (move a bottle) with the two vitality forms (gentle; rude) in Exp. 1 (ABCD) and by the male actor (move a bottle, can and jam) with three vitality forms (gentle, neutral, rude) in Exp. 2 (EFGH). Graphs A and E depict the velocity profiles (Y axes) and duration (X axes). In graph A are shown only the points in which V> 0.05 m/s. Graphs B and F depict the action trajectories (Exp. 1: gentle, green line; rude, red line; Exp. 2: gentle, blue line; neutral, green line; rude, red line). Graphs C and G depict the potential energy, that is the energy that the actor gave to the object during the lifting phase of the action, and the kinetic energy, that is the energy that the actor gave to the object to move it with a specific velocity from the start to the end point. Graphs D and H depict the power required to perform the action on the object with a gentle vitality (Exp. 1: blue dashed line; Exp. 2:blue line) and a rude vitality (Exp. 1: blue solid line; Exp. 2: red line). For Exp. 2, (graphs EGH) variance among objects is represented by the lines boundary.

In this experiment, the velocities and the trajectories of the actions (Figure 14 EF) were assessed using a reflective marker placed on the object and a 3D motion capture system (Vicon OMG, UK). Additionally the kinetic energy, the potential energy, and the power required to perform the action with the object were assessed. To this purpose, the mass of each object (0.456 Kg. for all 3 objects) was measured. The potential and kinetic energy curves related to the movements performed with these objects are shown in Figure 14 G. Finally, the power ($P = d(E_k + E_u)/dt$) used by the actor to move the objects in association with specific velocities and trajectories was calculated (Figure 14 H).

3.2.3 Paradigm and Task

In both Exp. 1 and 2, participants lay in the scanner in a dimly lit environment. The stimuli were viewed via digital visors (VisuaSTIM) with a 500,000 px x 0.25 square inch resolution and horizontal eye field of 30°. The digital transmission of the signal to the scanner was via optic fiber. The software E-Prime 2 Professional (Psychology Software Tools, Inc., Pittsburgh, USA, http://www.pstnet.com) was used both for stimuli presentation and the recording of participants' answers.

Experiment 1 (run 1)

In Experiment 1, participants were presented with pairs of video-clips, where the executed action could be the either same or different between the first and the second video-clip and where the vitality form could be the same or could change between videos. All video combinations were presented in two tasks (*what* and *how*). The *what* task required the participants to pay attention to the type of action observed in the two consecutive videos and to decide whether they represented the same or a different action, regardless of the associated vitality form. The *how* task required participants to pay attention to the vitality forms and to decide whether the represented vitality was the same or differed between the two consecutive videos, regardless of the type of action observed.

The two tasks started with the instructions "Pay attention to what", and "Pay attention to how", respectively. The "what" instruction was written in blue and the "how" instruction was written in green, in order to help the participants to focus on the type of task.

Each trial started with a colored fixation point (blue for *what* task and green for *how* task) positioned at the center of a black screen for 500ms. The color of the fixation point corresponded to the color of the instructions (see above). The first video-clip was presented for 2s followed by a 100ms fixed interval and by the second video-clip lasting 2s. The second video was followed by a jittered interval ranging between 2.5-4s (fixation cross), in which, in 16% of cases, the participants were cued presenting a task related question lasting 2s. During this time they had to provide an explicit response to the stimuli (catch trials). More specifically, during the view of the question cue, the participants had to indicate, on a response box placed inside the scanner, whether the two consecutive videos were the same or different according to the task type. All video-pairs were shown in only one functional run. In this run, the two tasks (*what* and *how)* were presented, each, in 5 independent mini-blocks in a sequential order. Within each mini-block/task, the video-pairs were presented 6 times in a randomized order. In total, the participants viewed 60 experimental video-pairs. This functional run lasted about 10min.

Experiment 2 (run 2-5)

Exp. 2 was composed of 4 functional runs (2 for *vitality* task, 2 for *velocity* task). In the first two runs, we presented participants with single video clips and asked them to pay attention to the style of the action (*vitality* task). In the last two runs, we presented participants with the same single video clips and asked them to pay attention to action velocity (*velocity* task). The 2 vitality runs were presented before the 2 velocity runs in order to avoid possible bias from the velocity task on the vitality task. A fixation cross was introduced in each video to restrain eye-movements.

Every run started with a white fixation cross, positioned at the center of a black screen for 12s. Each experimental trial presented a single video-clip for 2s followed by a jittered interval (fixation cross) ranging 12-16s. In 10% of cases, after 500ms from video viewing, the participants were cued presenting a task related question lasting 2.5s. During this time they had to provide an explicit response to the stimuli (catch trials). More specifically, during the view of question cue (2.5s), the

participants had to indicate, on a response box placed inside the scanner, whether the observed video was rude/fast, neutral/standard, gentle/slow according to the task-type. In total, participants viewed 50 video-clips (45 experimental trials, 5 catch trials) for each run, presented in a randomized order. Each functional run lasted about 14min.

Before the scanning session, participants underwent a training session with different stimuli than those used during scanning to familiarize with the experimental procedures and tasks.

fMRI data acquisition

Anatomical T1-weighted and functional T2*-weighted MR images were acquired with a 3 Tesla General Electrics scanner equipped with an 8-channel receiver head-coil. Functional images were acquired using a T2*-weighted gradient-echo, echo-planar (EPI) pulse sequence (acceleration factor asset 2, 37 interleaved transverse slices covering the whole brain, with a TR time of 2100ms. for Exp. 1 and 2000ms for the Exp. 2, TE = 30ms, flip-angle = 90 degrees, FOV = 205 x 205 mm^2, inter-slice gap = 0.5 mm, slice thickness = 3 mm, in-plane resolution 2.5 x 2.5 x 2.5 mm^3). In Exp. 1, the scanning sequence comprised 285 interleaved volumes; in Exp. 2, each scanning sequence comprised 416 interleaved volumes. After the third functional run, to allow participants to rest, a high-resolution inversion recovery prepared T1-weighted anatomical scan was acquired for each participant (acceleration factor arc 2, 156 sagittal slices, matrix 256x256, isotropic resolution 1x1x1 mm^3, TI=450ms, TR =8100ms, TE = 3.2ms, flip angle 12°).

3.2.3 Statistical analysis

Univariate analysis

Data analysis was performed with SPM8 (Statistical Parametric Mapping software; The Wellcome Department of Imaging Neuroscience, London, UK; http://www.fil.ion.ucl.ac.uk) running on MATLAB R2009b (The Mathworks, Inc., Natick, MA). The first four volumes of each run were discarded to allow for T1 equilibration effects. For each participant, all volumes were spatially

realigned to the first volume of the first session and un-warped to correct for between-scan motion, and a mean image from the realigned volumes was created. T1 weighted images were realigned to create a mean image and then segmented into gray, white and cerebrospinal fluid and spatially normalized to the Montreal Neurological Institute (MNI). Thereby derived spatial transformation by T1 normalization was applied to the realigned EPIs volumes, which after normalization were re-sampled in 2x2x2 mm^3 voxels using trilinear interpolation in space. All functional volumes were then spatially smoothed with a 6-mm full-width half-maximum isotropic Gaussian kernel for the group analysis.

Data were analyzed using a random-effects model (Friston et al., 1999), implemented in a two-level procedure. In the first level, single-subject fMRI responses were modelled in a General Linear Model (GLM) by a design-matrix comprising the onsets and durations of each event according to the experimental task for each functional run (Exp. 1 - run 1: *what* task, *how* task; Exp. 2 - run 2-3: *vitality* task; run 4-5: *velocity* task).

In Exp. 1, we modelled four regressors as follows: *What, How, Instruction* and *Response*. The two consecutive videos of each trial were modelled as one single epoch lasting 4.1s. The instruction was modeled with a duration of 2s. The response was modeled with a duration of 2s starting from the presentation of the task related question. In the second level analysis (group-analysis), corresponding contrast images of the first level for each participant were entered into a flexible ANOVA with sphericity-correction for repeated measures (Friston et al., 2002). This model considered the pattern of activation obtained in the 2 tasks (*what* and *how*) *versus* implicit baseline (fixation cross). Within this model, we assessed activations associated with each task (independently) *vs.* implicit baseline (P_{FWE} <0.05 corrected at the voxel level; FWHM: 6 mm), as well as activations resulting from the direct contrast between tasks (P_{FWE} <0.05 corrected at the cluster level).

In Exp. 2, at the first level, for the task *vitality* (run 2-3) we modelled 4 regressors as follows: *Rude, Neutral, Gentle, and Response*; for the task *velocity* (run 4-5) we modelled other 4 regressors as follows: *Fast, Standard, Slow, and Response*. The single video of each trial was modelled as a mini

epoch lasting 2s. The *Response* was modelled with a duration of 2,5s starting from the question was presented. In the second level analysis (group-analysis), corresponding contrast images of the first level for each participant were entered in one flexible ANOVA with sphericity-correction for repeated measures (Friston et al., 2002). This model was composed of six regressors (*Fast, Standard, Slow, Rude, Neutral, Gentle*) and considered the pattern of activation obtained for each level in the two tasks (*vitality*, *velocity*) *versus* implicit baseline.

Within this model, we assessed activations associated with each task *vs.* implicit baseline (P_{FWE} <0.05 corrected at the voxel level; FWHM: 6 mm). This model did not reveal significant main effect of task (vitality *vs.* velocity), levels (*Rude vs. Gentle*, *Neutral vs. Gentle*, *Rude vs. Neutral*), or interaction.

The location of the activation foci was determined in the stereotaxic space of MNI coordinates system. Those cerebral regions for which maps are provided were also localized with reference to cytoarchitectonical probabilistic maps of the human brain, using the SPM-Anatomy toolbox v1.7 (Eickhoff et al, 2005).

An introduction to the MVPA technique

Multi-voxel pattern analysis (MVPA) involves searching for highly reproducible spatial patterns of activity that differentiate across experimental conditions. MVPA is therefore considered as a supervised classification problem where a classifier attempts to capture the relationships between spatial patterns of fMRI activity and experimental conditions. More generally, classification consists in determining a decision function **f** that takes the values of various “features” in a data “example” ***x*** and predicts the class of that “example” considering a possible “bias” **b** (f = wx + b). In fMRI context, an “example” represents a trial in the experimental run, and the “features” represent the corresponding fMRI signals in a cluster of voxels. The experimental conditions represent the different classes (i.e vitality and velocity). To obtain the decision function f , data (i.e., trials and the corresponding class labels) must be split into two sets: “training set” and “test set” (Figure 15 A1, B1). The classifier is

trained using the training set (Figure 15A). Training consists of modeling the relationship between the voxels and the class label by assigning a weight ***w*** to each voxel. This weight corresponds to the relative contribution of the voxel to successfully classify the two classes (i.e. vitality and velocity). The classifier is then evaluated with the test set to determine its performance in capturing the relationship between voxels and classes (Figure 15 B2). The most popular classifier used for fMRI data is the Support Vector Machine (SVM).

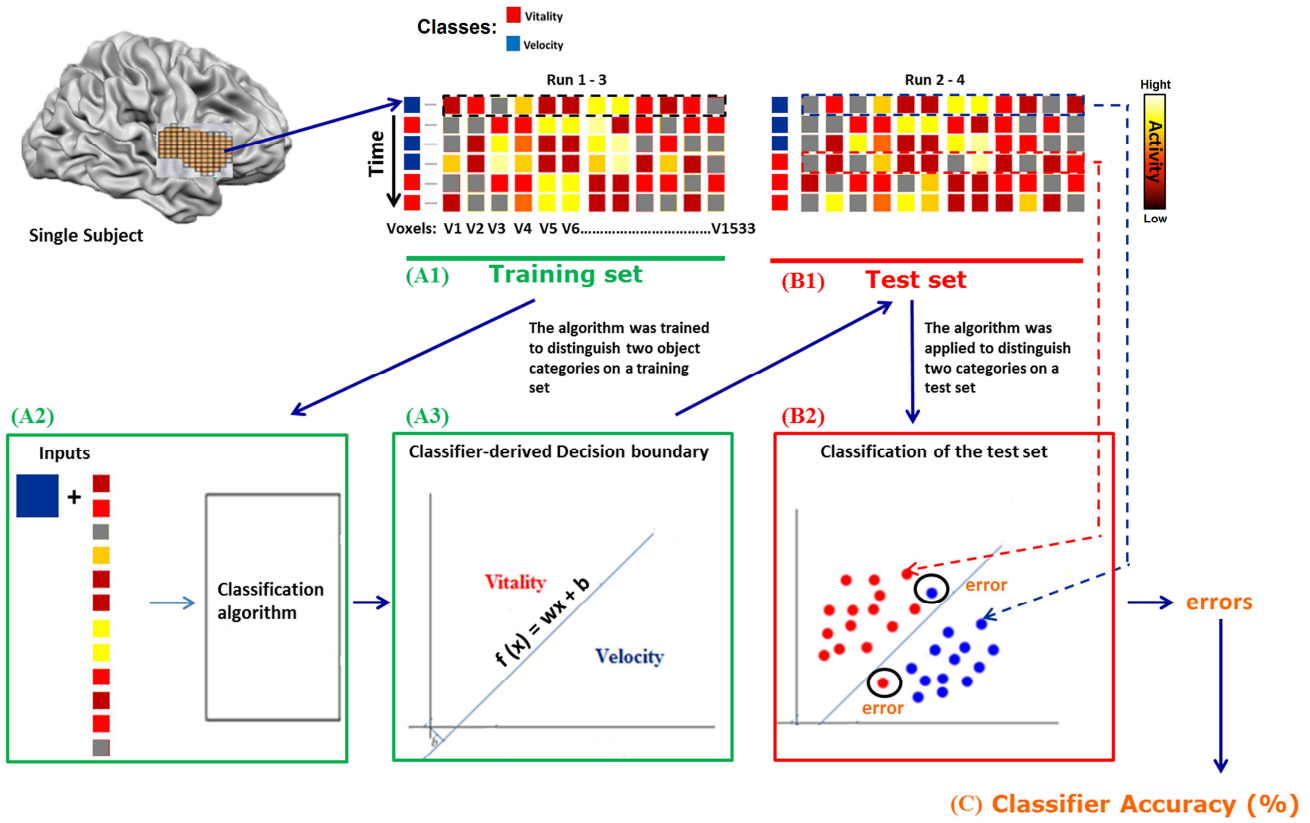

Figure 15: General schema of the Multivoxel Pattern Analysis. Using a training set of data related to the insula (A1) a SVM algorithm was trained. SVM algorithm learned the relation between the BOLD signal and the presented condition (A2) producing a rule (A3, Decision boundary) for the classification of the two classes (vitality and velocity). The trained algorithm was used for the classification of a new set of data (test set, B1, B2) determining the classifier accuracy (C). The classifier accuracy represents the number of the correct classified trials (vitality, velocity) respect to the all presented trials.

Multivoxel pattern analysis

A multivoxel pattern analysis was carried out with the data obtained from Exp. 2. This analysis aimed at assessing possible different patterns of activation in response to velocity (fast, medium, slow) and vitality form (rude, neutral, gentle). Imaging data were analyzed using Brain Voyager QX (Brain Innovation) and custom scripts on MATLAB R2013 (The Mathworks, Inc., Natick, MA). The raw images were pre-processed in BrainVoyager QX performing the following steps: sinc-interpolated slice-time correction, 3D motion correction to correct small head movements, temporal high-pass filtering to remove low frequency non linear drifts of seven cycles for time course. Functional slices were then coregistered to the anatomical volume and subsequently transformed into Talairach space. All individual brains were segmented at grey/white matter boundary using a semiautomatic procedure based on intensity values implemented in Brain Voyager QX.

We decoded multivariate pattern of BOLD activation using support vector machine (SVM) classifiers based on *vitality form* perception (see Figure 15). On the basis of our previous (Di Cesare et al., 2013) and present results, we tested the activation pattern characterizing the insular cortex in response to vitality forms as opposed to velocity. We built 2 regions of interest (ROIs), one at level of the left insula (size of 1533 voxels) and one in the right insula (size of 1346 voxels). In order to build the two ROIs we draw a line between the border of the insula and the parietal, frontal and temporal opercula cortices, which were all excluded from the ROIs. To make sure that each drawn point belonged to the insula, for each slice we checked the coordinates of 8 different border points with Talairach coordinates (Talairach Client – V. 2.4.3). We also built 2 control ROIs, one (CTRL 1) at level of the white matter (size of 46 voxels, coordinates -28 -41 26) and the other (CTRL 2) at level of Broadman Area 21 (size of 44 voxels, coordinates -48 -4 -22). The control ROIs served to test results reliability as a function of the multivoxel pattern model. All ROIs were built on the mean anatomical structure of the participants.

We estimated the response of every voxel in each trial by fitting a standard hemodynamic model to each voxel. The patterns of activation related to each given trial consisted of the set of beta

(% change) values associated with one of the six predictors (*task*levels model*) for all voxels considered in the analysis. The Inter-Stimulus-Interval ranged from 6 to 8 TRs (12 to 16s). For each trial, one pre-onset volume and 5 post-onset volumes were used to model the signal.

Since the multivoxel pattern model required a comparison between tasks that were presented in separate runs (*vitality task:* run 1,2; *velocity task*: run 3,4), we performed a cross-validation scheme considering alternate runs (1,3; 2,4; 2,3; 1,4), dividing them in two different groups (training runs and testing runs). More specifically, we trained linear SVMs on the training datasets (e.g., from runs 1,3) and evaluated the generalization of the model to new data (the test datasets example e.g., from runs 2,4). This procedure was repeated for four possible combinations (1,3 *vs*. 2,4; 2,4 *vs*. 1,3; 2,3 *vs*. 1,4; 1,4 *vs*. 2,3).

We reported accuracies for the classification of new trials. Using balanced datasets for training and testing (15 trials for each level, *rude/neutral/gentle*; 15 trials for each level, *fast/medium/slow*), we expected a rate higher than 50% (chance level, see Figure 20) for each different contrast (*rude vs. fast*, *neutral vs. medium*, *gentle vs. slow*). The significance of this difference was assessed by means of non-parametric Wilcoxon sign-rank one-sided test (α=0.05).

To visualize the spatial activation patterns that were used for classification and to assess consistency across participants, group discriminative maps were created. For each participant, these maps indicated the locations that contributed the most to the discrimination of conditions. After using the linear support vector machine we ranked the features (i.e., voxels) according to their contribution to the discrimination at each individual map level and selected the peaks through thresholding. For each participant, we selected the 50% most discriminative voxels and created group discriminative maps representing at least ten of 16 participants. It is worth noting that we obtained the same activation patterns selecting 35% threshold of most discriminative voxels with group maps representing eight of 16 participants. To account for the multiple tests performed in creating these maps, we thesholded the maps using false discovery rate (Benjamini and Hochberg, 1995, with q

=0.05). The classification accuracy for each participant was always calculated with respect to the whole set of features that did not depend on the threshold chosen for the creation maps.

3.3 Results

3.3.1 Behavioral study

E-Prime software converted automatically participants' judgments in scores (very rude/very fast=5; rude/fast=4; neutral/medium=3; gentle/slow=2; very gentle/very slow=1). Single participants judgments were then modeled using a General Linear Model (GLM) by a design matrix, comprising the participants' score related to each task (vitality, velocity), for each execution time (12 levels).

The results of the GLM analysis indicate a significant difference in judgments between the two *Tasks* ($F_{1,17}$=10.07, P<0.01, partial-η^2=0.37, δ=0.85) as well as among the different *Execution Times* ($F_{11,187}$=310.37, P<0.00, partial-η^2=1, δ=1). The interaction *tasks**execution time* was also significant ($F_{11,187}$=5.54, P=0.02, partial-η^2=0.90, δ=0.89). Post-hoc analysis revealed for the vitality task a significant difference in pairwise comparisons (p<0.01 Bonferroni corrected) except for 5 comparison (5-6, 7-8, 8-9, 9-10, 11-12; p>0.05 Bonferroni corrected). A significant difference between levels was also observed for the velocity task except for two pairwise comparison (8-9, 9-10; p>0.05 Bonferroni corrected).

A regression analysis was subsequently carried out to compare vitality and velocity judgment (dependent variable) as a function of execution time (independent variable). As shown in Figure 16, the curve that best fit the relation between vitality perception and execution time followed a logarithmic trend (R^2=0.94, F=3060, P<0.00, Figure 16) while, for velocity task, there was a linear relationship between velocity perception and execution time (R^2=0.86, F=1360, P<0.00). Taken together, these data indicate that vitality and velocity judgments differ one from another.

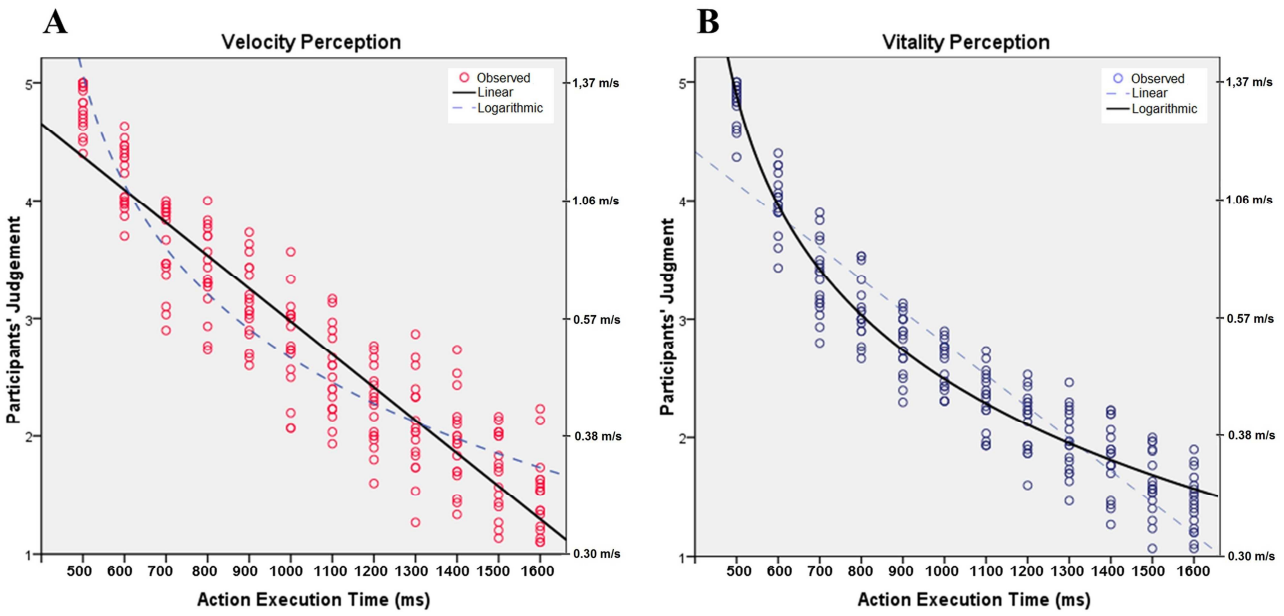

Figure 16: Regression graphs. Graph depicts the linear relation between participants' velocity judgment and action execution time (A). Graph depicts the logarithmic relation between participants' vitality judgment and action execution time (B). For each level, points indicates participants mean score (very rude/very fast=5; rude/fast=4; neutral/medium=3; gentle/slow=2; very gentle/very slow=1). The velocity peak corresponding to each judgment is reported on the right side.

3.3.2 fMRI Experiment 1

Overall effect of "what" and "how" tasks

The observation of all video-clips *vs.* implicit baseline revealed a rather similar pattern of activations for both tasks (*what* and *how*). There was a significant activation of occipital and posterior temporal areas, posterior parietal lobe and cerebellum bilaterally, as well as of the inferior frontal gyrus and of the insula bilaterally, more evident in the left hemisphere. Additional activations were found in the premotor cortex, particularly for *what* task (see Figure 17 and Table 1AB-S3 in Appendix).

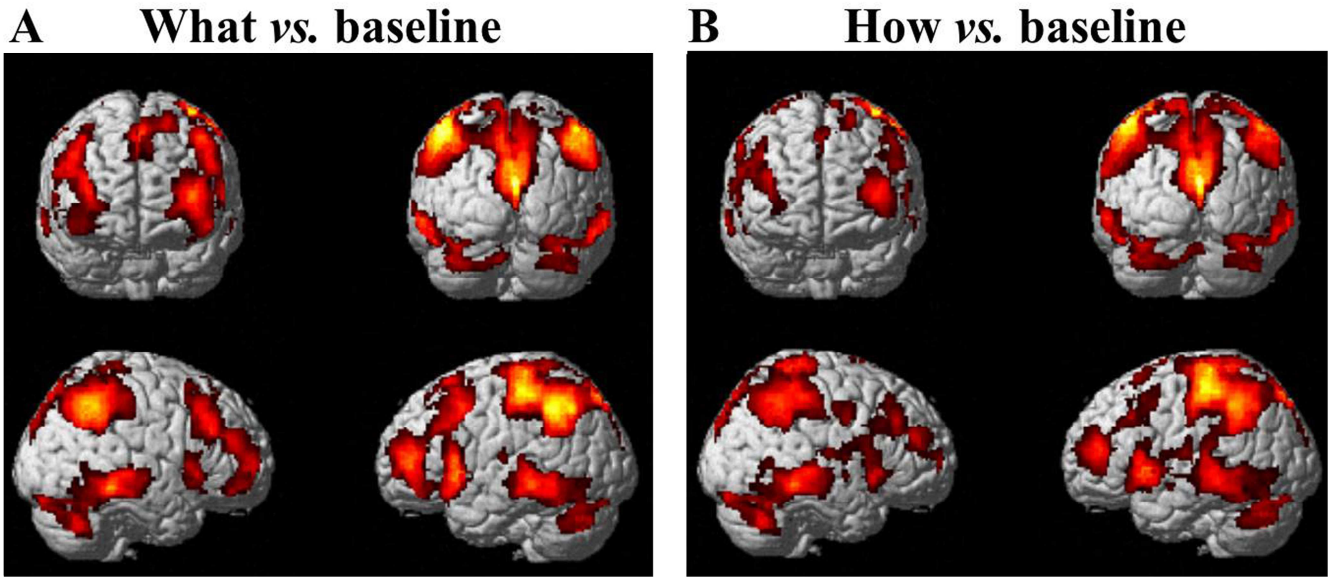

Figure 17: Signal change during (A) the task what and (B) the task how vs. implicit baseline (PFWEcorr<.05 at cluster level).

Contrast between what and how tasks

The contrast between *what vs. how* tasks revealed stronger activations for *what* task in the posterior parietal lobe bilaterally, left premotor and prefrontal cortex (Figure 18 A; see in Appendix Table 2C-S3). The opposite contrast (*how vs. what*), revealed specific activations in dorso-central insula bilaterally, with left prevalence (Figure 18 B left insula, and C right insula, in Appendix Table 2D-S3). Confirming the results from our previous study (Di Cesare et al., 2013), the present data show specificity of insular activation during the *how* task. On this basis, *insula* was used as the region of

interest for the multivoxel pattern analysis (see Exp. 2), in which we aimed at highlighting possible differences in activation patterns between velocity and vitality judgments.

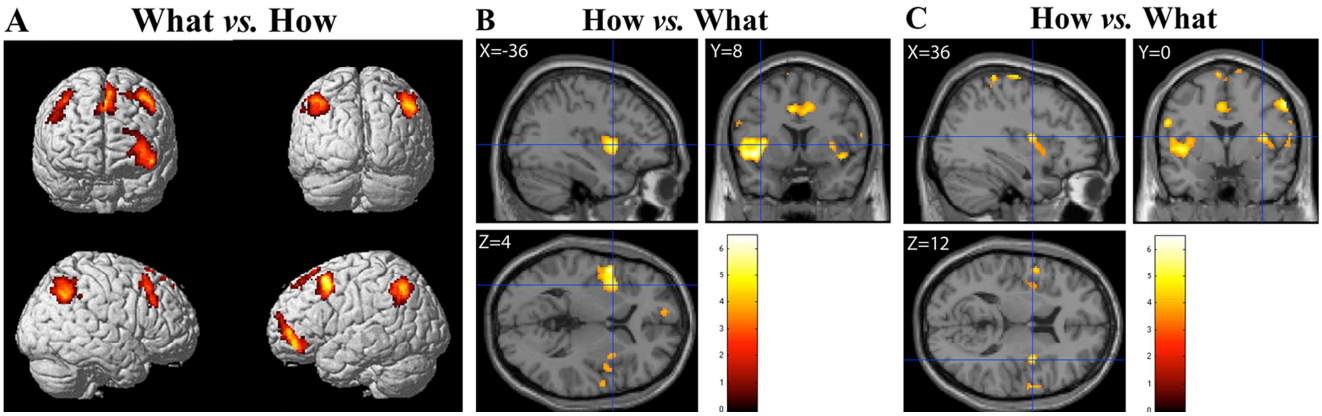

Figure 18: Brain activations resulting from the direct contrast between (A) what vs. how tasks and (BC) how vs. what tasks. These activations are rendered into a standard MNI brain template (PFWEcorr<.05 at cluster level).

3.3.3 fMRI Experiment 2

Response-based analysis testing for task complexity

This analysis was based on the participants' responses (catch trials) during vitality and velocity tasks (see Methods). Within this analysis, we used the number of correct responses (hits; i.e., when the subjects correctly perceived a specific velocity or vitality as falling into the pre-determined category, e.g. fast or rude) and response times (RTs) as dependent variables to assess possible effects of task difficulty on brain activations. To this purpose, independent repeated measure GLM analyses, with 2 levels of task (vitality and velocity) and 3 levels of execution times (600ms, 1000ms, 1400ms), were carried out. With respect to hits, the results revealed no difference between tasks ($P<0.05$), showing that vitality and velocity were equally simple to judge. Opposite, the analysis of RTs revealed a difference between the two tasks ($F_{1,15}$ =7, 7 P=.014, partial-η^2 =.34, δ=.74) showing that participants were significantly faster in judging movement velocity (mean RT time=0.8 s, DS=0.16) than vitality forms (mean RT time=0.9 s, DS=0.13). Altogether, these results suggest that possible differential activation patterns observed between vitality *vs*. velocity tasks cannot be ascribed to a complexity effect associated with vitality task.

Univariate analysis

Overall effect of "vitality" and "velocity" tasks

In Exp. 2, observation of the video-clips for each task (*vitality* and *velocity*) *vs.* implicit baseline revealed a very similar pattern of activation. In particular, there was signal increase in visual occipito-temporal areas, parietal lobe, SMA, premotor and prefrontal cortex (see Figure 19). Additionally, insular activation was observed bilaterally.

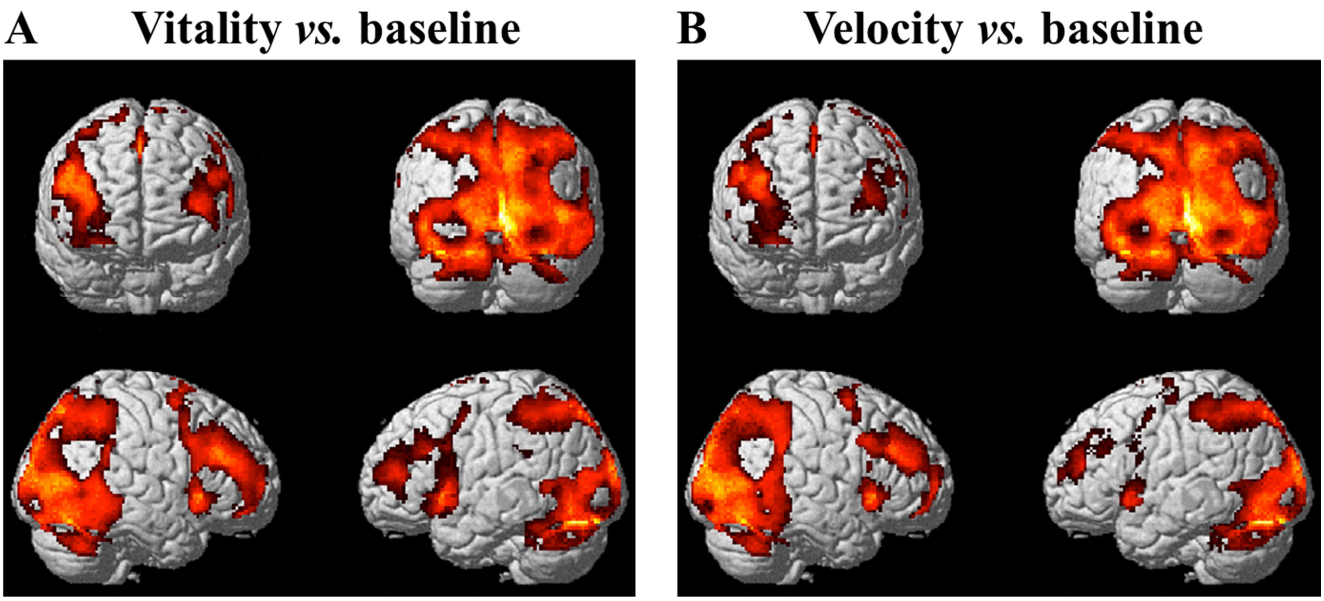

Figure 19: Signal change during (A) velocity task vs. implicit baseline and (B) vitality task vs. implicit baseline (fixation cross). The activations are rendered into a standard MNI brain template.

Contrasts between vitality and velocity tasks

The direct contrast *vitality vs. velocity* tasks revealed no significant activation pattern. The opposite contrast, *velocity vs. vitality* tasks, revealed no significant activations (P>.05).

Multivariate pattern analysis

On the basis of previous results (Di Cesare et al., 2013), confirmed in Exp. 1 of the present study, we assess possible differences in activation patterns as a function of vitality forms and velocity judgments within *insular cortex.* To this purpose, we performed a multivoxel pattern analysis using an algorithm to learn, on training trials, the relationship between *tasks* and *levels* (*rude vs. fast, neutral vs. medium,*

gentle vs. slow) and assessed each relative spatial activation pattern. This information was used to classify the patterns associated with the unlabeled trials (testing trials, see Method section).

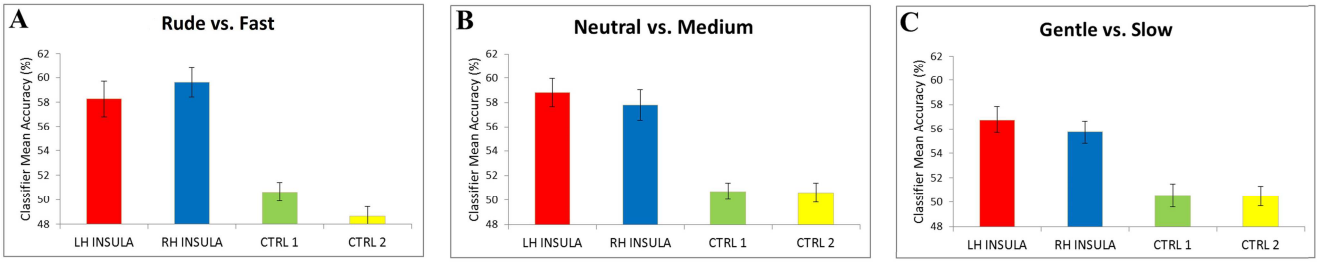

Figure 20: Mean classification accuracy for sixteen participants. Accuracies obtained for the contrasts: rude vs. Fast (A), neutral vs. medium (B), gentle vs. slow (C). Accuracies were significantly different respect to the chance level (50%) only in the left and right insula. Differently, in each contrast level, control areas (CTRL 1, CTRL 2) not differ significantly from chance (50%).

The multivoxel pattern analysis revealed that the classifier mean accuracy for the levels across 16 participants was, for the left and right insula, respectively: 58,2% (Wilcoxon, one sided; $p<0.01$) and 59,6% ($p<0.01$) for the contrast *rude vs. fast*, 58,8% ($p<0.01$) and 57,7% ($p<0.01$) for the contrast *neutral vs. medium* and 56,7% ($p<0.01$) and 55,7% ($p<0.01$) for *gentle vs. slow*. (Figure 20). For the two control areas (CTRL 1, CRTL 2), the classifier mean accuracy across the same 16 participants was, for the left and right insula, respectively: 50,6% ($p>0.05$) and 48,6% ($p>0.05$) for the contrast *rude vs. fast*, 50,7% ($p>0.05$) and 50,6% ($p>0.05$) for the contrast *neutral vs. medium* and 50,5% ($p>0.05$) and 50,5% ($p>0.05$) for *gentle vs. slow*, that is chance level.

Subsequently, group discriminative maps were constructed and inspected for consistency of spatial activation patterns across participants. Figure 21 shows the main pattern of discriminative maps clustered in the insula. The red color indicates positive weights, corresponding to voxels that were more selective for vitality tasks with respect to velocity task, while the blue color indicates negative weights corresponding to voxels that were more selective for velocity tasks with respect to vitality tasks. In the discriminative maps, the three different comparisons (*rude vs. fast, neutral vs. medium, gentle vs. slow*) were collapsed together. Single vitality forms comparisons (i.e., *rude vs. gentle, fast vs. slow*, etc.) as well as the analyses between different velocities (i.e., *fast vs. medium*, *medium vs. slow*, etc.) were not significant ($P>0.05$).

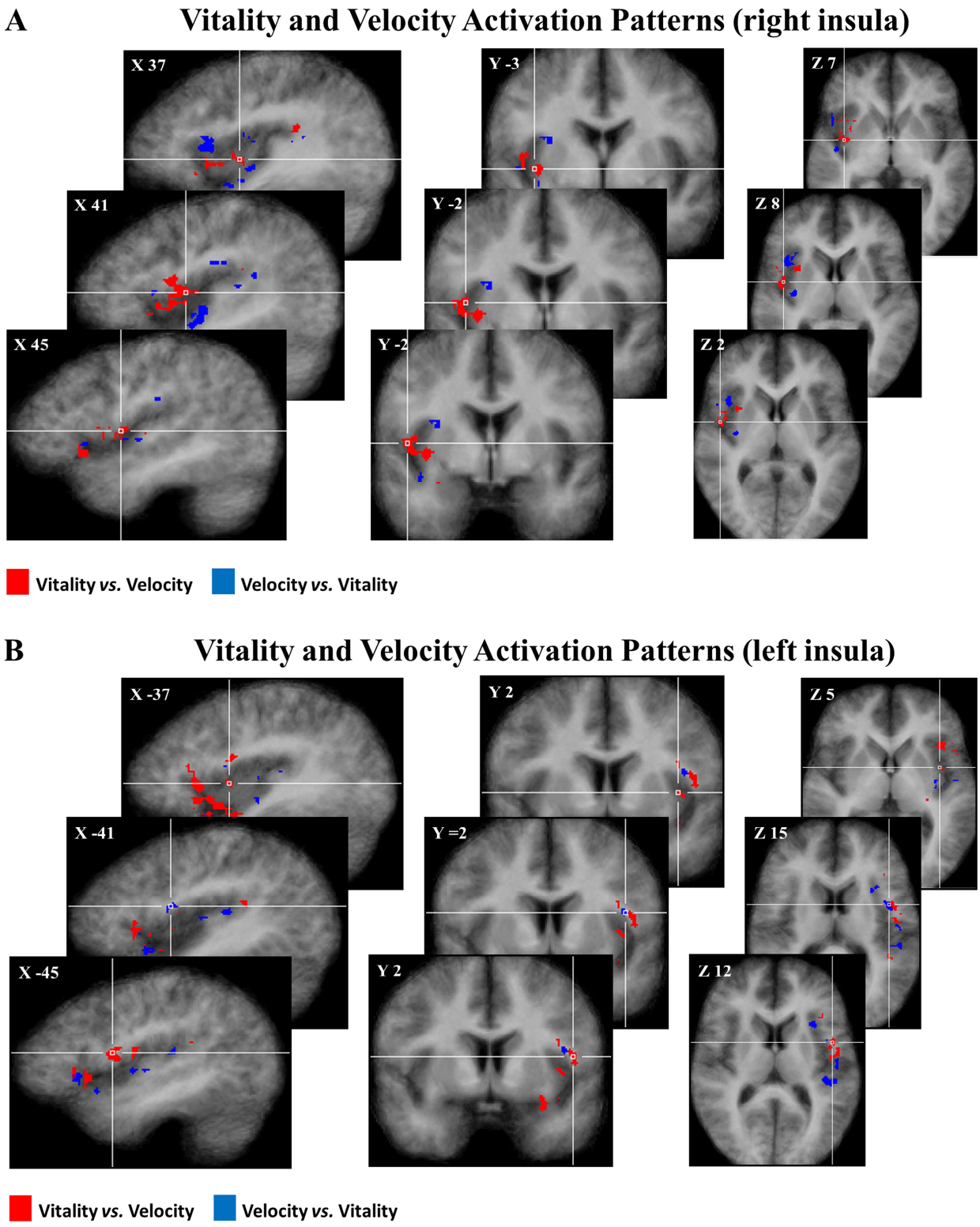

Figure 21: Maps group of 50% of active voxels most discriminative for the perceptual difference of vitality forms (red) and velocity (blue) collapsing three different contrasts (rude vs. fast, neutral vs. medium, gentle vs. slow) in the right (A) and in the left (B) insula. Each voxel was reported if it was present in at least 10 of the 16 participants. These activation patterns (FDRcorr <.05) are overlaid on the average anatomical template of 16 participants in Tailarach coordinates.

3.4 Discussion

The vitality forms or vitality affects is a psychological construct introduced several years ago by Stern (1985, 2010). According to Stern, vitality forms are composed of five dynamic events linked together: movement, time, force, space and direction. Globally these five components create a fundamental "dynamic pentad" which gives an appraisal of the relations between the agent and the action recipient. The description of vitality forms by Stern was based, however, exclusively on a qualitative assessment of observed actions.

In the present study, we first examined the kinematics properties of movement endowed with different vitality forms and described them in more standard physical terms (velocity, trajectory, energy and power). For this purpose, we presented participants with videos showing hand actions performed with twelve different velocities (and related different kinematic components) and asked them to judge their velocity and their vitality form. The results of the behavioral study showed that there was a significant difference between the psychophysical curves related to the action velocity and vitality form judgments. In particular, the regression analysis showed that the psychophysical curve of the vitality forms follows a logarithmic fitting, while this is less evident for velocity judgments. Taken together these results indicate that the perception of velocity and vitality forms falls into different perceptual constructs.

On the basis of these results, we further investigated, using the fMRI technique, the neural correlates of action vitality forms with respect to velocity encoding of the same actions. Previously, we found that observation of actions performed with different vitality forms (gentle, rude) determines an activation of a dorso-central sector of the right insula (Di Cesare et al., 2013). In the present study, using a multivolxel pattern analysis, we examined whether identical stimuli that had to be encoded either in terms of their velocity or vitality form, activate the same or different parts of the insula.

To confirm the activation of the dorso-central insula during action observation, we performed an initial experiment (Exp. 1), in which participants were instructed to discriminate between action goal (i.e., the "what" of an action) and the vitality form of the same action (i.e., "how" the action was

performed). The results confirmed the activation of dorso-central insula when the participants had to judge the vitality forms of the observed actions relative to the goal of the same actions.

On the basis of these findings, the same participants underwent a second experiment (Exp. 2), in which we used a multivoxel pattern analysis focusing on insular activation, with the aim to define the activation patterns during velocity and vitality assessment. The experiment revealed the presence of discriminative voxels preferring vitality forms in the dorso-central sector of the insula. Voxels preferring information about velocity were distributed around the preoviously mentioned region .This activation pattern was particularly evident in the right hemisphere. It should be noted that our data indicate only a preferential activation of given voxels rather than their exclusive activation. Thus, we cannot exclude that the observed pattern is more intermingled between vitality and velocity than here described.

In non-human primates, single neuron studies showed that dorso-central insula is endowed with sensorimotor properties (Schneider et al., 1993; Robinson and Burton, 1980a; see also Jezzini et al., 2012) somehow similar to those of the somatosensory cortex (e.g., Mishkin, 1979; Friedman et al., 1986; Augustine, 1996; Caruana et al., 2011). Additionally, there is evidence in humans that the caudal sector of the insula receives information from a specific set of unmyelinated cutaneous fibres. These fibres (CT-afferents; see Löken et al., 2009) are activated when the skin is stroked at a pleasant, caress-like, speed and their discharge correlates with the subjective hedonic experience of the caress (Morrison et al., 2011). Morrison et al. (2011) found that this sector of the insula, plus its dorso-central part, is also activated during the observation of others being caressed, suggesting that it may play a central role in the evaluation of others' affective interaction.

On these grounds, we suggest that the posterior insula, including its dorso-central part (in contrast with its ventral-anterior part that is more related to basic emotions, see Dolan 2002; Philips et al., 2003; Kurth et al., 2010) is the site of transformation of the physical aspect of an action into its affective/communicative values (vitality forms). Affective information is then processed and

consolidated within medial temporal areas (i.e. the hippocampus and the amygdala), with which dorso-central insula is anatomically connected (see, for example, Friedman et al., 1986).

The main finding of our study is that the key area for vitality forms processing is the dorso-central sector of the insular cortex. During social interactions, this area transforms the physical aspects of an observed action in a communicative/affective construct (vitality form). In virtue of this transformation mechanism, the observer is able to understand the others' internal state. The same mechanism is most likely involved also during vitality form production (i.e., action execution), allowing an individual to communicate his/her affective internal state to others. It is possible that the same neural mechanism underlies both observation and execution of vitality forms.

Fourth Study: Insular representation of vitality forms during observation, imagination and execution.

4.1 Materials and Methods

4.1.1 Participants

Two fMRI experiments were carried out. Fifteen healthy right-handed volunteers (6 females [mean age = 23.1, s.d. = 2.1] and 9 males [mean age = 26, s.d. = 3.9]) participated in experiment 1 (Exp. 1) and in the experiment 2 (Exp. 2, control experiment). All participants had normal or corrected-to-normal visual acuity. None reported a history of psychiatric or neurological disorders, or current use of any psychoactive medications. They gave their written informed consent to the experimental procedure, which was approved by the Local Ethics Committee (Parma).

4.1.2 Experimental Design

The two experiments were carried out in two different experimental sessions. Exp. 1 aimed at understanding if the activation of the dorso-central insula, found activated during vitality forms observation in previous studies, is also present during vitality forms imagination and execution. Exp. 2 aimed to avoid the possibility that the dorso-central sector of insula could be selective not only for vitality forms recognition (control experiment).

The experimental design of Exp. 1 was composed by two different models. The first model was a 1 x 3 factorial with one level of condition (control condition 1) and three levels of task (*observation, imagination, execution*); the second model was a 2 x 3 factorial with two levels of vitality forms (Gentle and Rude) and three levels of task (*observation, imagination, execution*). Finally, the experimental design of Exp. 2 was a 1 x 1 factorial with one level of condition (control condition 2: not biological movement) and one level of task (*observation*).

4.1.3 Stimuli

All video-clips were presented to the participants showing the right hand of an actor performing different leftward and rightward actions. In Exp. 1, video-clips showed the actor's hand performing four different actions (move a bottle; hand a cup; give a packet of crackers; pass a ball) towards another actor using two different vitality forms: rude or gentle (Vitality conditions: Rude and Gentle; Figure 22 A1, B1). Additionally, video-clips also showed the actor's hand placing a small ball in a box (Control condition 1: Ctrl 1; Figure 22 C1). In Exp. 2, video clips showed the actor's hand rotating with a not biological velocity (control condition 2: Ctrl 2; Figure 22 D1).

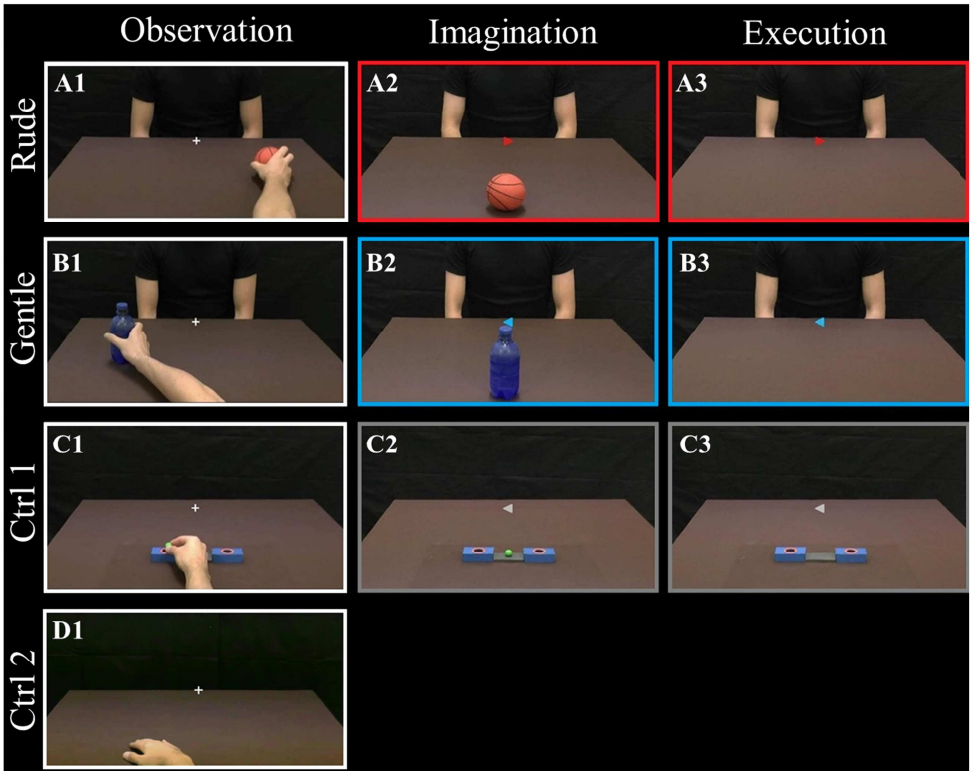

Figure 22: Example of video-clips as viewed by the participants in Exp. 1 (Rude, Gentle; Ctrl 1) and in Exp. 2 (Ctrl 2). In Exp. 1 for the Vitality condition, during imagination and execution tasks, the edge screen color indicated the vitality type (red: Rude; blue: Gentle). In the central part of the screen, a cue indicated the direction to follow during action imagination or action execution.

In all videos, the actor started from a start position and reached a final position. Each video lasted 3s. A total of 26 stimuli were shown (Vitality: 4 actions x 2 *vitality forms* x 2 directions*;* Ctrl 1: 1 action x 4 colors x 2 directions*;* Ctrl 2: 1 action x 2 directions). Using VirtualDubMod software v1.5, all the original videos (Exp. 1 and 2) were cropped to remove the head area. This was done to avoid the vision of the face area that represents a highly attractive social cue, which could have deviated the viewer's attention from the performed action on which the participants were required to give

judgments. Additionally, to focus participants' attention on performed actions, the videos were recorded in a dark scenario and actors wore black shirts to emphasize the forelimbs.

Kinematic and dynamic analysis of vitality forms

During action performance, all the actors' movement profiles were studied using the 3D point kinematics method. After video recording, using the software Avimeca v2.3, a specific point of the actor's hand was marked for all video clips. For all actions, the origin of the X/Y/Z was fixed in the position of the thumb at rest each position in the space every 20ms was marked until the end of action. Using MATLAB (The Mathworks, Natick, MA) software, we calculated the velocity and trajectory curves for all actions (Gentle, Rude; Ctrl 1, Ctrl 2). The module of velocity $\left(|v| = \sqrt{v_x^2 + v_y^2 + v_z^2}\right)$ was calculated using X, Y and Z values for each point during the execution of all actions and were averaged (red line: average of all Rude actions; green line: average of all Gentle actions; blue line: average of the Ctrl 1 actions; light blue line: average of the Ctrl 2 actions; Figure 23).

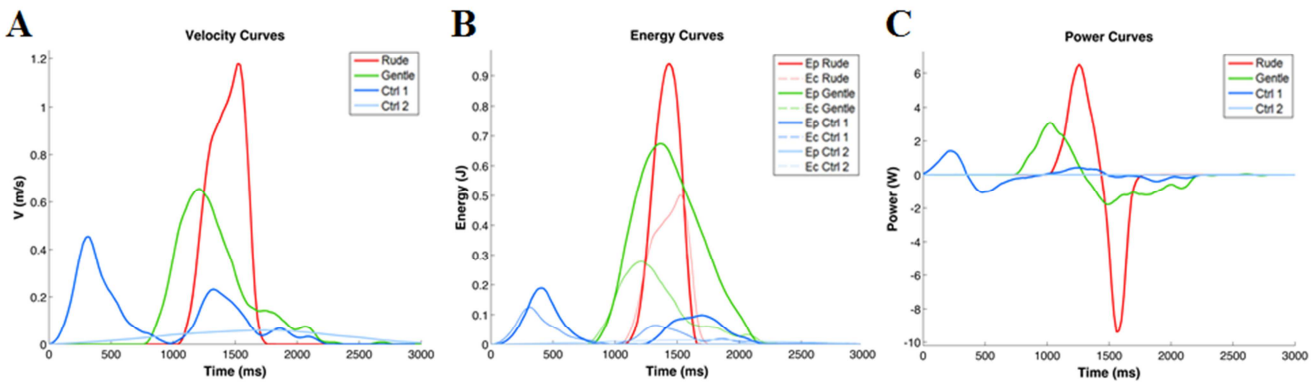

Figure 23: Kinematic and dynamic average profiles of the actions performed by the actor with different objects (Vitality: ball, cup, bottle and crackers; Ctrl 1: small ball) or without objects (Ctrl 2: hand rotation). Graph A depicts the velocity profiles and duration of the hand performing the action (Gentle, green line; Rude, red line; Ctrl 1, blue line; Ctrl 2, light blue line). Graph B depicts the potential and kinetic energy. Graph C depicts the power required to perform the action on the objects.

For each action, the kinetic energy ($E_k = ½\, mv^2$), the potential energy ($E_u = mgh$) and the power ($P = d(E_k + E_u)/dt$) required to perform the action with the object were estimated. To this purpose, the mass of each object (Exp. 1: bottle 0.350 Kg, cup 0.200 Kg, ball 0.200 Kg, cracker 0.025 Kg; Exp. 2: small ball 0,050 Kg) was measured and added to the mass of the actor's hand (0.5 Kg). The potential and

kinetic energy curves related to movements performed with these objects are shown in Figure 23 B. The potential and kinetic energy were normalized with respect to the mass (Nm/Kg) in order to compare the curves of the different objects that had different weights. Finally, the power ($P = d(E_k + E_u)/dt$) used by the actor to move with his hand the objects in association with specific velocities and trajectories was calculated (Figure 23 C).

4.1.4 Paradigm and Task

In both Exp. 1 and 2, participants lay in the scanner in a dimly lit environment. The stimuli were viewed via digital visors (VisuaSTIM) with a 500,000 px x 0.25 square inch resolution and horizontal eye field of 30°. The digital transmission of the signal to the scanner was via optic fiber. The software E-Prime 2 Professional (Psychology Software Tools, Inc., Pittsburgh, USA, http://www.pstnet.com) was used both for stimuli presentation and the recording of participants' answers.

Experiment 1

Exp. 1 was composed of 6 functional runs (2 runs for Control condition, 4 runs for Vitality condition). To avoid possible bias elicited by Vitality condition on Control condition, we decided to present Control condition before Vitality condition.

In the first run we presented participants with single video clips in two different tasks: *observation* and *imagination* (control condition). The two tasks were presented, each, in independent mini-blocks in a sequential order. The *observation task* started with the instruction "observe" and required the participants to pay attention to the action (Figure 22 C1). The *imagination task* started with the instruction "imagine" and required the participants to imagine to perform the action (Figure 22 C2). During *Imagination task*, in the central part of the screen, a cue indicated the direction towards to imagine to perform the action (left side or right side). In 10% of cases, participants had to provide an explicit response to the stimuli (catch trials). More specifically, they had to indicate, on a response box placed inside the scanner, the color of the small ball observed in the video-clip. In the second run, we presented a static image of two boxes (Figure 22 C3) and, during image viewing, asked

participants to place a small ball in the box (*execution task*). In the central part of the screen, a cue indicated the box towards to perform the action (left box or right box).

In the third and fourth runs, we presented participants with single video clips in two different tasks: *vitality observation* and *vitality imagination.* For each run, the two tasks were presented, each, in independent mini-blocks in a sequential order. The *vitality observation task* started with the instruction "observe" and presented to the participants video clips showing social interactions (passing an object towards another actor in rude or gentle way, see Figure 22 A1, B1). During this task participants had to pay attention to the style of the action (vitality form). The *vitality imagination task* started with the instruction "imagine" and required the participants to imagine to perform the action towards another actor seated in opposite side in gentle or rude way (Figure 22 A2, B2). During *vitality imagination task*, the edge screen color indicated the style of action in which to imagine to perform the action (blue color: Gentle; red color: Rude). Finally, in the central part of the screen, a cue indicated the direction toward to imagine to perform the action (left side or right side). In 10% of cases, participants had to indicate, on a response box placed inside the scanner, whether the vitality form of the observed or imagined action was rude or gentle. In the fifth and sixth run, we presented a static image of the actor seating opposite the observer and asked participants, simply rotating the wrist, to move in gentle way (Figure 22 B3) o in rude way (Figure 22 A3) a packet of crackers towards the opposite actor (*vitality execution task*). A cue indicated the direction (left side, right side) in which perform the action while the color of the edge screen indicated the style to use during the execution of action (blue color: Gentle; red color: Rude).

A fixation cross was introduced in each video to restrain eye-movements. Every run started with a white fixation cross, positioned at the center of a black screen for 500ms. For observation and imagination tasks (runs 1, 3, 4), each experimental trial presented a single video-clip for 3s followed by a jittered interval (fixation cross) ranging 3-6s. In total, participants viewed 71 video-clips (64 experimental trials, 7 catch trials) organized in mini-blocks and presented in a randomized order. In Each run every task were presented in 4 independent mini-blocks in a sequential order. Within each

mini-block, the video-pairs were presented 8 times in a randomized order. Each functional run lasted about 13min. For the execution task (runs 2, 5, 6) each experimental trial presented a static image lasting 3s during which participants had to perform the action (Vitality condition: pass a packet of crackers; Control condition: place a ball in the box). Each trial was followed by a jittered interval (fixation cross) ranging among 6-9-12s. In total, during the execution run, participants were presented 32 experimental trials.

Experiment 2 (Control Experiment)

Exp. 2 was composed of only 1 functional run. In this run, participants were presented with single video clips during the *observation task*. The task required the participants to pay attention to the action (Figure 22 D1). In 10% of cases, participants had to indicate, on a response box placed inside the scanner, the direction of the observed movement (left side, right side). For this task, each experimental trial presented a single video-clip for 3s followed by a jittered interval (fixation cross) ranging among 6-9-12s. In total, participants viewed 32 video-clips presented in a randomized order.

fMRI data acquisition

Anatomical T1-weighted and functional T2*-weighted MR images were acquired with a 3 Tesla General Electrics scanner equipped with an 8-channel receiver head-coil. Functional images were acquired using a T2*-weighted gradient-echo, echo-planar (EPI) pulse sequence (acceleration factor asset 2, 40 interleaved transverse slices covering the whole brain, with a TR time of 3000ms. for Exp. 1 and Exp. 2, TE = 30ms, flip-angle = 90 degrees, FOV = 205 x 205 mm^2, inter-slice gap = 0.5 mm, slice thickness = 3 mm, in-plane resolution 2.5 x 2.5 x 2.5 mm^3). In Exp. 1, the scanning sequence comprised 287 interleaved volumes for runs 1, 147 volumes for runs 2-5-6; 266 volumes for runs 3-4. In Exp. 2, each scanning sequence comprised 140 interleaved volumes. After the third functional run, to allow participants to rest, a high-resolution inversion recovery prepared T1-weighted anatomical scan was acquired for each participant (acceleration factor arc 2, 156 sagittal slices, matrix 256x256, isotropic resolution 1x1x1 mm^3, TI=450ms, TR =8100ms, TE = 3.2ms, flip angle 12°).

4.1.4 Statistical analysis

Data analysis was performed with SPM8 (Statistical Parametric Mapping software; The Wellcome Department of Imaging Neuroscience, London, UK; http://www.fil.ion.ucl.ac.uk) running on MATLAB R2009b (The Mathworks, Inc., Natick, MA). The first four volumes of each run were discarded to allow for T1 equilibration effects. For each participant, all volumes were spatially realigned to the first volume of the first session and un-warped to correct for between-scan motion, and a mean image from the realigned volumes was created. T1 weighted images were realigned to create a mean image and then segmented into grey, white and cerebrospinal fluid and spatially normalized to the Montreal Neurological Institute (MNI). Thereby derived spatial transformation by T1 normalization was applied to the realigned EPIs volumes, which after normalization were re-sampled in 2x2x2 mm^3 voxels using trilinear interpolation in space. All functional volumes were then spatially smoothed with a 6 mm full-width half-maximum isotropic Gaussian kernel for the group analysis. To control head movements, we modelled motion parameters as regressors.

Data were analyzed using a random-effects model (Friston et al., 1999), implemented in a two-level procedure. In the first level, single-subject fMRI responses were modelled in a General Linear Model (GLM) by a design-matrix comprising the onsets and durations of each event according to the experimental task for each functional run. In Exp. 1, at first level were used four different GLM: *observation and imagination control model* (run 1: *observation task, imagination task*), *execution control model* (run 2: *execution task*), *observation and imagination vitality model* (run 3-4: *vitality observation task, vitality imagination task*), *execution vitality model* (run 5-6: *vitality execution task*).

In Exp. 2, at the first level was used one GLM: *observation control model* (run 1: *observation task*).

In Exp. 1, Control condition (run 1) was modelled using four regressors as follows: *Observation (Obs Ctrl 1), Imagination (Img Ctrl 1), Instruction* and *Response*. Differently, Vitality condition (runs 3, 4) was modelled using six regressors as follows: *Observation Rude (Obs Rude), Observation Gentle (Obs Gentle), Imagination Rude (Img Rude), Imagination Gentle (Img Gentle), Instruction* and

Response. Single video was modelled as a single event lasting 3s. The instruction and response were modelled respectively with a duration of 3s and 2s. For the *execution task*, Control condition (run 2) was modelled using one regressor (*Execution*: *Exe Ctrl 1*). while Vitality condition (run 5, 6) was modelled using two regressors (*Execution Rude: Exe Rude; Execution Gentle: Exe Gentle).*

In Exp. 2, for the *observation* task, the second control condition (Ctrl 2), was modelled using two regressors: *Observation (Obs Ctrl 2) and Response*. The single video was modelled as a single event lasting 3s while the *Response* was modelled with a duration of 2s.

In the second level analysis (group-analysis), corresponding contrast images of the first level for each participant were entered into a flexible ANOVA with sphericity-correction for repeated measures (Friston et al., 2002). This model was composed of ten regressors (*Obs Rude, Obs Gentle, Img Rude, Img Gentle, Obs Ctrl 1, Img Ctrl 1, Exe Rude, Exe Gentle, Exe Ctrl 1, Obs Ctrl 2)* and considered the activation pattern obtained for different tasks (Obs, Img, Exe) in four different condition (Vitality: Gentle and Rude; Ctrl 1, Ctrl 2) *versus* implicit baseline. Within this model, we assessed activations associated with each task *vs.* implicit baseline and activations resulting from the direct contrast between tasks (P_{FWE} <0.05 corrected at the cluster level) and activations resulting from the direct contrast between task*conditions (*Obs Rude vs. Obs Ctrl 1, Obs Gentle vs. Obs Ctrl 1, Img Rude vs. Img Ctrl 1, Img Gentle vs. Img Ctrl 1, Exe Rude vs. Exe Ctrl 1, Exe Gentle vs. Exe Ctrl 1, Obs Rude vs. Obs Ctrl 2; Obs Gentle vs. Obs Ctrl 2*; P_{FWE} <0.05 corrected at the cluster level, cluster size estimated with a voxel-level threshold of *P*-uncorrected = 0.001).

The location of the activation foci was determined in the stereotaxic space of MNI coordinates system. Those cerebral regions for which maps are provided were also localized with reference to cytoarchitectonical probabilistic maps of the human brain, using the SPM-Anatomy toolbox v1.7 (Eickhoff et al, 2005).

To test the specificity of the dorso-central part of insula during the observation of the Gentle vitality form respect to the Ctrl 1 (Control condition 1), two ROIs were created on the basis of the functional maps (group analysis) resulting from the overlapping of the observation, imagination and

execution tasks obtained for Gentle vitality form. Using MarsBaR ROI toolbox for SPM (release 0.42), both ROIs were defined on the dorso-central insula, centering the sphere (radium 10 mm) around the maxima (x=38, y=4, z=-8 right insula; x=-38, y=4, z=2 left insula). Mean cluster values associated with Gentle vitality form and Ctrl 1 (Control condition) were then calculated for each subject on the basis of contrast images from the *observation vitality model* and *observation control model* of the first level (described above). Signal change for each subject was extracted using REX (http://web.mit.edu/swg/rex).

4.3 Results

Overall effect of "vitality forms" and "control" conditions

The observation of all video-clips *vs.* implicit baseline revealed a rather similar activation pattern for all conditions (Gentle, Rude, Ctrl 1, Ctrl 2, Figure 24).

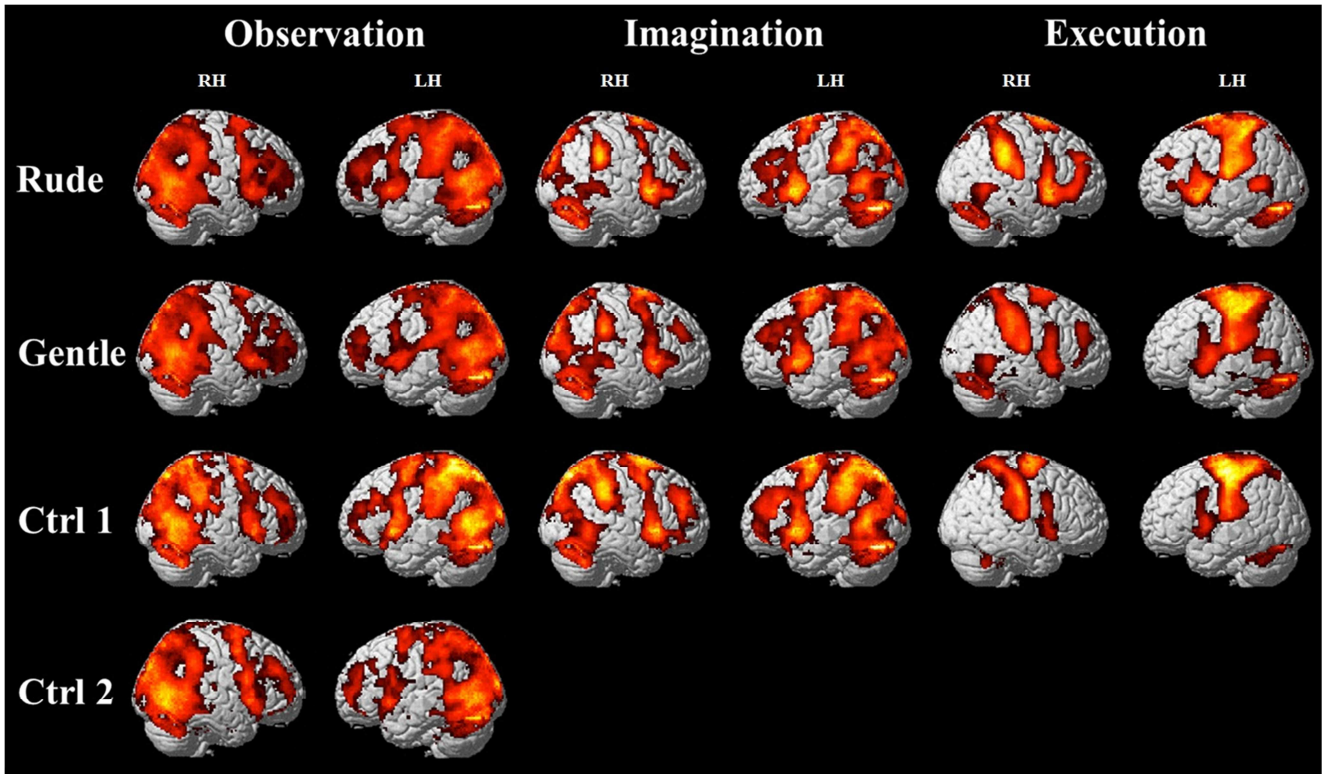

Figure 24: Brain activations resulting from different conditions (Rude; Gentle; Ctrl 1; Ctrl 2), vs. implicit baseline during three different tasks (Obs, Img and Exe). These activations (PFWE<0.05 at cluster level) are rendered into a standard MNI brain template.

There was a significant activation of occipito-temporal areas, parietal lobe, middle and inferior frontal gyrus, insula and cerebellum bilaterally. Additional activations were found in the premotor cortex (Figure 24). A very similar activation pattern was observed also for *imagination task* in vitality forms (Gentle, Rude) and Ctrl 1 conditions respectively.

The execution of an action performed with (Gentle, Rude) or without a vitality form (Ctrl 1) produced activation in parietal lobe, motor areas, premotor areas, insula and cerebellum bilaterally. Additional activations were found in the temporal area only during the execution of the action performed with a vitality forms (Figure 24).

Contrast between "vitality forms" and "control" conditions

The contrast between vitality forms (Gentle, Rude) and Ctrl 1 condition revealed activation in the dorso-central sector of insula for all three different tasks except for one condition (observation task: Gentle vs. Ctrl 1, Figure 25).

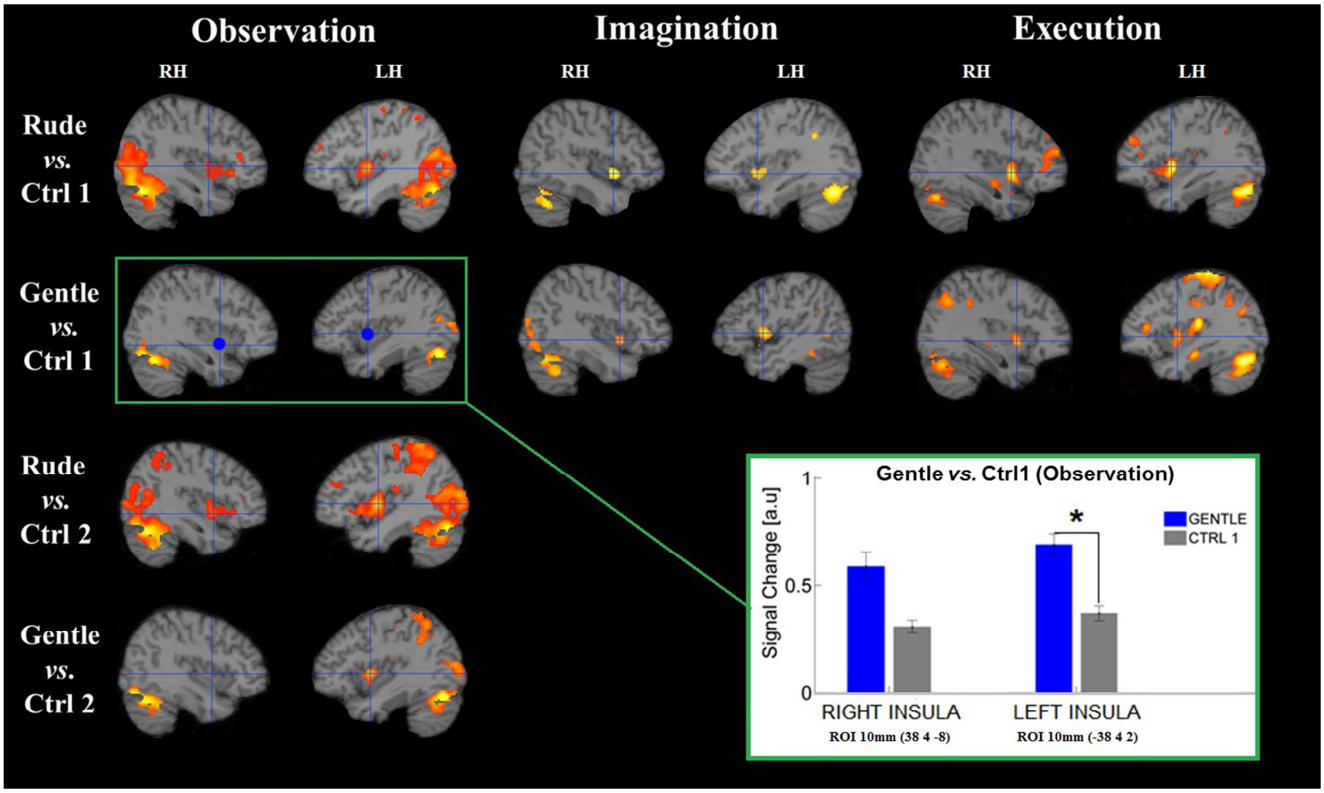

Figure 25: Signal change during the direct contrast between vitality type (Rude, Gentle) vs. Ctrl 1 during three different tasks (Obs, Img, Exe). In the observation task, the direct contrast Gentle vs. Ctrl 1 produced no activation in the dorso-central insula. However, a ROI analysis revealed in the left insula a significative increase of BOLD signal during the observation of Gentle vitality form respect to the control condition (T test a priori, * p<0.05). The present figure also shows the direct contrasts between vitality type (Rude, Gentle) vs. Ctrl 2 (not biological

movement). All these activations (PFWE<0.05 at cluster level) are rendered into a standard MNI brain template.

The contrast between vitality forms (Gentle, Rude) and Ctrl 2 condition, revealed activation in the occipito-temporal area, parietal lobe, dorso-central insula and cerebellum bilaterally (Figure 25, see Appendix Tables 1-S4 and 2-S4 for coordinates and statistical values).

Conjunction among Observation, Imagination and Execution

The conjunction analysis among all three different tasks (Obs, Img, Exe) revealed, for Vitality (Rude and Gentle) and Ctrl 1 conditions, activation in left premotor cortex in the parietal lobe, dorso-central sector of insula and cerebellum bilaterally. Additionally, only for Vitality conditions, activations were observed in the temporal area bilaterally (Gentle, Rude; see Figure 26, for coordinates see also Table 3-S4).

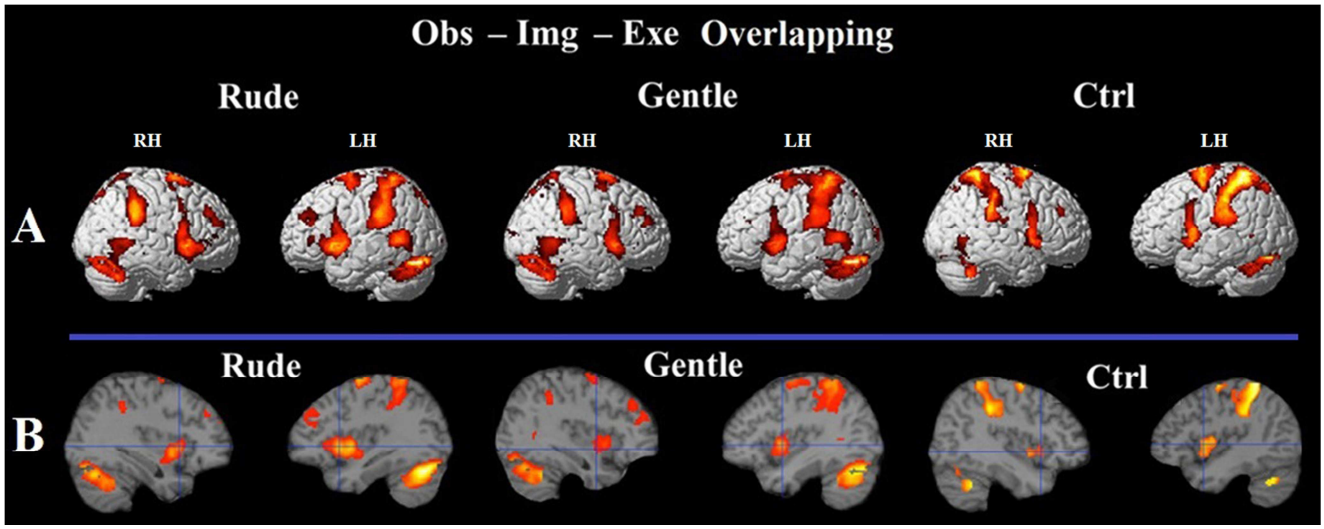

Figure 26: Brain activations resulting from the conjunction among three different tasks (Obs, Img, Exe) respectively, in Vitality (Rude, Gentle) and control conditions (Ctrl 1). These activations are shown at cluster level (PFWE<0.05) on a volume brain (A) and on section brain (B). These activations are rendered into a standard MNI brain template.

Contrast between Gentle and Control condition during observation task: ROI analysis

To test the specificity of the dorso-central part of insula during the observation of a Gentle vitality form respect to the control (Ctrl 1), two ROIs were created at level of dorso-central insula (see

Methods). Task-related process was tested in a T test that assessed the BOLD signal change during observation of Gentle vitality form and observation of Ctrl 1. The results revealed in the left dorso-central insula a significative difference between the Gentle vitality form and Ctrl 1 (T Test a priori $p<0.05$, see Box Figure 25).

4.4 Conclusions

In previous studies, we found that the observation of the style of others actions determined a selective activation of a dorso-central sector of the right insula (Di Cesare et al., 2013). In the present study we investigated whether the dorso-central insula is also involved during vitality forms imagination and execution. More specifically we studied if recognition, planning and execution of vitality forms share the same neural correlates.

For this purpose, we carried out two different fMRI experiments (Exp. 1 and Exp. 2). In Exp. 1, different video clips were presented in two different conditions: vitality and control. During control condition, participants were presented actions (placing a ball in the box) and were requested to observe the action (*observation task*), to image to perform (*imagination task*) or to perform the action (*execution task*). During vitality condition, participants were presented with videos showing actor's hand performing four different actions (move a bottle; hand a cup; give a packet of crackers; pass a ball) towards another actor using two different vitality forms (Gentle, Rude) and were requested to observe the style of action (*vitality observation task*), to image to perform (*vitality imagination task*) or to perform the action with a Gentle or Rude vitality form (*vitality execution task*).

The observation of all video-clips *vs.* implicit baseline revealed a rather similar activation pattern for all conditions (Gentle, Rude, Ctrl 1, Ctrl 2). There was a significant activation of occipito-temporal areas, parietal lobe, middle and inferior frontal gyrus, insula and cerebellum bilaterally. Additional activations were found in the premotor cortex. More interestingly, the direct contrast between Vitality (Gentle, Rude) and Ctrl 1 condition revealed activation in the dorso-central sector of insula for all three different tasks. These findings indicate that, during action observation the dorso-

central part of insula is involved in vitality form processing. This area is also activated during the control observation showing that the vitality processing is automatic and task independent.

The dorso-central insula is also activated during action imagination and execution showing a stronger activation when participants imagined or produced a vitality form. Pooling together, these data shows that vitality form recognition, planning and execution share the same activation pattern.

To avoid the possibility that this activation could be selective not only for vitality forms processing, a control experiment was carried on (Exp. 2). In Exp. 2 video clips were presented to participants showing a hand moving with a not biological velocity. The results of the control experiment showed that the observation of a human hand moving with a not biological kinematics produced no activation in the dorso-central sector of insula.

In conclusion, our data suggest that during observation, the perception of the kinematic/dynamic properties of movement allows one to understand the affective/communicative component of others' actions (vitality forms: Gentle, Rude). This mechanism is also involved in vitality form production. This mechanism, during social interactions, could be a link between our inside world with the outside, allowing us to understand others' internal state through action observation and, through action execution, to communicate our internal state to others.

General Discussion

The style of an action is the way in which the action is performed and it is characterized by kinematic parameters such as velocity and trajectory. In everyday life, during action execution is possible to perform the same action in different ways according to agent's intentions. The goal of the present thesis was to assess, with four different fMRI studies, the brain areas involved in the action style processing.

In the first study (preliminary study) was delineated brain activations during observation of reaching movements following *biological* and *non-biological* motion profiles and then was investigated whether these areas are sensitive to movement *velocity*. The results of this study showed that the observation of reaching movement produced activation of the dorsal fronto-parietal areas rather than inferior parietal lobule areas involved in grasping observation (grasp an object). Additionally, the dorsal fronto-parietal circuit was found active in responding to movement kinematics when a reaching action was performed by a *biological* effector. These data suggest that, during action observation, kinematic parameters underlined reaching are encoded in the superior parietal/dorso-premotor circuit.

The way in which an action is performed represents the style of that action. Action style is an important aspect that allows the observer to understand *how* the action is performed, providing also an appraisal of the affective/communicative quality underlying the relation between the agent and the action recipient. This information, carried by the dynamic and kinematic informations of the observed action, has been defined by Stern "vitality forms" (Stern, 2010). The aim of the second study was to delineate the neural correlates involved in vitality forms processing (the *how* of action) during action observation, investigating if they differed from those observed for goal action understanding (the *what* of action). The results of this study showed enhanced activations for the *how* task in the right dorso-central insular cortex. The dorso-central insula is a sector endowed with sensorimotor properties suggesting that vitality forms are not actions where the crucial information is related to the emotional

dimension, like actions conveying fear, anger, etc. Vitality forms are on another dimension of action describing both the affective and cognitive components of the action.

Different *vitality forms* are characterized by different physical properties such as velocity (fast, slow) and convey an affective content (gentle, rude). This strict relation between kinematics and affective state characterizing vitality forms introduces a new question: is vitality perception simply related to velocity perception or vitality forms are characterized by a different construct? This question has been addressed in the third study. In this study, the results of a preliminary behavioral experiment showed that there is a difference between the psychophysical curves related to the action velocity and vitality form perception. Additionally, using fMRI technique and multi-voxel pattern analysis (MVPA), were further explored, within the insula, the distributed activation pattern associated with vitality and velocity processing. The MVPA results showed that the most discriminative voxels for the comparison between vitality form and velocity were located, consistently across subjects, in the dorso-central sector of the insula (positive signs, exhibiting a preference for vitality) and a widespread set of voxels was found around this sector (negative signs, preference for velocity). These results suggest that dorso-central insula is the site where the kinematic aspects of the observed actions are transformed into vitality forms, enabling individuals to understand others' internal state through action observation.

In everyday life people not only observe vitality forms but also produce them. The same mechanism could be most likely involved also during vitality form production (i.e., action execution), allowing an individual to communicate his/her affective internal state to the others. The aim of the fourth study was to investigate whether the dorso-central sector of insula, found activated during vitality form observation, is also involved during vitality form imagination and execution. The results of the fourth study confirmed the activation of the dorso-central insula during action observation and demonstrated that this activation is task independent. Interestingly, the dorso-central insula is also activated during action imagination and action execution suggesting that vitality form recognition, planning and execution share the same activation pattern.

How these new data fit with previous findings on the functional properties of the dorso-central insula?

In non-human primates, single neuron studies showed that the dorso-central insula is endowed with sensorimotor properties (Schneider et al., 1993; Robinson and Burton, 1980a; see also Jezzini et al., 2012) somehow similar to those of the somatosensory cortex (e.g., Mishkin, 1979; Friedman et al., 1986; Augustine, 1996; Caruana et al., 2011). Additionally, there is evidence in humans that the caudal sector of the insula receives information from a specific set of unmyelinated cutaneous fibres. These fibres (CT-afferents; see Löken et al., 2009) are activated when the skin is stroked at a pleasant, caress-like, speed and their discharge correlates with the subjective hedonic experience of the caress (Morrison et al., 2011). Morrison et al. (2011) found that this sector of the insula, plus its dorso-central part, is also activated during the observation of others being caressed, suggesting that it may play a central role in the evaluation of others' affective interaction.

These grounds suggest that the posterior insula, including its dorso-central part (in contrast with its ventral-anterior part that is more related to basic emotions, see Dolan 2002; Philips et al., 2003; Kurth et al., 2010, Jezzini et al., 2012) is the site of transformation of the physical aspect of an action into its affective/communicative values (vitality forms). Affective information is then processed and consolidated within medial temporal areas (i.e. the hippocampus and the amygdala), with which dorso-central insula is anatomically connected (Friedman et al., 1986).

In conclusion, the main finding of this thesis is that besides goal and intention, there is another fundamental aspect of action: the style (*vitality form*). The encoding of vitality forms involves the dorso-central sector of the insular cortex, bilaterally. During social interactions, this area transforms the physical aspects of an observed action in a communicative/affective construct (*vitality form*). In virtue of this transformation mechanism, the observer is able to understand the others' internal state. The same mechanism is also involved during vitality form production (i.e., action execution), allowing an individual to communicate his/her affective internal state to others.

References

Augustine, J.R. (1996). Circuitry and functional aspects of the insular lobe in primates including humans. Brain Research Reviews, 2, 229-244.

Benjamin, Y., Hochberg, Y. (1995). Controlling the false discovery rate: a practical and powerful approach to multiple testing. J.R. Statist. Soc. B, 57 (1), 289-300.

Binder, J.R., Desai, R.H., Graves, W.W., & Conant, L.L. (2009). Where is the semantic system? A critical review and meta-analysis of 120 functional neuroimaging studies. Cerebral Cortex, 19, 2767–2796.

Binkofski, F., Buccino, G., Posse, S., Seitz, R., Rizzolatti, G., & Freund, H. (1999). A fronto-parietal circuit of object manipulation in man: evidence from an fMRI study. European Journal of Neuroscience, 11, 3276-3286.

Buccino, G., Binkofski, F., Fink, G. R., Fadiga, L., Fogassi, L., Gallese, V., et al. (2001). Action observation activates premotor and parietal areas in a somatotopic manner: an fMRI study. European Journal of Neuroscience, 13, 400–404.

Calvo-Merino, B., Glaser, D. E., Grèzes, J., Passingham, R.E., & Haggard, P. (2005). Action observation and acquired motor skills: an fMRI study with expert dancers. Cerebral Cortex, 15, 1243-1249.

Casile A., Dayan E., Caggiano V., Hendler T., Giese M., (2009). Neuronal encoding of human kinematic invariants during action observation. Cereb. Cortex 20, 1647-1655.

Caruana F., Jezzini A., Sbriscia-Fioretti B., Rizzolatti G., Gallese V. (2011). Emotional and social behaviors elicited by electrical stimulation of the insula in the macaque monkey, Current Biology, 21(3):195-199

Caspers, S., Zilles, K., Laird, A.R., Eickhoff, S.B. (2010). ALE meta-analysis of action observation and imitation in the human brain. Neuroimage, 50, 1148–67.

Colby C., Gattass R., Olson C., Gross C., (1988). Topographical organization of cortical afferents to extrastriate visual area PO in the macaque: a dual tracer study. J. Comp. Neurol. 269, 392-413.

Condon, W.S., Sander, L.S. (1974). Neonate movement is synchronized with adult speech: interactional participation and language acquisition. Science, 183, 99-101.

Cox, D.D., Savoy, R.L. (2003). Functional magnetic resonance imaging (fMRI) ‘‘brain reading’’: detecting and classifying distributed patterns of fMRI activity in human visual cortex. Neuroimage, 19, 261–70.

Dayan E., Casile A., Levit-Binnun N., Giese M.A., Hendler T., Flash T. (2007). Neural representations of kinemtic laws of motion: evidence for action-perception coupling. PNAS 104(51), 20582-20587.

Decety, J., Grèzes, J., Costes, N., Perani, D, Jeannerod, M., Procyk, E., et al. (1997). Brain activity during observation of actions. Influence of action content and subject's strategy. Brain, 120, 1763–1777.

Decety J. (1996). Neural representation for action. Review in Neurosciences 7, 285-297.

Dè Sperati C., Viviani P. (1997). The relationship between curvature and velocity in two-dimensional smooth pursuit eye movements. J. Neurosci. 17, 1244-59.

Di Cesare, G., Di Dio, C., Rochat, M.J., Sinigaglia, C., Bruschweiler-Stern, N., Stern, D.N., Rizzolatti, G. (2013). The neural correlates of "vitality form" recognition: an fMRI study. Social Cognitive and Affective Neuroscience, doi:10.1093/scan/nst068.

Dijkerman, H. C., & de Hann E. H. F. (2007). Somatosensory process subserving perception and action. Behavioral and Brain Sciences, 30, 189-239.

di Pellegrino G, Wise, S.P. (1991). A neurophysiological comparison of three distinct regions of the primate frontal lobe. Brain 114, 951–978.

Dolan, R.J. (2002). Emotion, cognition, and behavior. Science, 298, 1191–4.

Edelman S., Grill-Spector K., Kushnir T., Malach R. (1998). Toward direct visualization of the internal shape space by fMRI. Psychobiology 26, 309–321.

Eickhoff, S., Stephan, K. E., Mohlberg, H., Grefkes, C., Fink, G. R., Amunts, K., & Zilles, K. (2005). A new SPM toolbox for combining probabilistic cytoarchitectonic maps and functional imaging data. Neuroimage, 25(4), 1325-1335.

Engel, S. Furmanski, C. (2001). Selective adaptation to color contrast in human primary visual cortex. J. Neurosci. 21, 3949-3954.

Fang, S., Murray, D., Kersten, S. (2005). Orientation – tuned fMRI adaptation in human visual cortex. The Journal Of Neurophisiology 94, 4188-4195.

Ferri, S., Kolster, H., Jarstoff, J., Orban, G.A. (2011). The human extrastriate body area: selective body responses in human MT/V5 proper. Society for Neuroscience, program/poster: 486.14/OO24.

Filimon, F., Nelson, J., Hagler, D., Sereno, M. (2007). Human cortical representations for reaching: mirror neurons for execution, observation, and imagery. Neuroimage 37, 1315-1328.

Flom, R., & Bahrick, L. E. (2007). The development of infant discrimination of affect in multimodal and unimodal stimulation: The role of intersensory redundancy. Developmental Psychology, 43, 238-252.

Friedman, D. P., Murray, E.A, O'Neill, J.B., & Mishkin, M. (1986). Cortical connections of the somatosensory fields of the lateral sulcus of macaques: evidence for a corticolimbic pathway for touch. The Journal of Comparative Neurology, 252, 323–347.

Friston, K. J., Glaser, D. E., Henson, R. N., Kiebel, S., Phillips, C., & Ashburner, J. (2002). Classical and Bayesian inference in neuroimaging: applications. Neuroimage, 16, 484–512.

Friston, K. J., Holmes, A. P., & Worsley, K. J. (1999). How many subjects constitute a study? Neuroimage, 10, 1-5.

Fogassi, L., Ferrari, P., Gesierich, B., Rozzi, S., Chersi, F., Rizzolatti, G. (2005). Parietal Lobe: From Action Organization to Intention Understanding. Science 308, 662-666.

Gallese, V., Fadiga, L., Fogassi, L., & Rizzolatti, G. (1996). Action recognition in the premotor cortex. Brain, 119, 593-609.

Gallese, V., Keysers, C., Rizzolatti, G. (2004). A unifying view of the basis of social cognition**.** Trends in Cognitive Sciences, 8(9):396-403.

Galletti, C., Fattori, P., Kutz, D.F., Gamberini, M. (1999). Brain location and visual topography of cortical area V6A in the macaque monkey. Eur. J. Neurosci. 11, 575–582.

Galletti, C., Fattori, P., Battaglini, P.P., Shipp, S., Zeki, S. (1996). Functional demarcation of a border between areas V6 and V6A in the superior parietal gyrus of the macaque monkey. Eur. J. Neurosci. 8, 30–52.

Gamberini, M., Passarelli, L., Fattori, P., Zucchelli, M., Bakola, S., Luppino, G., Galletti, C. (2009). Cortical connections of the visuomotor parietooccipital area V6Ad of the Macaque monkey. The Journal of Comparative Neurology 513, 622-642.

Gibson, J. (1986). The ecological approach to perception. Hillsdale: Lawrence Erlbaum Associates.

Grafton, S.T., Arbib, M.A., Fadiga, L., Rizzolatti, G. (1996). Localization of grasp representations in humans by PET: 2. Observation compared with imagination. Exp. Brain Res. 112, 103–111.

Grafton, S.T., Arbib, M.A., Fadiga, L., Rizzolatti, G. (1996b). Functional anatomy of pointing and grasping in human. Cereb. Cortex 6(2), 226-237.

Grèzes, J., Armony, J.L., Rowe, J., Passingham, R.E. (2003). Activations related to “mirror” and “canonical” neurones in the human brain: an fMRI study. Neuroimage 18, 928–937.

Grill-Spector, K., Kushnir, T., Edelman, S., Avidan, G., Itzchak, Y., Malach, R. (1999). Differential

Processing of Objects under Various Viewing Conditions in the Human Lateral Occipital Complex. Neuron 24, 187–203.

Grill-Spector, K., Malach, R. (2001). fMR-adaptation: a tool for studying the functional properties of human cortical neurons. Acta Psychol (Amst) 107, 293-321.

Hamilton, A.F., Grafton, S.T. (2009). Repetition Suppression for Performed Hand Gestures Revealed by fMRI. Human Brain Mapping 30(9), 2898-2906.

Hadjikhani, N., & Roland, P. E. (1998). Cross-modal transfer of information between the Tactile and the visual representations in the human brain: A positron emission tomographic study. The Journal of Neuroscience, 18(3), 1072-1084.

Haynes, J.D., Rees, G. (2005). Predicting the orientation of invisible stimuli from activity in human primary visual cortex. Nature Neuroscience, 8, 686–91.

Haxby, J.V., Gobbini, M.I., Fury, M., Ishai, A., Schouten, J.L., Pietrini, P. (2001). Distributed and overlapping representations of faces and objects in ventral temporal cortex. Science, 293, 2425–30.

Hicheur, H., Vieelledent, S., Richardson, M., Flash, T., Berthoz, A. (2009). Velocity and curvature in human locomotion along complex curved paths: a comparison with hand movements. Exp. Brain Res. 162(2), 145-154.

Huk, A.C., Ress, D., Heeger, D.J. (2001). Neuronal basis of the motion aftereffect reconsidered. Neuron 32, 161-172.

Iacoboni, M. (2009). Imitation, empaty, and mirror neurons. Annual Reviews of Psychology, 60, 653-70.

Iacoboni, M., Woods, R.P., Brass, M., Bekkering, H., Mazziotta, J.C., Rizzolatti, G. (1999). Cortical mechanisms of human imitation. Science 286, 2526–2528.

Jezzini, A., Caruana, F., Stoianov, I., Gallese, V., & Rizzolatti, G. (2012). The functional organization of the insula and of inner perisylvian regions: an intracortical microstimulation study. Proceedings of the National Academy of Sciences, in press.

Keysers, C., Fadiga, L. (2008). The mirror neuron system: new frontiers. Social Neuroscience. 3, 193-8.

Kolster, H., Peters, R., Orban, G., (2010). The retinotopic organization of the human middle temporal area MT/V5 and its cortical neighbors. J. Neurosci. 30, 9801-9820.

Kourtzi, Z., Grill-Spector, K., Planck, M. (2005). fMRI adaptation: a tool for studying visual representations in the primate brain. In Fitting the mind into the World. Adaptation e after-effects in high-level vision, Clifford C Edition WG E Rodhes G, Oxford University Press, USA, pp. 173 D.

Kurth, F., Zilles, K., Fox, P. T., Laird, A.R., & Eickhoff, S. B. (2010). A link between the systems: functional differentiation and integration within the human insula revealed by meta-analysis. Brain Structure Function, 214, 519-534.

Kriegeskorte, N., Bandettini, P. (2007a). Analyzing for information, not activation, to exploit high-resolution fMRI. NeuroImage 38, 649-662.

Kriegeskorte, N., Goebel, R., Bandettini, P. (2006). Information-based functional brain mapping. PNAS 103, 3863–3868.

Laquaniti, F., Terzuolo, C., Viviani, P. (1983). The law relating the kinematic and figural aspects of drawing movements. Acta Psycol. (Amst) 54(1-3), 115-130

Lestou, V., Pollick, F., Kourtzi, Z. (2008). Neural substrates for action understanding at different description levels in the human brain. J. Cogn. Neuroscience 20, 324-341.

Löken, L. S., Wessberg, J., Morrison, I., McGlone, F., & Olausson, H. (2009). Coding of pleasant touch by unmyelinated afferents in humans. Nature Neuroscience, 12, 547-548.

Luppino, G., Ben Hamed, S., Gamberini, M., Matelli, M., Galletti, C. (2005). Occipital (V6) and parietal (V6A) areas in the anterior wall of the parieto-occipital sulcus of the macaque: a cytoarchitectonic study. Eur. J. Neurosci. 21, 3056-3076.

Matelli, M., Luppino, G. (2001). Parietofrontal circuits for action and space perception in the macaque monkey. Neuroimage 14, 27-32.

Mishkin, M. (1979). Analogous neural models for tactual and visual learning. Neuropsychologia, 17, 139–51.

Molenberghs, P., Cunnington, R., Mattingley J., B. (2012). Brain regions with mirror properties: A meta-analysis of 125 human fMRI studies. Neuroscience and Biobehavioural Reviews, 36, 341-349

Morrison, I., Bjsdotter, M., & Olausson, H. (2011). Vicariuos responses to social touch in posterior insular cortex are tuned to pleasant caressing speeds. The Journal of Neuroscience, 31(26), 9554-9562.

Mesulam, M. M., &Mufson, E. J. (1982). Insula of the old world monkey. (III): Afferents cortical output and comments on the claustrum. The Journal of Comparative Neurology, 212, 38–52.

Nadel, J., & Butterworth, G., editors. (1999). Imitation in infancy. Cambridge University Press.

Norman K.A., Polyn S.M., Detre G.J., Haxby J.V. (2006). Beyond mind-reading: multi-voxel pattern analysis of fMRI data. Trends of Cognitive Science,10(9):424–30.

Peelen, M.V., Downing, P.E. (2007). The neural basis of visual body perception. Nature Reviews Neuroscience 8, 636-648.

Phillips, M.L., Drevets, W.C., Rauch, S.L., Lane, R. (2003). Neurobiology of emotion perception I: the neural basis of normal emotion perception. Biological Psychiatry, 54, 504–14.

Pitzalis, S., Sereno, M., Committeri, G., Fattori, P., Galati, G., Patria, F., Galletti, C., (2009). Human V6: the medial motion area. Cereb. Cortex 20(2), 411-424.

Rizzolatti, G., Cattaneo, C., Fabbri-Destro, M., Rozzi, S. (2014). Cortical Mechanisms underlying the organization of goal-directed actions and mirror neuron-based action understanding. Physiological Review, 94(2): 655-706.

Rizzolatti, G., & Sinigallia, C. (2010). The functional role of the parieto-frontal mirror circuit: Interpretations and misinterpretations. Nature Review Neuroscience, 11, 264-274.

Rizzolatti G. (2005). The mirror neuron system and its function in humans. Anat. Embryol. 210, 419–421.

Rizzolatti, G., & Craighero, L. (2004). The mirror-neuron system. Annual Review Neuroscience, 27, 169-192.

Rizzolatti, G., Fogassi, L., Gallese, V. (2001). Neurophysiological mechanisms underlying the understanding and imitation of action. Nature Rev. Neurosci. 2, 661–670.

Rizzolatti, G., Fadiga, L., Fogassi, L., & Gallese, V. (1996). Premotor cortex and the recognition of motor actions. Cognitive Brain Research, 3, 131–141.

Rizzolatti, G., Fadiga, L., Gallese, V., & Fogassi, L. (1996a). Premotor cortex and the recognition of motor actions. Cognitive Brain Research, 3, 131-141.

Rizzolatti, G., Fadiga, L., Matelli, M., Bettinardi, V., Paulesu, E., Perani, D., Fazio, F., (1996b). Localization of grasp representation in humans by PET: 1. Observation versus execution. Exp. Brain Res. 111, 246–252.

Rozzi, S., Ferrari, P.F., Bonini, L., Rizzolatti, G., Fogassi, L., (2008). Functional organization of inferior parietal lobule convexity in the macaque monkey: electrophysiological characterization of motor, sensory and mirror responses and their correlation with cytoarchitectonic areas. European Journal of Neuroscience 28, 1569-1588.

Rozzi, S., Calzavara, R., Belmalih, A., Borra, E., Gregoriou, G.G., Matelli, M., Luppino, G. (2005). Cortical connections of the inferior parietal cortical convexity of the macaque monkey. Cereb. Cortex 16, 1389-1417.

Robinson, C. J., & Burton, H. (1980a). Somatotopographic organization in the second somatosensory area of M. fascicularis. The Journal of Comp Neurology, 192, 43– 67.

Rochat, P. (2009) Others in Mind: The origins of self-consciousness. Cambridge Univ. Press.

Schneider, R., Friedman, D., & Mishkin, M. (1993). A modality-specific somatosensory area within the insula of the rhesus monkeys. Brain Research, 621, 116–120.

Spiridon, M., Fischl, B, Kanwisher, N. (2006). Location and Spatial Profile of Category-Specific Regions in human Extrastriate Cortex. Human Brain Mapping 27, 77-89.

Seltzer, B. & Pandya, D.N. (1991). Post-Rolandic cortical projections of the superior temporal sulcus in the rhesus monkey. The Journal of Comp Neurology, 312, 625-640.

Stern, D.N. (1984). Affect attunement. In: J.D. Call, E. Galenson, R. Tyson (eds). Frontiers of Infant Psychiatry. New York: Basic Books.

Stern, D. N. (1985). The interpersonal world of the infant. New York: Basic Books.

Stern, D. N. (2004). The present moment in psychotherapy and everyday life. New York: Norton.

Stern, D. N. (2010). Forms of vitality exploring dynamic experience in psychology, arts, psychotherapy, and development. Oxford: Oxford University press.

Strange, B. A., Portas, C.M., Dolan, R., A.P. Holmes, & Friston, K.J. (1999). Random effects analyses for event-related fMRI. Neuroimage, 9, 36.

Sunaert, S., Van Hecke, P., Marchal, G., Orban, G. (1999). Motion-responsive regions of the human brain. Exp. Brain Res. 127, 355-370.

Tolias, A., Smirnakis, S., Augath, M., Trinath, T., Logothetis, N. (2001). Motion processing in the macaque: revisited with functional magnetic resonance imaging. J. Neurosci. 21(21), 8594-8601.

Trevarthen, C. (1998). The concept and foundations of infant intersubjectivity. In: S. Braten (eds.). Intersubjective communication and emotion in early ontogeny. Cambridge: Cambridge University Press.

Trevarthen, C., & Aitken, K.J. (2001). Infant intersubjectivity: research, theory and clinical applications. Journal of Child Psychology and Psychiatry, 42(1), 3-48.

Viviani, P., Stucchi, N. (1992). Biological movements look uniform: evidence of motor-perceptual interactions. Journal of Experimental Psycology 18(3), 603-623.

Viviani, P., Flash, T., (1995). Minimum-jerk, two third power law, and isocrony: converging approaches to movement planning. Journal of Experimental Psycology: Human Perception and Performance 21, 32-53.

Zeki, S., Watson, J.D., Lueck, C.J. et al. (1991). A direct demonstration of functional specialization in human visual cortex. J. Neurosci. 11, 641-649.

Acknowledgments

I would like to express my special appreciation and thanks to Professor Giacomo Rizzolatti, he has been a brilliant mentor for me. I would like to thank him for encouraging my research and for allowing me to grow as a research scientist. I would also like to thank my supervisor, Dr. Cinzia Di Dio for supporting and guiding me through the realization of this work. I also want to thank Dr. Fabrizio Fasano and Dr. Massimo Marchi for their good comments and suggestions. I would like to thank radiology technicians of Ospedale Maggiore di Parma to support me to collect data for my PhD thesis.

A special thanks to my family. Words cannot express how grateful I am to my mother, and father for all work that they did to support me in this project. I would also like to thank to my sister Rosita and my little nephew Giuseppe to be present every day in my life. Thanks to all my friends who supported me in all this period.

I would like to express gratitude to my girlfriend Simona that with her smile and love supports me in everyday life.

Appendix

Table 1 S1: A. Activations during the observation of the Arm vs. control still image (minus still images); B. activations during the observation of the Cylinder vs. control still image (minus still images). Local maxima of activated areas as shown in 4, given in MNI standard brain coordinates at cluster-level 0.05 and voxel level p<0.001 [ATB: most probable anatomical region in the Anatomy Toolbox 1.7, Eickhoff et al., 2005; asterisks (*) denote assigned areas].

Anatomical region	Left					Right				
	x	y	z	Z-score	ATB	x	y	z	Z-score	ATB
A. Arm (Arm)										
Superior Occipital Gyrus/V6	-20	-80	28	4.49		22	-80	28	3.54	
Lingual Gyrus	-18	-86	-2	5.65	30% hOC3V (V3v)*					
Middle Occipital Gyrus/V5	-40	-70	8	5.87	30% hOC5 (V5)	48	-76	0	5.33	20% hOC5 (V5)
Superior Temporal Gyrus	-44	-42	12	4.92						
Middle Temporal Gyrus/V5						48	-70	12	6.73	
Superior Parietal Lobule	-28	-46	56	5.76	40% Area 2*	22	-50	54	4.70	60% SPL
(SPL)										(7PC)*
IPS	-42	-28	40	4.33	40% IPC (Pft)*					
Superior Marginal Gyrus	-48	-28	28							
Rolandic Operculum						60	-28	24	4.27	40% OP1*
Postcentral Gyrus (PMd)	-22	-8	60	4.50	30% Area 6	42	-4	54	4.25	40% Area 6
Postcentral Gyrus (PMv)	-52	-6	40	5.14	60% Area 6					
Insula						38	8	2	4.49	
Cerebellum	-28	-72	-20	5.48	51% Lobule VI*					
B. **Cylinder (C)**										
Middle Occipital Gyrus	-40	-70	6	4.76	20% hOC5 (V5)	48	-78	2	4	20% hOC5 (V5)
Middle Temporal Gyrus/V5						46	-68	8	4.91	30% hOC5 (V5)

Table 2 S1: A. Activations during the observation of Arm, Arrow, and Colored Arm vs. control still image (minus still images); B. global activations during the observation of reaching movement independently of the stimulus-type. Local maxima of activated areas as shown in Figure 5, given in MNI standard brain coordinates at cluster-level 0.05 and voxel level p<0.001 [ATB: most probable anatomical region in the Anatomy Toolbox 1.7, Eickhoff et al., 2005; asterisks (*) denote assigned areas].

Anatomical region	Left					Right				
	x	y	z	Z-score	ATB	x	y	z	Z-score	ATB
Arm (Arm)										
Superior Occipital Gyrus/	-16	-98	20	7.17	60% Area 18*					
V6	-20	-82	28	4.35						
Middle Occipital Gyrus/V5	-42	-72	8	7.59	40% hOC5 (V5)*	48	-70	2	7.50	20% hOC5 (V5)*
Middle Temporal Gyrus/	-56	-68	12	4.30	20% IPC (PGp)					
STS	-48	-52	8	3.89						
Superior Parietal Lobule (SPL)	-32	-50	68	5.76	30% SPL (7PC)					
Precentral Gyrus (PMd)	-28	-14	56	4.74	60% Area 6					
SMA	-8	14	48	4.45	20% Area 6	8	12	54	4.31	40% Area 6
Middle Cingulate Cortex						12	20	42	5.37	10% Area 6
Inferior Frontal Gyrus						48	18	4	4.21	20% Area 45
Superior Frontal Gyrus (medial)						6	28	46	3.93	10% Area 6
Middle Frontal Gyrus						38	46	20	4.39	
Insula	-36	20	-6	4.18		32	24	12	3.92	
Putamen	-28	24	-2	4.53						
Arrow (A)										
Superior Occipital Gyrus/	-16	-100	20	7.32	20% Area 18					
V6	-20	-82	24	3.53						
Middle Occipital Gyrus/V5	-44	-76	6	6.70	50% hOC5 (V5)*					
Superior Parietal Lobule	-32	-50	68	5.73	30% SPL (7PC)					
Inferior Parietal Lobule	-38	-38	38	4.66	30% hIP3*					
SupraMarginal Gyrus (TPJ)	-46	-40	30	4.50	40% IPC*					
Precentral Gyrus (PMd)	-36	-2	52	5.06	30% Area 6	36	-4	46	4.17	40% Area 6
SMA	-6	2	54	4.69	80% Area 6	6	16	50	3.91	40% Area 6
Middle Cingulate Cortex						10	20	42	5.03	10% Area 6
Superior Medial Gyrus						6	28	48	3.31	10% Area 6
Insula	-30	24	-2	4.88		32	22	-2	4.66	
Cerebellum	-20	-64	-30	4.43	81% Lob VI (Hem)*					

Colored Arm (CArm)										
Superior Occipital Gyrus/	-18	-92	24	6.66	10% Area 18					
V6	-20	-82	28	4.34						
Middle Occipital Gyrus/V5	-44	-74	8	7.49	20% hOC5 (V5)*					
Middle Temporal Gyrus/V5						46	-68	4	6.34	40% hOC5(V5)*
Superior Parietal Lobule	-30	-50	70	6.60	20% SPL (7PC)					
Precentral Gyrus (PMd)	-34	-2	54	4.62	20% Area 6					
SMA	-6	4	52	4.92	70% Area 6	8	18	50	3.62	20% Area 6
Middle Cingulate Cortex						10	20	42	3.92	10% Area 6
Arm+A+CArm										
Superior Occipital Gyrus/	-16	-94	34	Inf	10% Area 17					
V6	-20	-82	24	7.04						
Middle Occipital Gyrus/V5	-44	-76	6	Inf	50% hOC5(V5)*					
Middle Temporal Gyrus/V5						48	-68	2	Inf	30% hOC5(V5)
Superior Parietal Lobule	-32	-50	68	Inf		30	-56	68	6.10	40% SPL (7PC)*
SupraMarginal Gyrus (TPJ)	-48	-38	32	Inf	30% IPC (PFcm)					
Inferior Parietal Lobule	-42	-32	40	5.35	40% IPC (PFt)*					
Precentral Gyrus (PMd)	-34	-2	54	Inf	20% Area 6	40	-2	54	6.74	40% Area 6
SMA	-4	4	56	7.50	70% Area 6	8	18	50	6.72	20% Area 6
Middle Cingulate Cortex						10	20	42	7.05	10% Area 6
Inferior Frontal Gyrus						34	30	10	5.04	
Middle Frontal Gyrus	-36	48	20	5.68		36	44	16	7.20	
Insula	-30	20	2			28	20	-4	5.85	

Table 3 S1: Descriptive analyses and the statistical values relative to the direct comparison between conditions *same* and *different* for each stimulus-type (Arm, A, CArm) in PMd and SPL ROIs. Asterisk (*) indicates Bonferroni correction for per multiple comparisons (p≤.017).

Location	Maxima	Condition	Mean	SEM	F-test (P)	Part-η^2
Left SPL	(-30 -56 68)	Hsame	0.92	0.37	0.005*	0.44
		Hdiff	1.49	0.36		
		Asame	1.15	0.28	0.65	0.01
		Adiff	1.21	0.27		
		HCsame	1.20	0.30	0.71	0.01
		HCdiff	1.25	0.31		
Left PMd	(-28 -4 44)	Hsame	0.73	0.22	0.000*	0.69
		Hdiff	1.23	0.24		
		Asame	0.97	0.15	0.28	0.08
		Adiff	1.12	0.15		
		Hcsame	0.77	0.19	0.36	0.05
		Hcdiff	0.89	0.22		

Table 1 S2: Cerebral activity during A. the observation of *what* task *vs.* implicit baseline; B. during the observation of *how* task *vs.* implicit baseline. Local maxima, as shown in Figure 10, are given in MNI standard brain coordinates at voxel-level PFWE <0.05 [ATB: most probable anatomical region in the Anatomy Toolbox 1.7, Eickhoff et al., 2005; asterisks (*) denote assigned areas].

Anatomical region	Left					Right				
	x	y	z	Z-score	ATB	x	y	z	Z-score	ATB
A. What *vs.* implicit baseline										
Calcarine Gyrus	-10	-78	10	7.36	80% Area 17 *	12	-78	14	6.89	80% Area 18 *
Lingual Gyrus	-12	-70	-8	6.43	50% hOC3V (V3v)*	12	-66	-4	7.10	60% Area 18 *
Middle Occipital Gyrus	-38	-80	4	6.70		36	-92	8	6.21	
Inferior Occipital Gyrus	-48	-76	-8	6.02	10% hOC5(V5)	42	-84	2	5.84	40% hOV4v (V4)
Fusiform Gyrus	-40	-72	-18	6.30	30% hOV4v (V4)					
Superior Temporal Gyrus						56	-38	8	4.77	
Middle Temporal Gyrus	-60	-46	0	6.20		50	-68	4	7.06	10% hOC5(V5)
Inferior Temporal Gyrus	-46	-64	-8	5.30		54	-68	-8	6.91	30% hOC5(V5)
Superior Parietal Lobule	-32	-62	58	5.23	80% SPL (7A)	30	-66	54	6.12	
Inferior Parietal Lobule	-42	-48	52	6.68	40% IPC *	34	-52	40	5.86	40% hIP3 *
Postcentral Gyrus	-38	-20	44	5.56	80% Area 4p *					
Precentral Gyrus	-46	2	54	6.17	40% Area 6					
SMA	0	12	52	6.06	20% Area 6					
Middle Frontal Gyrus	-50	26	34	6.06	30% Area 45	50	40	26	5.38	
Inferior Frontal Gyrus	-44	48	-12	6.16						
Insula	-28	20	2	5.65						
Hippocampus	-26	-28	0	5.78		24	-26	-6	5.50	
Cerebellum	-48	-60	-24	6.29		46	-56	-30	6.40	69 % Lobule VIIa
B. How *vs.* implicit baseline										
Calcarine Gyrus	-10	-76	8	7.46	70% Area 17 *	12	-78	14	6.94	80% Area 18 *
Lingual Gyrus	-12	-70	-8	6.62	50% hOC3V (V3v)*	12	-66	4	7.17	60% Area 18 *
Middle Occipital Gyrus	-42	-82	4	6.68		36	-92	8	6.36	
Inferior Occipital Gyrus	-44	-72	8	6.07	20% hOC5(V5)	48	-82	-4	6.19	30% hOV4v (V4)
Fusiform Gyrus										
Middle Temporal Gyrus	-60	-46	0	5.58		56	-38	6	4.88	
Inferior Temporal Gyrus						54	-68	-8	6.87	30% hOC5(V5)
Superior Parietal Lobule										
Inferior Parietal Lobule	-42	-48	52	6.10	40% IPC *	42	-38	48	6.24	50% hIP2
Postcentral Gyrus	-38	-20	44	5.75	80% Area 4p *					

Precentral Gyrus	-38	-18	64	5.67	90% Area 6				
SMA	0	10	50	5.47	60% Area 6				
Middle Frontal Gyrus	-50	26	34	5.21	30% Area 45				
Inferior Frontal Gyrus	-56	10	12	5.24	50% Area 44 *				
Insula	-34	14	0	4.97					
Hippocampus	-26	-28	0	5.97		24	-26	-4	5.00

Table 2 S2: Brain activations resulting from the direct contrast between A. *what*-task *vs. how*-task and B. *how*-task *vs. what*- task. Local maxima of activated areas, as shown in Figure 11A, B, are given in MNI standard brain coordinates at cluster-level PFWE <0.05 [ATB: most probable anatomical region in the Anatomy Toolbox 1.7, Eickhoff et al., 2005; asterisks (*) denote assigned areas].

Anatomical region	Left					Right				
	x	y	z	Z-score	ATB	x	y	z	Z-score	ATB
A. What *vs.* How										
Superior Occipital Gyrus						32	-76	42	4.49	
Middle Occipital Gyrus						36	-72	32	3.90	20% IPC
Inferior Temporal Gyrus	-56	-52	-16	3.74						
Superior Parietal Lobule	-32	-62	58	4	80% SPL (7A)	36	-52	56	4.69	40% SPL (7A)
Inferior Parietal Lobule	-34	-60	48	4.60	30% hIP3 *					
Angular Gyrus						30	-64	48	3.97	
Middle Frontal Gyrus						34	8	40	4.52	
Inferior Frontal Gyrus	-40	10	24	3.98	20% Area 44	42	26	28	4.17	
Middle Orbital Gyrus	-42	46	-2	4.38						
B. How *vs.*What										
Rolandic Operculum						50	0	8	4.55	20% OP
Putamen						32	8	8	4.41	
Insula						34	12	12	4.23	20% OP 4

Table 3 S2: A. Percentages of correct responses (hits) related to the task type indicate that the SASV (same action/what-same vitality/how) combination was the simplest, whereas the most complex combination was DASV (different action/what-same vitality/how). The other two combinations, DADV (different action/what-different vitality/how), SADV (same action/what-different vitality/how), fell in between. Descriptive analyses and statistical values based on percentages of the correct responses (hits) relative to: B. the main effect of stimulus combination in the behavioral analysis testing for task complexity (N=16); C. the direct comparison between the stimuli combinations (SASV, SADV, DASV, DADV).

A. Percentages of hits related to the task type

	DADV	DASV	SADV	SASV
WHAT hits %	97.31	89.06	93.75	100
HOW hits %	90.63	87.50	95.31	100

B. Main effects of stimulus comb. for task complexity

	F	Sig.	Part-η^2	Power
Task	0.58	0.46	0.04	0.11
Comb	4.47	0.02	0.23	0.72

C. Contrasts between stimuli combinations

Comb	F	Sig.	Part-η^2	Power
DADV vs. DASV	1.2	0.29	0.07	0.18
DASV vs. SADV	5	0.04	0.25	0.55
SADV vs. SASV	4.6	0.05	0.24	0.52
SASV vs. DADV	6.4	0.02	0.30	0.66

Table 1 S3: Cerebral activity during A. the observation of *what* task *vs.* implicit baseline; B. during the observation of *how* task *vs.* implicit baseline; C. during the observation of *what* task *vs. how* task. Local maxima, as shown in Figure 17, are given in MNI standard brain coordinates at voxel-level PFWE <0.05 [ATB: most probable anatomical region in the Anatomy Toolbox 1.7, Eickhoff et al., 2005; asterisks (*) denote assigned areas].

Anatomical region	LH					RH				
	x	y	z	Z-score	ATB	x	y	z	Z-score	ATB
A. What *vs.* baseline										
Cuneus	-2	-84	20	6.87	70% Area 18*	8	-84	20	7.00	80% Area 18*
Inferior Temporal Gyrus	-56	-40	-16	6.00						
Middle Temporal Gyrus						58	-40	-12	7.12	
Inferior Parietal Lobule	-42	-58	50	6.96	40% IPC(PGa)	44	-54	54	6.70	50% IPC(PGa)
Postcentral Gyrus	-44	-26	60	6.74	80% Area 1*					
Precentral Gyrus	-38	-22	66	5.90	60% Area 6					
Middle Frontal Gyrus	-42	14	50	5.63		48	32	38	5.65	
Inferior Frontal Gyrus	-52	24	32	4.84	40% Area 45*	58	16	2	4.88	50% Area 44*
Cerebellum	-34	-70	-38	5.09	78% Lobule VIIa*	30	-70	-38	4.61	76% Lobule VIIa*
B. How *vs.* baseline										
Calcarine Gyrus						6	-74	10	7.75	80% Area 17*
Cuneus	-8	-84	20	5.37	30% Area 18*					
Inferior Temporal Gyrus	-56	-40	-16	6.01						
Middle Temporal Gyrus	-58	-40	-12	5.15		58	-40	-12	7.05	
Inferior Parietal Lobule	-46	-48	42	6.43	30%IPC(PF)*	50	-40	56	6.27	
Postcentral Gyrus	-46	-30	56	7.26	70% Area 1*	48	-38	60	6.17	70% Area 2*
Middle Frontal Gyrus	-40	48	18	6.28		46	34	38	5.01	
Inferior Frontal Gyrus	-46	48	10	5.37		46	34	38	5.01	
Temporal Pole						54	16	-8	4.76	
Cerebellum	-40	-66	-28	6.21	100% Lobule VIIa*	42	-60	-34	6.33	100% Lobule VIIa*

Table 2 S3: Cerebral activity during C. during the observation of *what* task *vs. how* task*;* D. during the observation of *how* task *vs. what* task. Local maxima, as shown in Figure 18, are given in MNI standard brain coordinates at voxel-level PFWE <0.05 [ATB: most probable anatomical region in the Anatomy Toolbox 1.7, Eickhoff et al., 2005; asterisks (*) denote assigned areas; K: cluster size].

Anatomical region	LH						RH					
	x	y	z	Z-score	K	ATB	x	y	z	Z-score	K	ATB
C. What *vs.* How												
Angular gyrus	-38	-62	46	5.20	799	30% IPC(PFm)*	48	-58	36	4.66	696	
Superior Medial Gyrus	-2	40	46	4.61	750							
Middle Frontal Gyrus	-40	14	48	5.51	680		44	24	46	4.57	402	
	-38	52	0	5.54	618							
D. How *vs.* What												
Supramarginal Gyrus	-60	-32	26	4.81	644	60 % IPC(PFm)*						
Precentral Gyrus	58	0	44	4.73	469		58	0	44	4.73	469	
Cingulate cortex	-6	6	40	4.40	541							
Orbital Gyrus	-6	50	-6	3.81	209							
SMA							16	-6	74	4.48	722	
Insula	-44	6	-4	5.19	824		36	2	12	4.59	247	

Table 1 S4: Cerebral activity during A. the observation task of *vitality forms (Rude and Gentle) vs. control conditions (Ctrl 1 and Ctrl 2)*. Local maxima, as shown in Figure 25, are given in MNI standard brain coordinates at cluster-level PFWE <0.05 [ATB: most probable anatomical region in the Anatomy Toolbox 1.7, Eickhoff et al., 2005; asterisks (*) denote assigned areas].

Anatomical region	LH					RH				
	x	y	z	Z-score	ATB	x	y	z	Z-score	ATB
($P_{FWE\text{-}COR\ CLUSTER\ LEVEL}$=<.05)										
A Observation Task										
Rude vs. Ctrl 1										
Calcarine Gyrus	-8	-84	6	Inf	90% Area 17*					
Lingual Gyrus						8	-72	2	Inf	70% Area 18*
Middle Temporal Gyrus	-56	-64	8	5.41		54	-60	2	5.34	
Fusiform Gyrus	-32	-70	-18	4.96						
Parietal Lobule	-52	.-34	38	4.86	50% IPC (PFT)					
SMA	-2	8	46	3.99	30% Area 6	2	18	46	4.01	Area 6 40%
Insula	-40	-2	2	4.96		36	16	4	3.63	
Middle Frontal Gyrus						50	48	10	3.51	
Inferior Frontal Gyrus						52	18	-10	4.14	
Gentle vs. Ctrl 1										
Calcarine Gyrus	-8	-84	6	6.54	70% Area 17*					
Lingual Gyrus						8	-72	2	6.45	70% Area 18*
Middle Occipital Gyrus	-50	-78	-2	5.12		50	-76	2	5.98	
Middle Temporal Gyrus	-56	-58	10	4.20		58	-66	6	4.38	
Fusiform Gyrus	-26	-80	-18	6.36	70% hOC4(V4)					
Insula										
Rude vs. Ctrl 2										
Calcarine Gyrus	-8	-84	6	Inf	90% Area 17*					
Lingual Gyrus						10	-80	-14	Inf	70% Area 18*
Superior Temporal Gyrus						56	-32	-10	3.33	
Middle Temporal Gyrus						66	-38	-4	4.06	
Precentral Gyrus	-56	14	34	4.10	20% Area 44					
SMA	-4	8	44	4.16						
Insula	-40	-2	4	5.57		40	6	-6	4.12	
Superior Frontal Gyrus	-32	-4	68	4.44	Area 6 30%					
Middle Frontal Gyrus	-48	34	30	3.91						
Inferior Frontal Gyrus	-48	40	18	4.05		50	40	8	4.01	
Middle Cingulate						12	6	42	3.54	
Amygdala						24	0	-22	4.91	40% Amyg (LB)
Gentle vs. Ctrl 2										
Calcarine Gyrus	-8	-84	6	6.61	70% Area 17*					
Inferior Parietal Lobule	-52	-34	38	4.24	50% IPC (PF)*					
Supra Marginal Gyrus	-52	-22	16	4.18	70% OP1*	60	-42	28	3.55	50% IPC (PFm)*
Superior Temporal Gyrus	-52	-34	18	4.44		66	-28	18	3.93	60% IPC (PF)*
Fusiform Gyrus	-26	-80	-18	6.44	70% hOC4(V4)					
Insula	-38	4	4	4.17						
Temporal Pole						58	14	-4	3.88	
Cerebellum	-16	-80	-16	6.67	30% hOC4(V4)					

Table 2 S4: Cerebral activity during A. the imagination task of *vitality forms (Rude and Gentle) vs. Ctrl 1*; B. the execution task of *vitality forms (Rude and Gentle) vs. Ctrl 1*. Local maxima, as shown in Figure 25, are given in MNI standard brain coordinates at cluster-level PFWE <0.05 [ATB: most probable anatomical region in the Anatomy Toolbox 1.7, Eickhoff et al., 2005; asterisks (*) denote assigned areas].

Anatomical region	LH					RH				
	x	y	z	Z-score	ATB	x	y	z	Z-score	ATB
($P_{FWE\text{-}COR\ CLUSTER\ LEVEL}$=<.05)										
B. Imagination Task										
Rude vs. Ctrl 1										
Calcarine Gyrus						2	-86	-2	5.37	80% Area 17*
Inferior Parietal Lobule	-52	-48	48	3.87	60%IPC(PFm)*					
Supra Marginal Gyrus	-64	-36	34	4.08	90% IPC(PF)*	60	-40	32	4.64	100% IPC(PF)*
Insula	-36	10	-4	3.81		44	10	-6	4.81	
Inferior Frontal Gyrus						58	10	4	4.27	40% Area 44*
						56	34	0	4.21	50% Area 45*
Rolandic Operculum	-54	6	2	4.62						
Temporal Pole	-50	14	-6	4.56						
Cerebellum	-32	-70	-22	5.17	71% VIIa CrusI*	26	-72	-18	5.26	30% hOC4v(V4)
Gentle vs. Ctrl 1										
Calcarine Gyrus	0	-84	-2	6.19	100% Area 17*					
Lingual Gyrus						8	-76	-4	6.18	90% Area 18*
Precuneus	-12	-70	62	4.37	40% SPL (7A)					
SMA	-12	0	66	4.18	50% Area 6					
Insula	-46	6	4	4.69		42	0	-6	4.15	
Rolandic Operculum	-52	4	2	4.78		60	10	6	4.43	60% Area 44*
Inferior Frontal Gyrus						58	26	4	4.46	100% Area 45*
Amygdala						26	0	-14	3.63	90% Amyg (SF)
Putamen	-22	10	4	4.39		32	0	6	3.46	
C. Execution Task										
Rude vs. Ctrl 1										
Lingual Gyrus						4	-76	-2	6.18	90% Area 17*
Inferior Parietal Lobule	-60	-40	46	6.16		56	-42	52	6.11	50% IPC (PF)
Supra Marginal Gyrus	-58	-40	36	6.21	80% IPC (PF)*	62	-38	34	6.28	100% IPC (PF)*
Middle Temporal Gyrus	-56	-52	6	5.03		62	-56	2	4.53	
SMA	-8	6	76	4.39		4	20	68	5.07	
Insula	-36	4	2	6.19		38	8	-2	5.74	
Inferior Frontal Gyrus	-50	40	6	5.43	50% Area 45*	52	14	10	6.35	70% Area 44*
Middle Cingulate	0	20	34	4.44						
Temporal Pole	-50	14	-10	7.14						
Cerebellum	-32	-70	-24	6.58	78% VIIa CrusI*	26	-80	-20	5.97	45% VIIa CrusI*
Gentle vs. Ctrl 1										
Calcarine	-2	-78	8	6.42	90% Area 17*	10	-74	16	6.59	80% Area 18*
Lingual Gyrus	-6	-80	-8	6.07	50% Area 18*	8	-76	-4	6.84	90% Area 18*
Inferior Parietal Lobule						48	-40	52	5.27	40% IPC (PFm)*
Supra Marginal Gyrus						56	-34	50	5.10	80% IPC (PF)*
Inferior Temporal Gyrus						58	-56	-6	4.32	
Postcentral Gyrus	-44	-38	64	6.17	70% Area 1*					
Precentral Gyrus	-30	-20	74	6.17						
Insula	-36	2	2	4.27		36	8	-2	4.67	
Inferior Frontal Gyrus	-44	36	12	4.46	30% Area 45	54	8	18	4.15	40% Area 44*
Temporal Pole						52	12	-10	4.88	
Cerebellum	-32	-70	-22	6.78	71% VIIa CrusI*					

Table 3 S4. Cerebral activity obtained with the overlapping of three different tasks (Observation, Imagination and Execution) for each condition: A. Rude condition; B. Gentle condition; C. Ctrl 1 condition. Local maxima, as shown in Figure 26, are given in MNI standard brain coordinates at cluster-level PFWE <0.05 [ATB: most probable anatomical region in the Anatomy Toolbox 1.7, Eickhoff et al., 2005; asterisks (*) denote assigned areas].

Anatomical region	LH					RH				
	x	y	z	Z-score	ATB	x	y	z	Z-score	ATB
Overlapping among Tasks (Obs, Img, Exe)										
($P_{FWE\text{-}COR\ CLUSTER\ LEVEL}$=<.05)										
A. Rude										
Calcarine Gyrus	0	-82	8	Inf	80% Area 17*					
Lingual Gyrus						4	-76	-2	Inf	90% Area 17*
Inferior Parietal Lobule						52	-42	48	5.31	40% IPC(PF)*
Supra Marginal Gyrus	-58	-34	30	6.04	60% IPC(PF)*	60	-40	30	6.23	90% IPC(PF)*
Middle Temporal Gyrus	-52	-58	4	5.54						
SMA						2	12	60	5.19	
Insula	-36	14	0	5.92		36	14	2	4.93	
Superior Frontal Gyrus	-30	-4	68	5.16						
Middle Frontal Gyrus						42	40	38	4.22	
Middle Cingulate Cortex						2	16	38	4.79	
Cerebellum	-32	-70	-22	Inf	71% VIIa CrusI*	32	-72	-28	6.28	96% VIIa CrusI*
B. Gentle										
Calcarine Gyrus	-2	-82	10	Inf	70% Area 17*	12	-74	16	Inf	40% Area 18*
Lingual Gyrus						4	-74	-4	Inf	70% Area 17*
Inferior Parietal Lobule						52	-42	50	4.24	40% IPC(PF)
Supra Marginal Gyrus						60	-40	32	5.56	100% IPC(PF)*
Insula	-38	4	2	5.52		38	4	-8	4.23	
Middle Frontal Gyrus						40	50	24	4.06	
Amygdala										
Putamen										
C. Ctrl 1										
Lingual Gyrus										
Precuneus	-12	-56	66	6.89	50% SPL (7A)	10	-54	68	6.81	50% SPL (5L)*
Superior Parietal Lobule	-38	-46	64	6.72						
Insula	-42	8	4	4.63		46	6	6	4.32	
Inferior Frontal Gyrus						62	12	22	4.49	
Cerebellum	-18	-76	-20	6.53	80% Lob VI (Hem)*	20	-72	-20	5.87	92% Lob VI (Hem)*

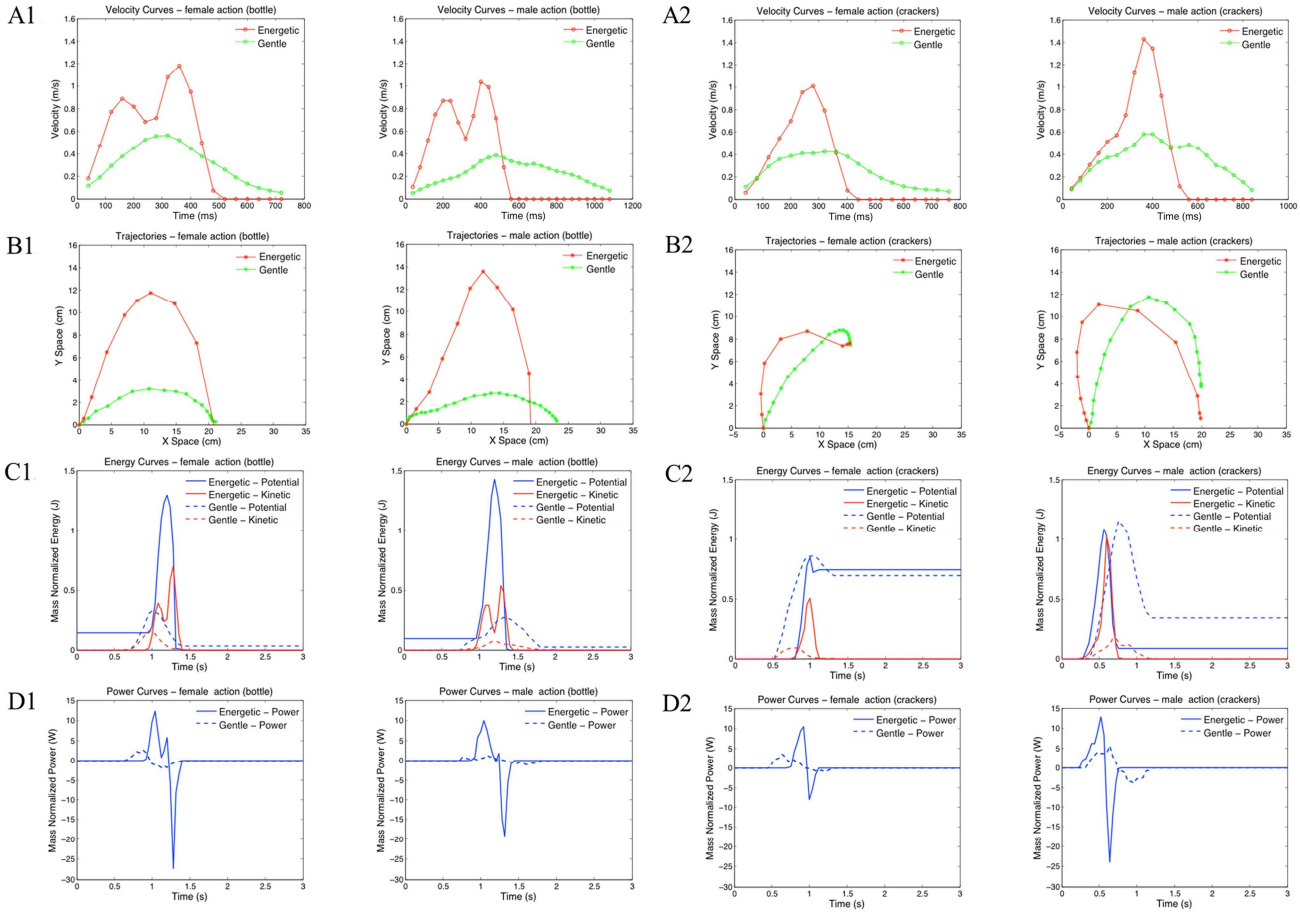

Figure 1 S2: Kinematic and dynamic profiles related to actions performed with object (1. move a bottle towards the other actor; 2. give a packet of crackers) performed by the female (graphs on the left) and the male (graphs on the right) actor with the two vitality forms (gentle; energetic). A. Velocity profiles (Y axes) and duration (X axes). In the graphs are shown only the points in which V > .05 m/s. B. Trajectories (gentle, green line; energetic, red line). C. Potential energy (blue line), that is the energy that the actor gave to the object during the lifting phase of the action; kinetic energy (red line), that is the energy that the actor gave to the object to move it with a specific velocity from the start to the end point. D. Power required to perform the action on the object in an energetic (blue solid line) and gentle (blue dashed line) vitality forms.

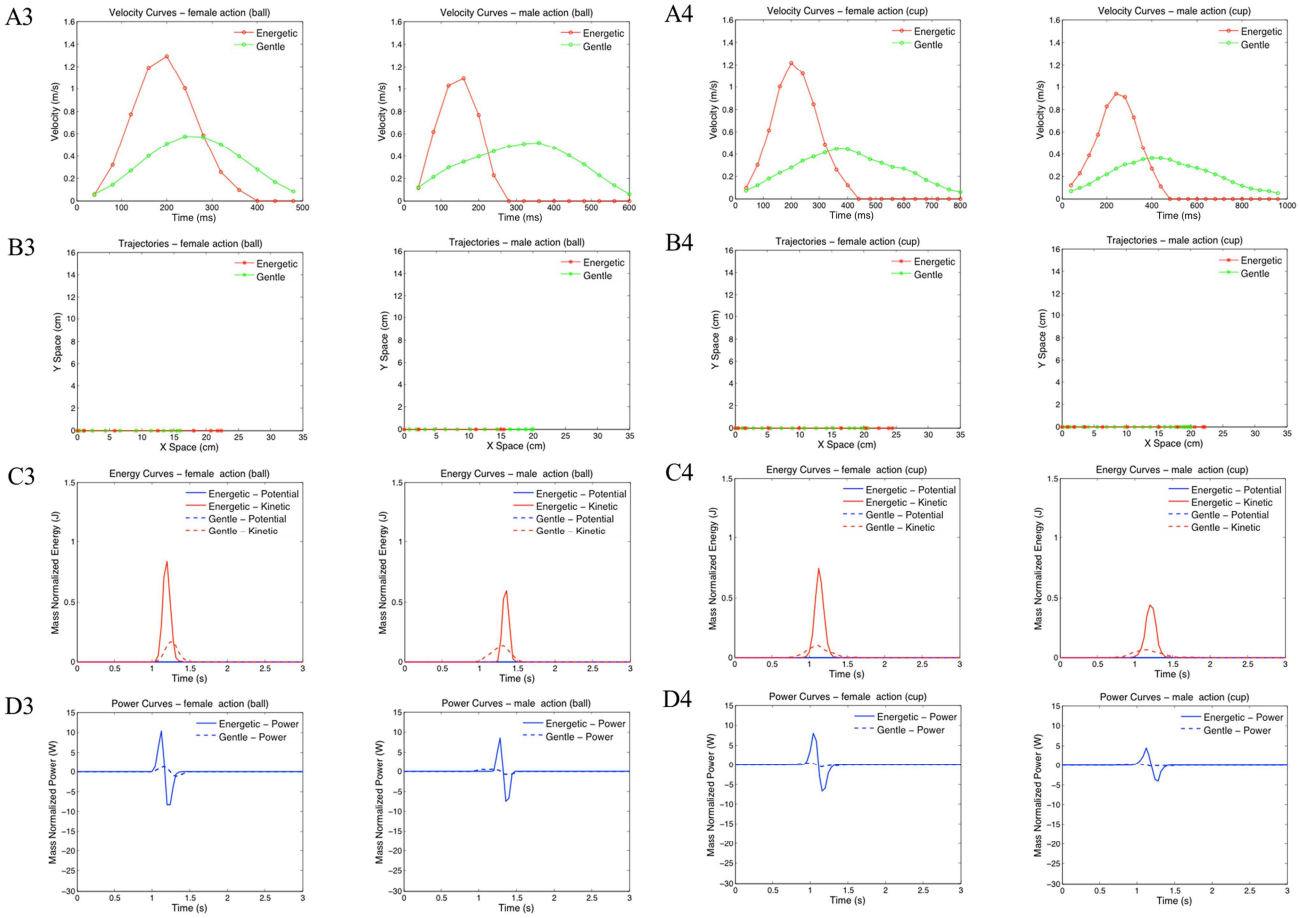

Figure 2 S2: Kinematic and dynamic profiles related to actions performed with object (1. pass a ball; 2. hand a cup) performed by the female (graphs on the left) and the male (graphs on the right) actor with the two vitality forms (gentle; energetic). A. Velocity profiles (Y axes) and duration (X axes). In the graphs are shown only the points in which V > .05 m/s. B. Trajectories (gentle, green line; energetic, red line). C. Potential energy (blue line), that is the energy that the actor gave to the object during the lifting phase of the action; kinetic energy (red line), that is the energy that the actor gave to the object to move it with a specific velocity from the start to the end point. D. Power required to perform the action on the object in an energetic (blue solid line) and gentle (blue dashed line) vitality forms.

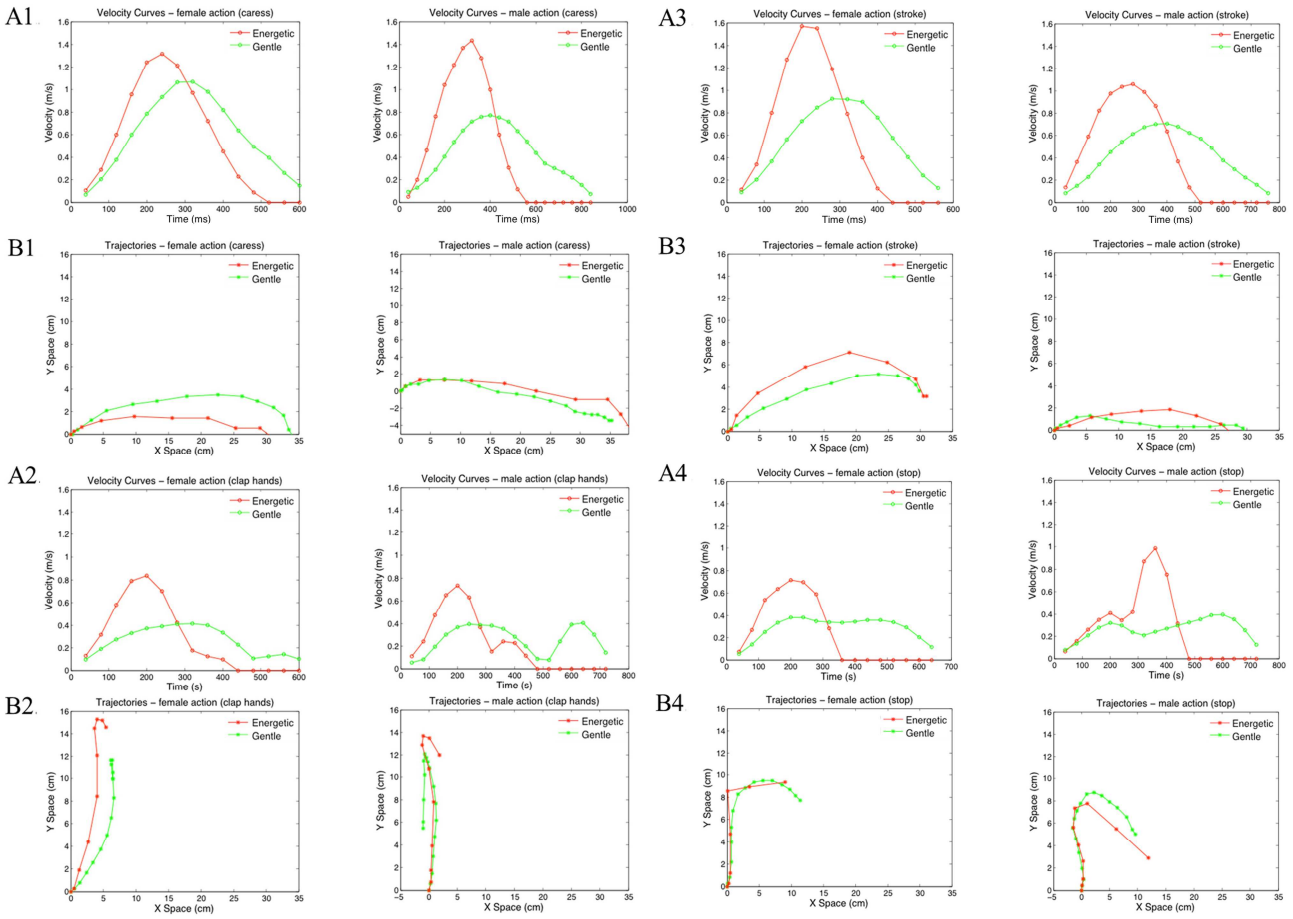

Figure 3 S2: Kinematic profiles related to the actions executed without object (1. caress; 2. clap hands; 3. stroke the other actor's backhand; 4. stop gesture) performed by the female (graphs on the left) and male (graphs on the right) actor with the two vitality forms (gentle; energetic). A. Velocity profiles (Y axes) and duration (X axes) of each action. In the graphs are shown only the points in which V > .05 m/s. B. Trajectories (gentle, green line; energetic, red line). The dots indicate the X and Y position occupied by the hand in space every 40ms.